الجمهورية الجزائرية الديمقراطية الشعبية

République Algérienne Démocratique et Populaire

Ministère de l'Enseignement Supérieur et de la Recherche Scientifique

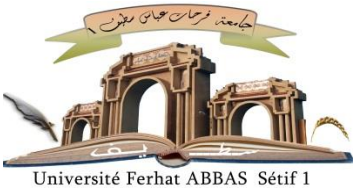

UNIVERSITÉ FERHAT ABBAS – SETIF 1

FACULTÉ DE TECHNOLOGIE

THÈSE

Présentée au Département d'Electronique

Pour l'obtention du diplôme de

DOCTORAT

Domaine : Sciences et Technologie

Filière : Electronique **Option : Systèmes Embarqués et Technologie**

Par

MEDKOUR Hicham

THÈME

Conception et Réalisation d'Antennes Reconfigurables

Soutenue le 04 / 07 / 2019 devant le Jury :

KRIM Fateh	**Professeur**	**Univ. Ferhat Abbas Sétif 1**	**Président**
ZEGADI Ameur	**Professeur**	**Univ. Ferhat Abbas Sétif 1**	**Directeur de thèse**
AIDEL Salih	**Professeur**	**Univ. Mohamed El Bachir El Ibrahimi de BBA**	**Examinateur**
ZEBIRI Chemseddine	**MCA**	**Univ. Ferhat Abbas Sétif 1**	**Examinateur**

People's Democratic Republic of Algeria

Ministry of Higher Education and Scientific Research

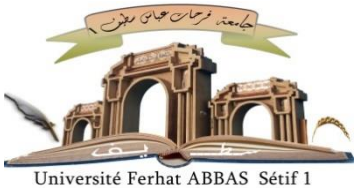

Ferhat Abbas University of Setif 1

Faculty of Technology

Thesis

Presented at the Department of Electronics

For the award of the degree of

DOCTORATE

Field: Sciences and Technology

Specialty: Electronics **Option: Embedded Systems and Technology**

By

Hicham MEDKOUR

Title

Design and Implementation of Reconfigurable Antennas

Defended on the 4th July 2019 before the Jury:

KRIM Fateh	**Professor**	**Ferhat Abbas Univ. of Setif 1**	**President**
ZEGADI Ameur	**Professor**	**Ferhat Abbas Univ. of Setif 1**	**Supervisor**
AIDEL Salih	**Professor**	**Mohamed El Bachir El Ibrahimi Univ. of BBA**	**Examiner**
ZEBIRI Chemseddine	**MCA**	**Ferhat Abbas Univ. of Setif 1**	**Examiner**


C2NS

Abstract

In this thesis we describe novel approaches in designing reconfigurable antennas. The proposed reconfigurable layouts are intended for integration into compact UWB communication systems and are characterized by their low profile and easy fabrication processes. Initially, the project was to design et implement some reconfigurable antennas based on conductive polymers. As a result, the first part of this thesis provides an advanced literature survey as well as an investigation on the use of tunable permittivity or conductivity in designing antennas based on conductive polymers. The second part of this thesis reports on the design of planar reconfigurable UWB antennas with interference filtering capabilities. Firstly, a planar monopole UWB reconfigurable antenna has been designed showing filtering capabilities in three narrow bands which could potentially interfere in this particular region of the spectrum. Reconfigurability allows the antenna to match to any interference cases. The presented design uses low-cost FR 4 substrates known for being light. Secondly, an extremely compact UWB single-sided reconfigurable designed antenna is described. Unlike the previous antenna, the reconfigurable filtering circuit has been exclusively implemented in the ground plane rather than in the radiating patch in order to optimize the radiation performance of the antenna. By doing so, the new design is cost effective, allowing interferences' filtering at the antenna level rather than at a later stage and avoids complex biasing control antenna circuitry.

Keywords: Antennas; Microstrip; UWB; Conductive polymers; Reconfiguration.

العنوان: تصميم وصناعة هوائيات ذات خصائص قابلة لإعادة الهيكلة

ملخص

في هذه الرسالة وصفنا طرائق جديدة في تصميم هوائيات ذات الخصائص القابلة للتحكم. فقد تم تقديم تصاميم لهوائيات مناسبة للإدماج في أنظمة الاتصالات الصغيرة الحجم وذو ترددات واسعة النطاق المنحصرة بين 3 و10 GHz. تتميز هذه الهوائيات بخاصيتين هامتين هما الهيئة الفزيائية الأقل جاذبية وسهولة التصنيع. أصلا في بداية المشروع، كنا نرغب إلى تصميم وصنع بعض الهوائيات القابلة لإعادة التكوين استنادًا إلى البوليمرات الموصلة. على هذا الأساس، يوفر الجزء الأول من هذه الرسالة مسحًا متقدمًا للأدب بالإضافة إلى دراسة حول استخدام السماحية القابلة للضبط أو الموصلية في تصميم الهوائيات باستعمال البوليمرات الموصلة. يقدم الجزء الثاني من هذه الرسالة تقريراً عن تصميم هوائيات **UWB** المستوية القابلة لإعادة التشكيل مع إمكانيات تصفية التداخل. أولاً، تم تصميم هوائي قابل لإعادة التشكيل أحادي القطب **UWB** لإظهار إمكانيات التصفية في ثلاث نطاقات ضيقة يمكن أن تتداخل في منطقة الطيف المعينة. تسمح إعادة التكوين للهوائي بالتطابق مع أي حالات تداخل. يستخدم التصميم المقدم ركائز **FR 4** منخفضة التكلفة معروفة بكونها خفيفة. ثانياً، يوصف هوائي مصمم بدقة **UWB** أحادي الجانب قابل لإعادة التحكم. بخلاف الهوائي السابق، تم تنفيذ دائرة الترشيح القابلة لإعادة التحكم على وجه الحصر في المستوى الأرضي بدلاً من التصحيح المشع من أجل تحسين أداء إشعاع الهوائي. القيام بذلك، يكون التصميم الجديد منخفض التكلفة مما يسمح بترشيح التداخلات على مستوى الهوائي بدلاً من مرحلة لاحقة ويتجنب الدوائر المعقدة لهوائي التحكم في التحيز.

الكلمات المفتاحية: الهوائيات؛ النواقل المطبوعة؛ UWB؛ لدائن ذات ناقلية كهربائية؛ عالية إعادة الهيكلة.

Titre : Conception et Réalisation d'Antennes Reconfigurables

Résumé

Dans cette thèse, nous décrivons de nouvelles approches dans la conception d'antennes reconfigurables. Les schémas reconfigurables proposés sont destinés à être intégrés dans des systèmes de communication UWB compacts et se caractérisent par leur profil bas et leurs processus de fabrication faciles. Au départ, le travail consistait à concevoir et à mettre en œuvre des antennes reconfigurables à base de polymères conducteurs, par conséquent, la première partie de cette thèse propose une étude bibliographique avancée ainsi qu'une étude sur l'utilisation de la permittivité ou de la conductivité accordables dans la conception d'antennes à base de polymères conducteurs. La deuxième partie de cette thèse porte sur la conception d'antennes UWB planes reconfigurables dotées de capacités de filtrage aux interférences. Premièrement, une antenne reconfigurable UWB monopolaire plane a été conçue, montrant des capacités de filtrage dans trois bandes étroites susceptibles d'interférer dans cette région spectrale. La reconfiguration permet à l'antenne de s'adapter à tous les cas d'interférences. La conception présentée utilise des substrats à faible coût de FR 4 connus pour leur légèreté. Deuxièmement, Nous décrivons une seconde reconfigurable antenne UWB et qui est extrêmement compacte. Contrairement à l'antenne précédente, le circuit de filtrage reconfigurable a été mis en œuvre exclusivement dans le plan de masse plutôt que dans le patch rayonnant afin d'optimiser les performances de rayonnement de l'antenne. La nouvelle conception est peu coûteuse et permet de filtrer les interférences au niveau de l'antenne plutôt qu'à un stade ultérieur, en évitant le besoin aux circuits complexes de commande de polarisation.

Mots-clés : Antennes ; Microruban ; UWB ; Polymères conducteurs ; Reconfiguration.

Acknowledgments

I first thank **ALLAH**, the Almighty, who lights us the right way.

I would like to express my sincere gratitude to everyone and organisations whose support, skills and encouragement were crucial to the successful completion of this thesis.

This work has been conducted in the laboratory: Croissance et Caractérisation de Nouveaux Semiconducteurs (LCCNS), Electronics Department, Technology Faculty of Ferhat Abbas University of Setif 1.

First and foremost, I would like to convey my deep gratitude to my principal supervisor, Professor Ameur Zegadi for his constant support throughout my doctorate research time at the University of Ferhat Abbas Setif 1. His encouragement and critical comments are all essential factors that led me throughout my work.

I am so thankful to Professor Ahmed Zouaoui, head of the laboratory, for his support.

I would like to mention my previous teacher and supervisor in Master's degree, Professor Hamimi Chemali. He has not only inspired me the research passion but also helped me to balance it with my social life and professional progress.

I am also deeply indebted to Professor Tan-Phu Vuong and all the technical staffs at the Institute of Microelectronics Electromagnetics and Photonic in Grenoble who received me and allowed me to carry out my experimental work. Special thanks are due to Miss Erika Vandelle who has patiently helped me in the antenna fabrication and measurement processes as well as during the papers writing.

I thank Professor Fateh Krim, at Ferhat Abbas University of Setif 1, for having accepted to chair the jury of this thesis, I am very honoured.

I extend my warmest thanks to Professor Salih Aidel of Mohamed El Bachir El Ibrahimi University of Bordj Bou Arreridj and Dr. Chemseddine ZEBIRI, MCA at Ferhat Abbas University of Setif 1 for having accepted to be part of the jury of this thesis as examiners.

My doctorate research would not be possible without the assistance from the University of Ferhat Abbas Sétif 1, the faculty of Technology, from which I received financial support for my

short training stay abroad. Indeed, I would like to thank the administrative team, including the head of the department Professor Abdelouahab Hassam.

Throughout my doctorate, I have received valuable help from many friends and colleagues. I would like to thank Dr. Ali Mansoul from the Development Centre of Advanced Technologies (CDTA) in Algiers, Dr. Idris Messaoudene from National School of Computer Science in Algiers,

Dr. Abou Djamal form the University of Science and Technology Houari Boumediene in Algiers. I will never forget the fruitful assistance I received from Dr. Adam Narbudowicz from the Dublin Institute of Technology in Ireland. I wish to acknowledge my deep appreciation to my dear friends and doctorate colleagues Abdelbaset Laib and Imededdin Djadour who have always been to my side in any case and supported me unconditionally.

Last but not least, I would like to give my infinite love and appreciation to my father, my mother, my brothers and sisters for their infinite care and encouragement.

Hicham Medkour,

February 2019,

Setif.

List of Acronyms

AC	Alternative Currents
BST	Barium Strontium Titanate
CSRR	Complementary Split Ring Resonators
CCo	Carbon coated Cobalt
CPW	Coplanar Waveguide
CST	Computer Simulation Technology
DMS	Defected Microstrip Structure
DFX	Drawing Interchange Format or Drawing Exchange Format
DC	Direct Current
DGS	Defect Ground Structure
FR	Flame Retardant
HFSS	Higher Frequency Spectrum Simulator
IMEP	Institut de Microélectronique Electromagnétisme et Photonique
ITU	International Telecommunication Union
LCP	Liquid Crystal Polymer
MWCNT	Multiwall Carbon Nanotubes
MSA	Microstrip Antenna
MIMO	Multiple Input Multiple Output
MgO	Magnesium Oxide
MEMS	Micro-Electro-Mechanical System
NASA	National Aeronautics and Space Agency
PIN	P-Intrinsic-N
POE	Polyolefin Elastomer
PANI	Polyaniline
PET	Polyethylene Terephthalate
PPy	Polypyrrole
PCB	Printed Circuit Board
PUT	Prototype Under Test

PEDOT	Poly(3,4-ethylenedioxythiophene)
PEDOT:PSS	Poly(3,4-ethylenedioxythiophene): Polystyrene sulfonate
RCS	Radar Cross Section
RF	Radio Frequency
RFID	Radio Frequency Identification
SMA	Sub-Miniature version A
SRR	Split Ring Resonator
WIMAX	Wireless Interoperability Medium Access
WBAN	Wireless Body Area Network
WLAN	Wireless Local Area Network
UWB	Ultra-Wide Band
VNA	Vector Network Analyser

List of Figures

List of Tables

Contents

General Introduction

1. Advantages of Reconfigurable Antennas

Assigning different antennas for each wireless protocol in a single device is no longer the best solution. There is an increased call today for further size miniaturization of wireless communication devices and henceforth the limited available space has to be shared carefully. Separate antennas of type monopole or microstrip are typically used in these devices and in many cases they may not have multiple-frequency capabilities. Generally, multiple antennas are integrated on a single device in order to enhance its reception capabilities but in sending mode only single antenna is used. Transmission from a portable device to a base station is the weakest mission in bidirectional communication links because of movability constraints like power, size, and cost. The portable handsets are commonly working in unexpected and rough electromagnetic environment which affects and decreases antenna performances. As a solution, antenna reconfigurability provides substantial help to deal with this problem. Tuning antenna's operating frequency could be utilized to change operating bands, filtering interfering signals, or allowing antenna to accommodate with new unexpected working environments. In addition, antenna radiation pattern reconfiguration permits to focus maximum radiation power into privileged directions and therefore use less power for transmission and consequently extends battery life. Besides the two previous alternative options, reconfigurable polarization provides also several possibilities to a single antenna to perform transmission/reception through multiple types of polarization including horizontal/vertical linear polarizations and left/right hand circular polarizations. At present, low-profile and miniaturization are two highly desirable characteristics in today's communication handsets and so the adoption of reconfigurable antennas would certainly respond to these requests through processing and managing these two properties. Hence, reconfiguration would assure additional operational freedom degrees in terms of adaptation, functionality and versatility.

2. Challenges in Reconfigurable Antennas

The integration of new features into conventional antennas presents not only a real challenge in terms of norms but certainly would arise several questions about cost, technology and efficiency [1]. The addition of antenna reconfigurability induces extra design complexities in control system implementation. These challenges should not only cover production of the desired levels of antenna functionality but also the integration of this new smart feature into a

complete cost-effective system. The overall design system cost of the antenna will be largely balanced by the associated technologies for implementing this valuable reconfiguration.

The complete antenna functionality task requires dedicated signal processing and feedback circuitry and will certainly face further complications when adding different components. However, if a single reconfigurable antenna could deliver the same functionality of more than one traditional single-purpose system, significant savings in cost, weight, volume, and maintenance/repair resources may be realizable. Of course, integrating new kinds of functionality into antennas will not automatically result in higher or comparable performance and lower costs. System designers need to be willing to exploit these new degrees of freedom and functionality so that the antenna becomes a more active part of the communication link, working together with new circuits, signal processing techniques, communication and radar protocols. The difficulty lies also in the fact that reconfigurable antennas often take on non-canonical forms and there is interaction between closely spaced elements. The influence of switches and their biasing lines is a real problem and basically their behaviour is quite difficult to be predicted.

3. Benefits of Conductive Polymers based Antennas

For such important wireless applications like RFID (radio frequency identification), WBAN (wireless body area network) antennas are required with low-profile, light weight, compact size (xy-plane), resistant to deformation and robust to electromagnetic impact. Antennas made of conventional materials such as metals and ceramics do not satisfy the aforesaid characteristics. In the last few years, many researches have been performed on conductive polymers and eventually they have showed very interesting electrical and mechanical properties which are a very promising for application in antennas designing **[2]**. Conductive polymers such as Polypyrrole (PPy), Graphene, Polyaniline and PEDOT expose these highly potential assets. In addition to their high electrical conductivity, high mechanical elasticity and being light, they can be implemented easily at a low-cost. Furthermore, they have low density and are highly resistant to corrosion with their production process is friendly to environment. Henceforth, there is high motivation to take advantage from their interesting properties to produce flexible, low-cost and easily foldable antennas and hence be able to produce reconfigurable antennas based on conductive polymers owing to the fact that the electrical conductivity of conductive polymers is adjustable **[3]**.

4. Challenges of Conductive Polymers based Reconfigurable Antennas

It is desirable to take advantages of the properties of conductive polymers in designing reconfigurable antennas. This combination would result into the development of highly efficient, multi-functional, low-cost and conformal antennas. Reconfigurability enhances the functionality of the antenna and multiplies its operating capabilities while the properties of conductive polymer. However, the challenge in today's reconfigurable conductive polymer antenna designs lie in how to integrate a robust reconfiguration mechanism onto the polymer antenna structure. Experimentally, there are two kinds of used polymer substrates: rigid and flexible substrates. In the last decade, there have been significant advances in the development of conductive polymer using rigid substrates. It is easy to integrate different control mechanisms onto conductive polymer surfaces, which are deposited on rigid substrates to achieve not only the frequency reconfiguration but also adjust the radiation pattern or polarization. However, the task is practically difficult when it comes to the integration of reconfigurability in flexible and plastic based substrate antennas. For instance, it is hard to associate lumped components (RF switches) onto conductive polymers that are deposited on plastic substrates. Furthermore, for the case of wearable antennas' applications, the presence of lumped elements on top of the polymer antenna represents a risk of being detached due to repeated physical deformations, which are possible in a realistic human-body environment (e.g. bending, stretching and twisting), and also when washing. Hence, the robustness of flexible reconfigurable conductive polymer antennas is a research challenge to find the right substrate that will be convenient to reconfiguration mechanisms.

5. Thesis Road Map

The objective of this thesis is to develop some antennas that offer certain additional functionalities while providing better performances to meet today's requirements and/or to solve certain problems linked to some wireless applications. The road map undertaken is as illustrated in **Fig. 1**. There are two main axes we started with:

1. The synthesis of a conductive polymer;
2. The design and implementation of some reconfigurable antennas.

In the first path, an experimental investigation has been carried out on preparing and characterizing some samples of conductive polymers in our laboratory (LCCNS). During a period of time, chemical polymerization of pyrrole was done and polypyrrole (PPy) has been

synthesised. The measurement of the conductivity using the method of four points has shown that the samples had low electrical conductivity. However, this requird additional chemical processing to enhance the electrical conductivity which is a crucial parameter for the antenna. Nevertheless, the tasks of conductivity enhancement, characterization of the polymer and the exploration of its interaction with electromagnetic environment are postponed and left as future work due to the lack of characterization facilities. Herein, we confined ourselves to give only the state of the art on antennas and reconfigurable antennas based on conductive polymer. Still, we present a theoretical study on conductive polymer properties with particular attention given to their electromagnetic behaviour.

In the meantime, work has been carried out in the second axe in which reconfigurable antennas based on copper were investigated. The objective is to come up with compact reconfigurable antennas that are capable to deal with the problem of interference that suffer some wireless systems in the electromagnetic spectrum 3.1 to 10 GHz. Indeed, two reconfigurable monopole antennas have been conceived, simulated and optimized using the commercial software CST [4]. In the first antenna conception, our work was limited to the design, the simulation and the optimization. While in the second, in addition to the simulation study the antenna was fabricated and its performances were measured.

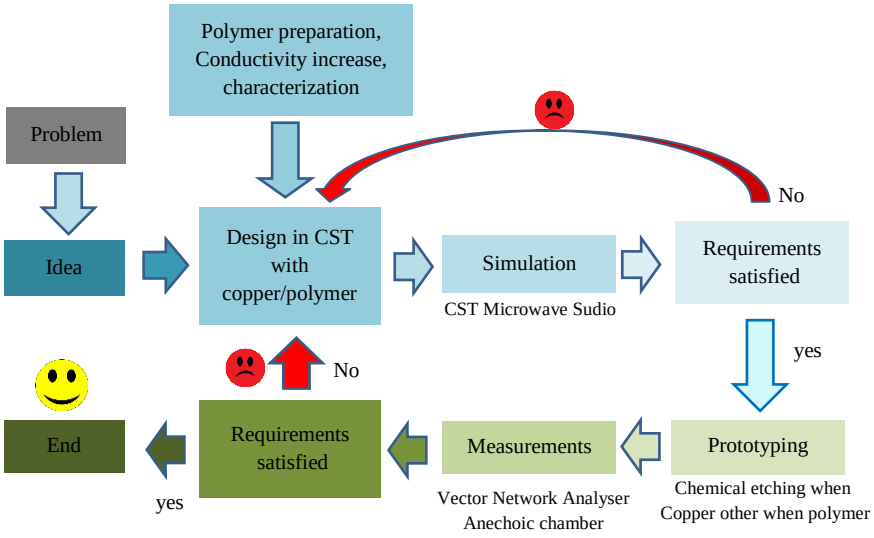

Figure 1. Flow diagram of the followed research road map to achieve the final objective.

6. Thesis Layout

The thesis is divided into four chapters:

- Chapter 1: contains some highlights on the state of the art of reconfigurable antennas. We review recent works that have been conducted on reconfigurable microstrip antennas using different reconfiguration mechanisms in planar structures. A particular attention is given to published literature on conductive polymer antennas and on the efforts being done in designing reconfigurable antennas based on conductive polymers.
- Chapter 2: a review on the electrical and mechanical properties of conductive polymers is presented as well as their behaviour in electromagnetics media. The preliminary simulation results of an antenna conception based on conductive polymers are discussed. The frequency reconfiguration through the use of tuning permittivity was also investigated.
- Chapter 3: include the design of a reconfigurable monopole ultra wideband antenna. The results thus obtained are discussed in the light of current literature.
- Chapter 4: discusses and presents the results of the second ultra-wideband antenna conception. We also report on the steps taken in implementing experimentally the antenna. We present the results on the antenna performances.

Bibliography

[1] N.O. Parchin, H.J. Basherlou, Y.I. Al-Yasir, R.A. Abd-Alhameed, A.M. Abdulkhaleq, J.M. Noras, “Recent Developments of Reconfigurable Antennas for Current and Future Wireless Communication Systems”, *Electronics 8*(2), p.128, 2019.

[2] S.J. Chen, "Flexible, Wearable and Reconfigurable Antennas based on Novel Conductive Materials: Graphene, Polymers and Textiles", PhD dissertation, Adelaide University Australia, 2017.

[3] R.L. Haupt, “Reconfigurable Patch with Switchable Conductive Edges”, *Microwave Opt. Technol. Lett.*, *51*(7), pp. 1757-1760, 2009.

[4] https://www.cst.com.

Chapter 1

State of the Art of Reconfigurable Antennas

RECONFIGURABLE antennas have been a dynamic field of research during the last two decades in which the motivation is to provide antennas with additional functionalities and better performance. We aim in this introductory chapter to give an overview on the state of the art of reconfigurable microstrip antenna based on both copper and conductive polymers. Radiation properties of a microstrip antenna are strongly linked to the geometry and substrate material of the antenna. The sizes of the radiating patch in one hand control the resonance frequency and in the other hand; the resonance frequency is inversely proportional to the relative permittivity and permeability of the substrate. Besides, the operating bandwidth is technically proportional to the substrate electrical height. This is the principle of reconfiguration which has been recently proposed in microstrip antennas and which will be reviewed in this chapter. The reconfiguration based on frequency, radiation pattern and polarization will be discussed.

1.1 Copper based Reconfigurable Microstrip Antennas

Reconfiguration of a microstrip antenna can be achieved through two methods. The first consists of modifying the dimensions of the radiating elements (patch/ground plane) and therefore metallic stubs or slots can be add to reduce or extend the dimensions of the current surfaces. While the second method lays on modifying the parameters of the dielectric substrate such as the high or the permittivity or permeability. In this case, tunable materials based on dielectric are used as substrates which can be controlled through an external effect like light, temperature, electric/magnetic field, etc…

1.1.1 Reconfiguration through Tunable Material substrates

1.1.1.1 Polarization Reconfigurability using Liquid Crystals Substrates

Liquid crystals are auspicious materials in microwave engineering since they have emerged as potential materials for applications in antenna technologies **[1-2]**. Liquid crystal (LC) materials have been used to construct a planar antenna with reconfigurable polarization **[3]**. As shown in **Fig 1.1**, the design proposed consists of 2×2 dual-fed microstrip patch array and two distinct feeding systems for each feeding of the dual-fed antenna. The design is capable of switching between dual circular and dual linear polarizations according to the variance phase shift between feedings networks of the antenna. The feeding systems are realized in inverted microstrip line topology with the liquid crystal material as a tunable substrate. When altering the liquid crystal, the differential phase shift is acquired between the feeding systems. Additionally, due to the continuous change of the LC material, the polarization can be switched between linear and circular polarizations. This antenna operates at 13.75 GHz which is in Ku and W frequency bands since LC materials decrease the dielectric losses which makes it suitable for applications at higher frequencies. Another microstrip patch antenna with reconfigurable polarisation was proposed in **[4]**. As demonstrated in **Fig 1.2**, a tuneable coupled line loaded with liquid crystal-based varactors is used to reconfigure the polarization of the antenna. Therefore, when a bias voltage is applied, the proposed antenna can be continuously reconfigured to give circular or linear polarization. The prototype is validated by simulation and measurements. Tuneable liquid crystals based dielectric substrate is investigated again for the development of frequency reconfigurable microstrip antenna as proposed in **[5].**

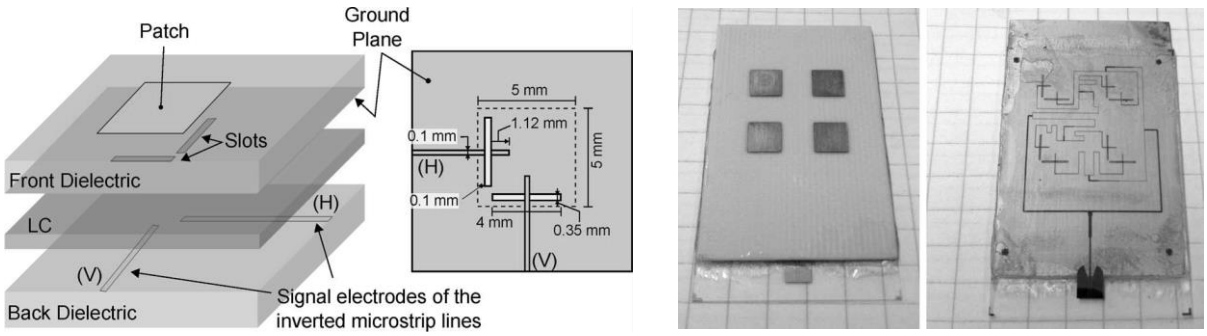

Figure 1.1. MSA array with reconfigurable polarization [3]. (a) schematics of the single radiating element and explode d perspective and (b) bottom view; (c, d) pictures of the fabricated antenna form the top (left) and bottom (right) views.

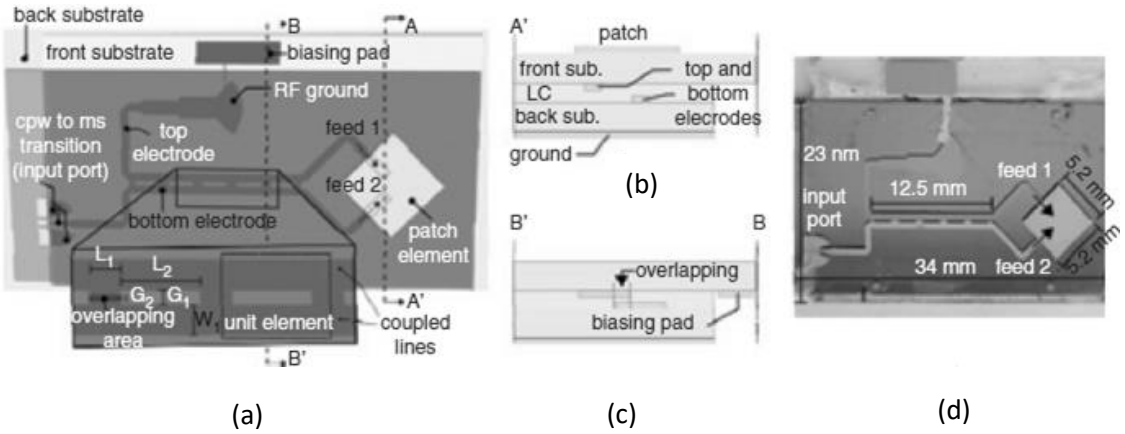

Figure 1.2. Single coupled feed MSA with reconfigurable polarization [4]. (a) top view; (b) and (c) cross section views; (d) photograph of the fabricated prototype (dimensions: G_1= 0.3 mm, G_2= 0.1 mm, L_1= 0.7 mm, L_2 =1.8 mm, W_1=0.6 mm).

The proposed design is illustrated in **Fig 1.3**. Reconfiguration is achieved by applying a low frequency AC bias voltage. The amplitude of the external applied electric field panels the tilt angle of the crystal liquid molecules which in turns work as directors that changes the constitutive properties of the LC dielectric material. Hence, various bias voltage values that varies between 0 and 10 Volts are applied continuously, helped to tune the antenna frequency range between 5.45 and 5.84 GHz.

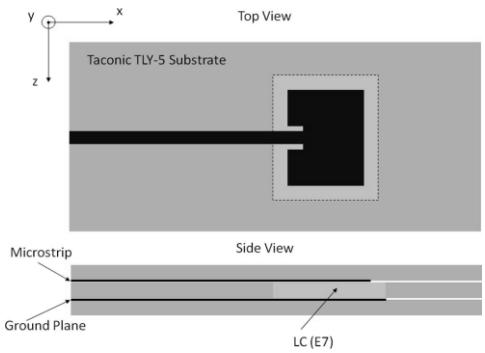

Figure 1.3. LC-based microstrip patch antenna [5].

1.1.1.2 Frequency Reconfiguration using Ferroelectric BST Substrates

Barium Strontium Titanate (BST) ceramic belongs to ferroelectric materials whose relative permittivity can be tuned by applying different voltages. Because of their high permittivity, BST materials have been utilized as substrates to achieve size reduction in different types of antenna such as dielectric resonator antennas. In recent years, BST has appealed for significant attention owing to its potential of low dielectric loss and high tunability **[6-7]**. It has been useful in several microwave devices, such as compact sized antennas **[8-9]**, phased array antennas **[10]**, and reconfigurable antennas based on BST varactors **[11-12]**. The structure shown in **Fig 1.4** is a frequency reconfigurable microstrip antenna with a wide instantaneous operation band based on BST/MgO composite films **[13]**. The objective of adding MgO to BST composite is to efficiently dilute the permittivity and keep a considerable dielectric tunability. The frequency reconfigurability is attained by changing the permittivity of BST film, and an extra Fabry-Perot resonant structure is adopted to increase the instantaneous operation band. As a result, a wide instantaneous band that is closely 26% superior is acquired in measurement, which means that the working band of this antenna can be tuned from 9.9–13.5 GHz to 10.9–14.2 GHz.

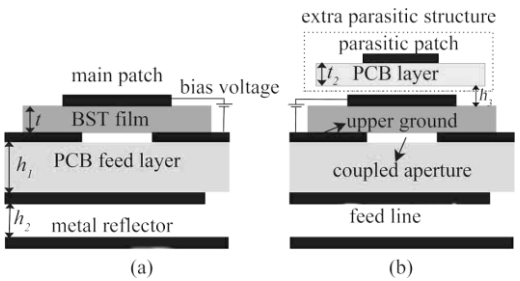

Figure 1.4. BST based frequency reconfigurable antenna [13]. (a) The original reconfigurable model and (b) the modified instantaneous wideband reconfigurable model.

This antenna is highly suitable for wireless communication systems due to its attractive feature of instantaneous frequency reconfigurable. The geometry shown in **Fig 1.5** shows another frequency reconfigurable microstrip antenna for which BST substrate material is adopted again **[14]**. The relative permittivity of BST material used in this design is approximately 100, and a thin BST film of 0.3 mm is used as the primary substrate. A tuneable bias voltage is applied between the metal patch and the ground plane to control the relative permittivity of BST material. As a consequence, the antenna frequency resonance is tuned of 10% from 13.3 to 14.7 GHz by changing the bias electric field from 0 to 10 V/µm. Nguyen et al. proposed a compact frequency reconfigurable planar antenna based on ferroelectric (BST) TiO_3 thin films **[15]**.

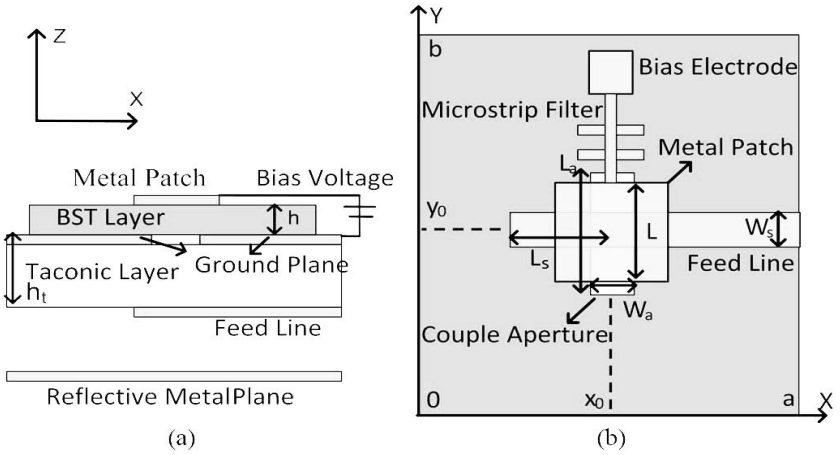

Figure 1.5 BST based frequency reconfigurable antennas [14]. (a) Side view; h=0.3 mm, the thickness of the Taconic Layer: h_t =1 mm; (b) the top view of the antenna: $W_a \times L_a$ rectangular aperture arranged on the $a \times b$ top surface of the PCB layer, and a $(L_s + a - x_0) \times W_s$ feed line arranged on the bottom side.

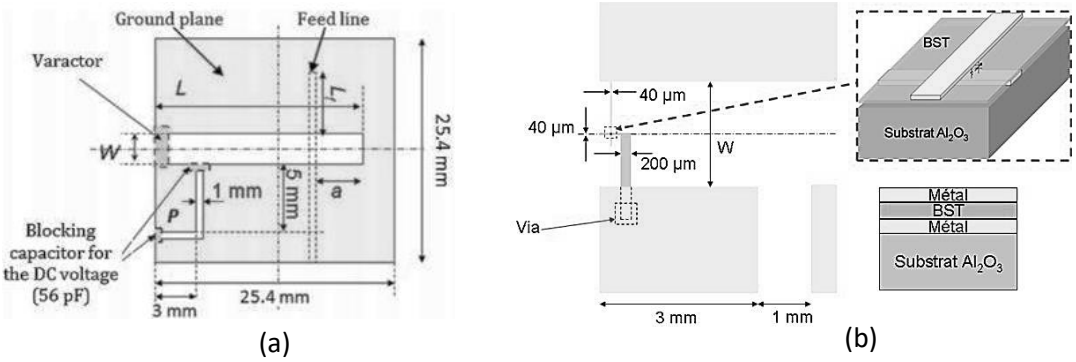

Figure 1.6. BST base frequency reconfigurable antennas [15]. (a) schematic of the notch antenna; (b) the varactor based on BST thin film.

As shown in **Fig 1.6** the notch antenna is loaded with a variable metal/insulator/metal (MIM) capacitor and is achieved by a monolithic method. The design delivers frequency tunability rate of 14.5% under an electric field of 375 kV/cm.

1.1.2 Reconfiguration through Conductor Modification using PIN Diodes

Altering the conductors shape and dimensions of planar/microstrip antenna (MSA) affect considerably the antenna radiation properties. This aspect is used as the basis to reconfigure the antenna operating frequency, bandwidth, pattern, and polarization. Basically, the modifications in the radiating patch or ground plane alter in fact the normal current distributions and contribute to other new current maps which change the antenna radiation properties. Therefore, if one can objectively control the current distribution it becomes possible to control the radiation properties of the antenna which becomes reconfigurable. There are different kinds of switches used to control current circulation in microstrip antennas, among which there are PIN diodes.

1.1.2.1. Frequency Reconfiguration using PIN Diode

The microstrip slot antenna proposed in **[16]** is capable to change its frequency between nine distinct narrow bands from 1.98 to 3.59 GHz. The configuration of the antenna is shown in **Fig 1. 7**. It is fabricated on a Taconic RF-35 dielectric substrate with a thickness of 3.04 mm having a permittivity of 3.5. It includes a rectangular patch and a slotted ground-plane beneath it. The design of the slot under the patch delivers extra operating bands to the antenna. Five PIN diodes are used to control the length of the slot which help to switch the operating frequency between nine different frequencies from 1.98 to 3.59 GHz. The antenna has a dimension of 50×50 mm^2. The frequency switchability of this antenna makes it suitable for cognitive radio applications. The antenna proposed in **[17]** is a monopole microstrip antenna with a slotted ground plane, shown in **Fig 1.8**. It consists of an inverted U-shape radiating patch fed by a microstrip line and a rectangular ground plane underneath. The radiating element offers a wide operating band between 2.63 and 3.7 GHz. Additionally, four horizontal slots were inserted in the ground plane to help the antenna to resonate at four different resonant narrow bands. To switch between the four narrow band frequencies, the slot's lengths are controlled using PIN diodes. The fabricated prototype has a size of 68×51 mm^2 and offers an omnidirectional radiation pattern. This antenna is suitable for cognitive radio applications.

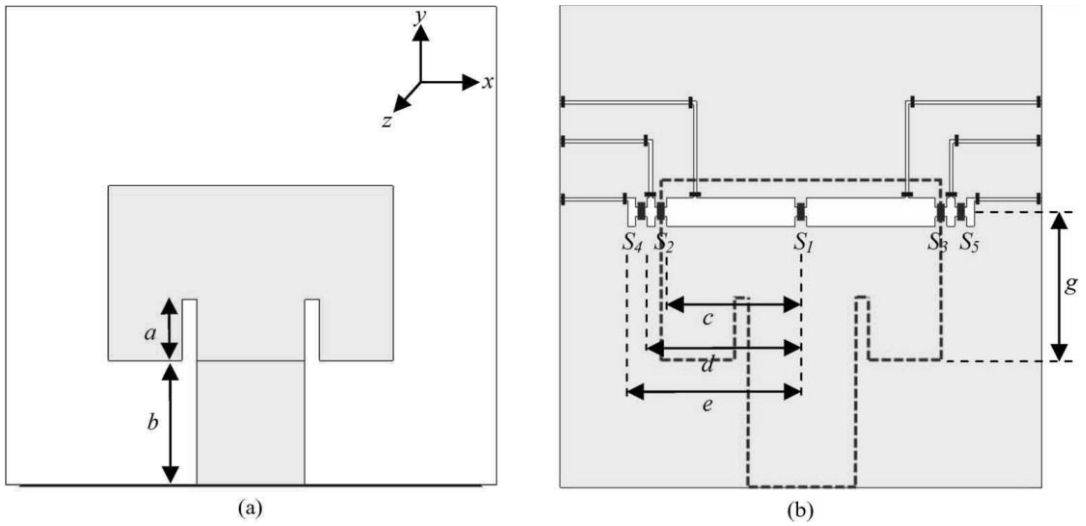

Figure 1.7. Frequency reconfigurable microstrip antenna [16]. (a) top view on patch; (b) the bottom view on the modified ground plane. Dimensions (mm) a= 6.4, b=13, c = 13.95, d= 16, e=18, g=15.38, S_1 to S_5 are PIN diodes.

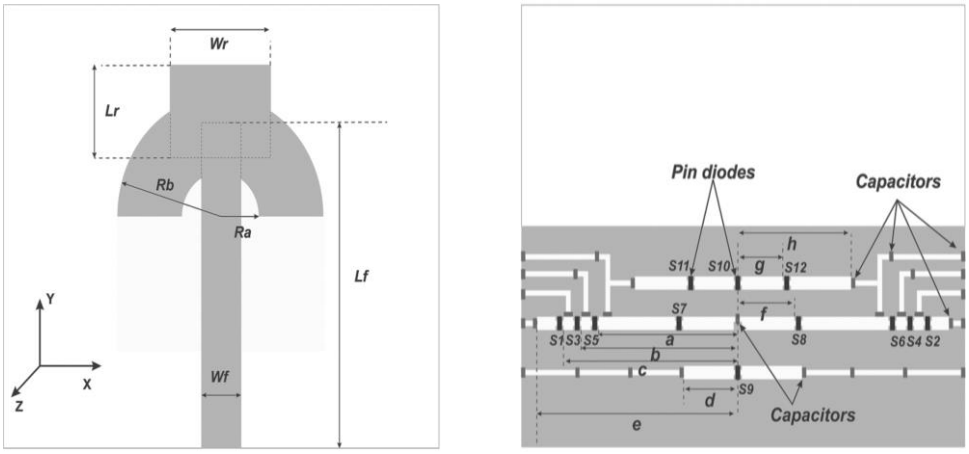

Figure 1.8. Selective frequency reconfigurable monopole planar antenna [17]. (a) top view on patch; (b) the bottom view on the modified ground plane. Dimensions (mm) a= 6.4, b=13, c = 13.95, d= 16, e=18, g=15.38, S_1 to S_5 are PIN diodes.

1.1.2.2. Radiation Patterns Reconfiguration using PIN Diode

A microstrip antenna was proposed in **[18]** to operate at the WiMAX frequency range 3.44 to 3.6 GHz with the capability to reconfigure its radiation pattern. As seen in **Fig. 1.9**, the antenna is designed on dielectric substrate with a permittivity of 3.5 and thickness of 3 mm. A circular

coaxially feed patch is on the upper side of the substrate with four quasi-rectangular radiation elements coupled to the patch using PIN diodes in symmetrical positions. The radiation pattern reconfiguration is achieved by switching the state of the four PIN diodes and thus, the antenna main beam can be switched between $\varphi = 0°$, $\varphi = 90°$, $\varphi = 180°$ or $\varphi = 270°$ while $\theta = 30°$. Four different radiation patterns state can be performed at WiMAX band. Besides, the proposed configuration has a small size and very acceptable realised gains which is more than 8 dBi. A similar reconfigurable radiation pattern microstrip antenna is proposed in **[19]**, shown in **Fig. 1.10**. Circular patches surrounded by four other parasitic circular patches are printed on the upper side of Taconic substrate of 2.2 permittivity and a thickness of 1.6 mm. The ground plane is printed on the lower side of the substrate which has a full size of 120×120 mm^2. The surrounding parasitic patches are shorted to the ground plane using four pins named S1, S2, S3 and S4. Four PIN diodes are used to connect the four shorting pins to each one of the parasitic patches. The parasitic patches work as director/reflectors which are controlled by the switching of the PIN diodes and as such, beam reconfiguration is achieved. Hence this antenna can switch its main radiation pattern into nine different directions: $(\varphi, \theta) = (0°, 0°)$, $(0°, 23°)$, $(45°, 22°)$, $(90°, 24°)$, $(135°, 22°)$, $(180°, 24°)$. Besides, the antenna yielded a gain greater than 7 dB for the nine possible pattern configurations.

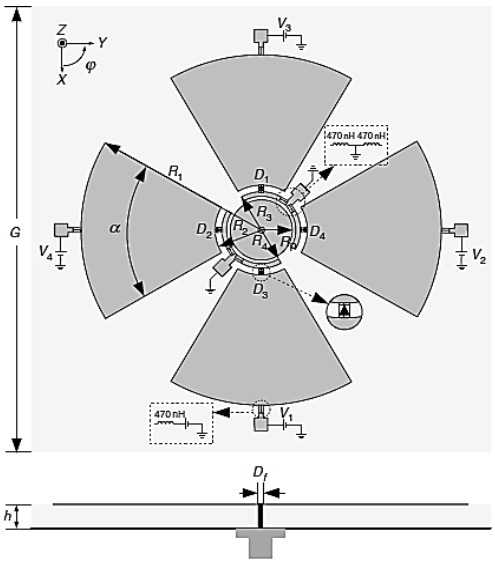

Figure 1.9. Radiation pattern reconfigurable Microstrip antenna [18]. (a) top view on patch; (b) the bottom view on the modified ground plane. Dimensions (mm): a = 60°, *G* = 6.4, *h*= 3, D_f = 1.2, R_p = 5, R_1 = 27.5, R_2 = 7, R_3 = 6, R_4 = 5.3.

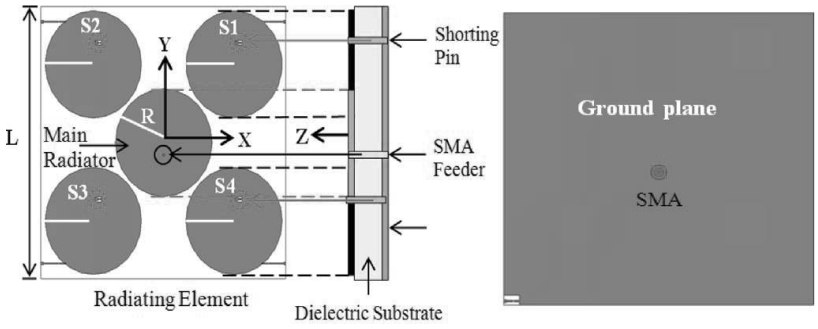

Figure 1.10. Multi-beam radiation pattern reconfigurable microstrip antenna [19]. (a) top view; (b) side view; (c) back view. Dimensions (mm): L=120, *R*= 23.7.

1.1.2.3. Polarization Reconfiguration using PIN Diodes

Polarization diversity can help to avoid fading losses caused by multipath effects. Therefore, there has been an increasing interest in implementing antennas with reconfigurable polarization. The design shown in **Fig. 1.11** illustrates the structure of a microstrip antenna which is capable to alter its polarization between three types: linear, left-hand and right-hand circular polarizations **[20]**. The structure consists of circular patch printed on the top of Taconic substrate having the permittivity of 3.52 and a thickness of 1.52 mm. Two pairs of L-shape slits are created symmetrically along *x* and *y* axis on the patch edges. In order to activate and deactivate the electrical length of the slits, four different PIN diodes are placed at the open end of each slit. This approach helped to obtain reconfigurable polarization at the WLAN frequency band 2.4 to 2.48 GHz.

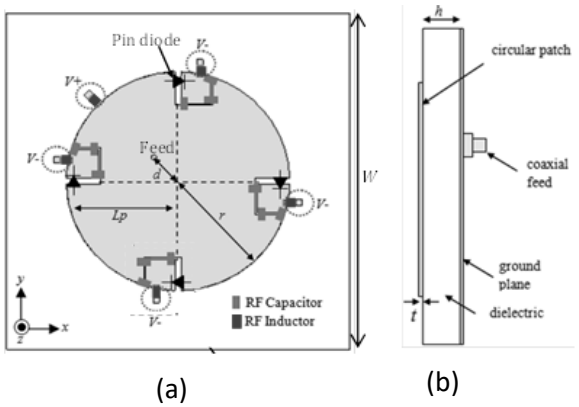

Figure 1.11. Reconfigurable polarization microstrip circular patch antenna [20]. (a) top view; (b) side view. Dimensions (mm): *d*= 5.5, *h*= 1.524, L_p= 15.3, r= 17.9, *t*= 0.035, W=55.

A microstrip ring antenna with reconfigurable circular polarisation has been proposed [21]. Its geometry is shown in Fig. 1.12. It comprises a FR-4 substrate with dielectric constant of 4.2 and a thickness of 1.57 mm with an overall size of 70×70 mm^2. Square ring patches with a T-shaped microstrip feed are printed on the top face of the substrate. A square loop is created at the centre of the ground plane on the lower face of the substrate. The antenna is fed by a gap-coupled through inductors across a distance *g*. Two gaps *gap1* and *gap2* are inserted in the patch and across which two PIN diodes are inserted to electrically connect/disconnect the two parts of the square ring. The reconfiguration of the polarization is achieved by controlling the switching states of the two PIN didoes at the frequency of 3.45 GHz. When diode 1 is *ON* and diode 2 is *OFF*, the antenna resonates with a right-hand circular polarization. When diode 1 is *OFF* and diode 2 is *ON*, the antenna resonates with a left-hand circular polarization. The obtained antenna gain was greater than 3 dBi.

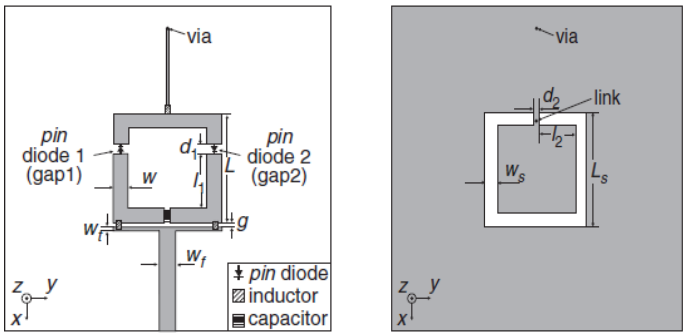

Figure 1.12. Reconfigurable polarization square ring circular microstrip antenna [21]. (a) top view; (b) side view. Dimensions (mm): d_2= 1, d_2= 1, g=0.3, h= 1.6, L= 55, l_1=10, l_2=7.5, W = 55, t= 0.035, W=8.2, W_f= 3, W_t= 0.8, W_s=2.5.

1.1.2.4. Frequency/radiation pattern reconfigurable antennas

The slot microstrip antennas of [22] offers a reconfiguration capability in two ways: frequency and radiation pattern. As shown in Fig. 1.13, the antenna is designed on Taconic FR35 substrate with the permittivity of 3.5 and a thickness of 1.52 mm. The rectangular patch is on the top of the substrate while the slot ground plane is on the back. The slot in the ground plane generates a bidirectional radiation pattern, therefore, a metallic sheet is placed behind the antenna in order to produce a directional radiation pattern. Frequency reconfiguration is achieved by controlling the electrical length of the slot using two PIN diodes denoted S1 and S2. Thus, the

antenna is capable to work at three distinct frequencies 1.82, 1.93 and 2.10 GHz. Radiation pattern reconfigurability is ensured through the introduction of four slits near to the corners of the ground plane. The control of the slits' length helped to alter the angle of the main radiation beam of the antenna and as such, it became capable to tune the beam angle between 0°, +15° and −15° at each one of the operating frequency bands.

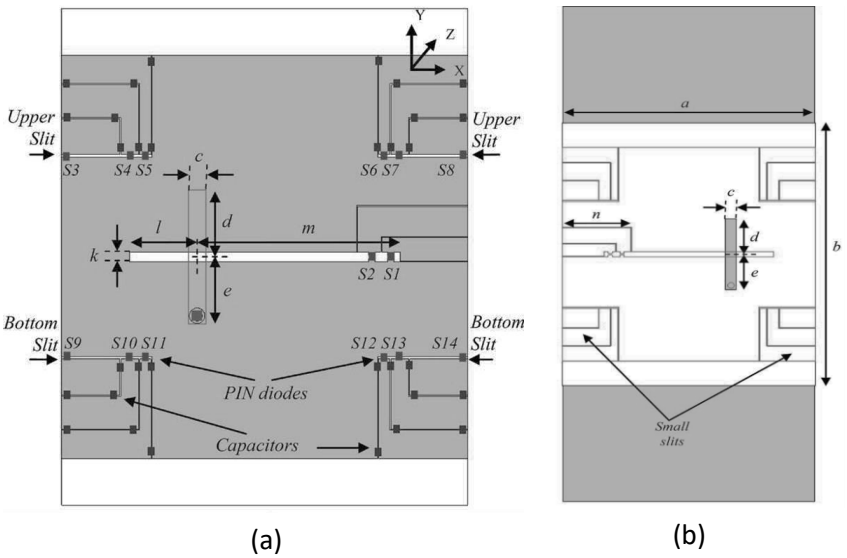

Figure 1.13. Frequency and radiation pattern reconfigurable MPA [22]. (a) Top view; (b) side view. Dimensions (mm): *a*= 130, *b*= 160, *c*= 33, *d*=21.75, *e*= 21.75, *n*=29, *m*=65.25, *l*=21.75, *k*=3.2.

The antenna proposed in **[23]** is a microstrip antenna, shown in **Fig. 1.14**, featuring reconfigurability in frequency and in radiation pattern. It consists of small patch which is surrounded by a square ring called internal ring and in between are two PIN diodes D3, D4 to ensure switchable contacts. Both metallic parts are surrounded by another square ring named external ring. Again, two PIN diodes D1 and D2 connect the internal and external rings together. According to the switching states of the PIN diodes, the antenna is capable to operate in three distinct modes, with resonance frequencies: 2.84, 3.84 and 3.85 GHz. Meanwhile, radiation pattern changes in accordance with the diodes switching states.

- In mode 1, the antenna produces 3 dB beam width from −30° to 25° with 7.4 dBi of gain.
- In mode 2, it provides 3 dB beam width from −80° to −15° with 5.7 dBi of gain.
- In mode three, it produces 3 dB beam from 5° to 60° with the maximal gain of 5.7 dBi.

These results were checked through both numerical simulations and performance measurements of an experimental prototype.

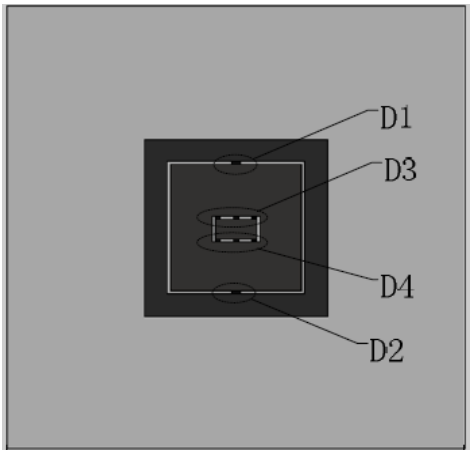

Figure 1.14. Frequency and radiation reconfigurable antenna MPA [23]. Dimensions (mm): a= 4.6, *b* = 7, c= 28.5, *d*=40, *L*= 100.

1.1.2.5. Frequency/Polarization Reconfigurable Antennas using PIN Diode Switches

In some antenna designs, the objective was to combine reconfigurable frequency with reconfigurable polarization in a single microstrip antenna structure. The proximity coupled fed configuration proposed in **[24]** consists mainly of a rectangular patch printed on Neltec N9000 substrate with a permittivity 2.2 and a thickness 0.762 mm, shown in **Fig. 1.15**. In order to implement the frequency reconfiguration feature, an additional small patch is positioned next to the central patch and connected to each other through a PIN diode. Frequency reconfiguration is established in the following way:

- When the diode is switched *OFF*, the antenna frequency resonance is due to only the central patch which resonates at the first band 5.7 GHz.
- When the diode is switched *ON*, the antenna resonance is due to both central and small patches and thus another resonant band at 5.2 GHz is produced.

To get polarization reconfigurability at either of two operational bands, each corner is cut off from the main and additional patches are inserted through a narrow L-shaped cut to generate polarization reconfigurability. A couple of PIN diodes named D1, D2, D3, D4, D5, D6 and D7 are employed to control the polarization of the antenna. Hence, to produce a circular polarization at 5.2 GHz, the pair of small parasitic patches placed diagonally is coupled to the main patch by

switching *ON* the two corresponding diodes and therefore, by changing the diagonal pair of small patches the polarization can be altered between left-hand circular polarization and right hand-circular polarization. Furthermore, the antenna is capable to offer circular polarization at the higher band 5.7 GHz when the additional patch is connected to the main patch and two small parasitic patches at the diagonal ends are disconnected from the circuit. This disconnection serves to generate two orthogonal components of currents which yields a circular polarization at 5.7 GHz.

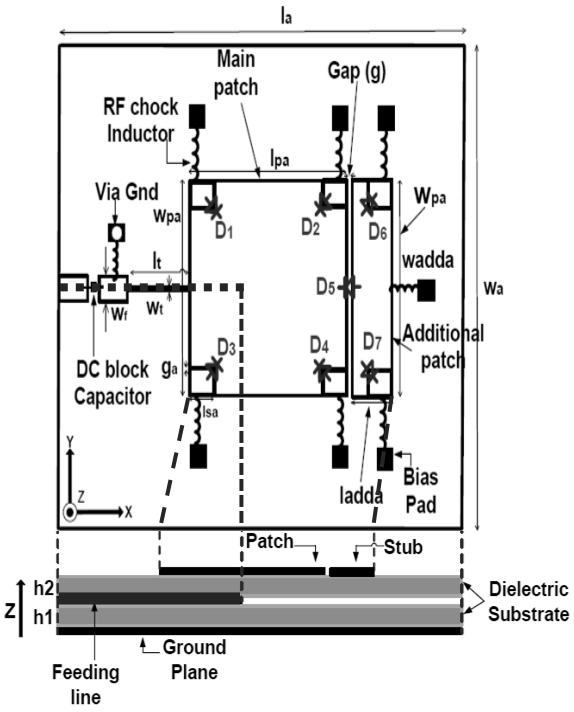

Figure 1.15. Frequency and polarization reconfigurable proximity Coupled fed MPA [24]. Top and side views. Dimensions (mm): g = 0.3, g_b = 0.3, l_b = 65, lp_b = 17.8, $Ladd_b$ = 4, l_f =28, W_b =60, $Wadd_b$ =18.15, Wp_b = 18.15, W_f= 2.4, W_t= 0.58, ls_b =2.2, l_t = 11.9.

Another example of frequency and polarization reconfigurabilities in microstrip antennas has been proposed recently **[25]**. The diagram is shown in **Fig. 1.16**. The antenna is realized on Rogers 5880 substrate of permittivity 2.2 and a thickness of 3.175 mm. The structure is composed of a square patch, three groups of switchable shorting pins (group 1, group 2, group 3) connected to the ground plane, and four controllable perturbation pads coupled to the corner of the patch through PIN diodes D1, D2, D3 and D4. The antenna is fed by a coaxial probe through a microstrip line. Polarization reconfigurability is achieved by controlling the switching state of

the four PIN diodes. When the two diodes in the opposite direction (D1 & D2 or D3 & D4) are switched *ON*, the two orthogonal modes will be split in resonant frequency with equal amplitude and 90° phase difference which can yield a circular polarization. When all the four PIN diodes are turned *ON*, linear polarization can be generated from the symmetrical structure of the antenna. Hence, by governing the states of the diodes *D1-D4*, the polarization of the antenna can alter the polarization between left-hand, right-hand and linear. The antenna operating frequency can be switched between eight distinct narrow bands by properly shorting the patch to the ground plane via the three groups of the shorting pins which are controlled by the PIN diodes.

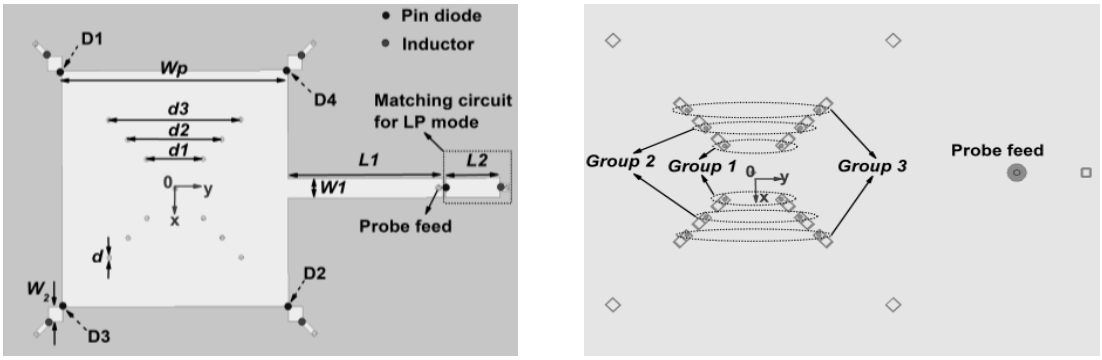

Figure 1.16. Frequency and polarization reconfigurable MPA [25]. (a) top view; (b) bottom view. Dimensions (mm): *d* = 1, *d1* = 12, *d2* = 20, *d3* = 28, *W1* = 4, *W2* = 3, *Wp* = 48, *L1* =33, *L2* = 12.

1.1.2.6. Pattern/Polarization Reconfigurable Antennas using PIN Diode Switches

The compact microstrip antenna proposed in **[24]** offers reconfigurability of both radiation pattern and polarization. The antenna, shown in **Fig 1.16**, comprises two truncated monopoles arranged orthogonally and connected to the microstrip lines via ideal switches named S1 and S2. It is intended for applications in 2.4 GHz IEEE 802.11 WLAN and Bluetooth bands. Radiation pattern and polarization reconfiguration can be conducted through the tow switches S1 and S2. At state 1, when S1 is switched *ON* and S2 is *OFF*, the vertical monopole is excited (parallel to the *y* axis). Hence, the antenna radiation is maximally on *xz*-plane and null along positive and negative *y* axis. At state 2, S1 is switched *OFF* and S2 is *ON*, the horizontal monopole is exited (parallel to *x* axis). In this case, the maximum radiation is along *yz*-plane and null along the positive and negative *x* axis. Meanwhile, polarization also can be reconfigured into horizontal or

vertical since, in state 1, the antenna provides linear polarization on the *y* axis, whereas in state 2, it provides also linear polarization but on the *x* axis.

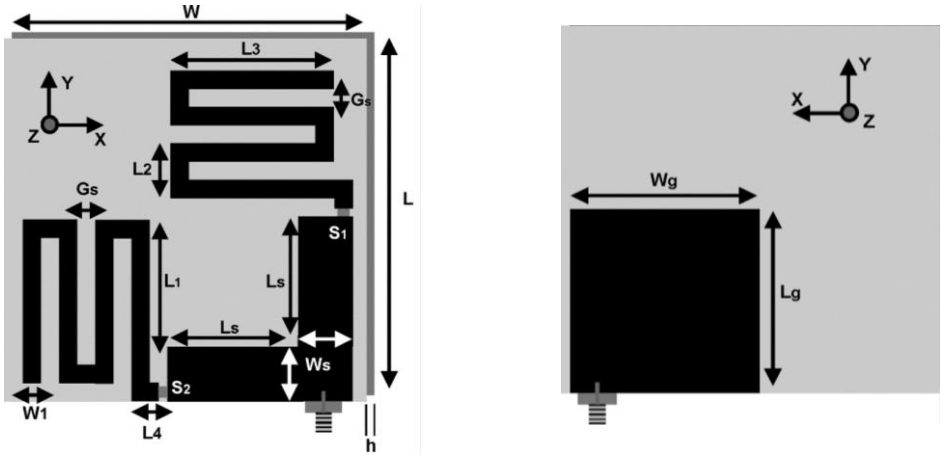

Figure 1.17. Pattern and polarization reconfigurable MSA [24]. (a) top; (b) back view. Dimensions (mm): Wg = 10, Lg = 10, Ls = 6.75, L = 19, W = 19, Ws = 3, Gs = 1.2, W1 = 0.8, L1 = 8, L2 = 3, L3 = 9, L4 = 2, h = 1.6.

A circular microstrip patch antenna with reconfigurable pattern and polarization was proposed **[25]**. As shown in **Fig. 1.18**, the antenna includes a circular patch whose structure is changeable trough PIN diode switches used to control radiation patterns and polarization. The antenna is fed by two coaxial ports carefully positioned orthogonally to maintain simultaneous radiation patterns and high isolation between the ports. Fourteen PIN diodes (switches D1), located radially on the antenna, are forwardly biased and used to dynamically change the radius of the circular patch and thus, alterations in the shape of the radiation pattern are attained by exciting different electromagnetic modes in the antenna structure. Four PIN diodes (switches D2) are reversely biased and connect or disconnect two perturbation segments to the inner circular patch. Therefore, the antenna can offer three different types of polarization:

- When both switches D1 and D2 are switched *OFF*, the antenna offers an elliptical polarization.
- When the switches D1 are switched *OFF* and the switches D2 are switched *ON*, the antenna offers a linear polarization with the mode TM_{21}.

- When the switches D1 are switched *ON* and the switches D2 are switched *OFF*, the antenna offers a linear polarization with the mode TM_{31}.

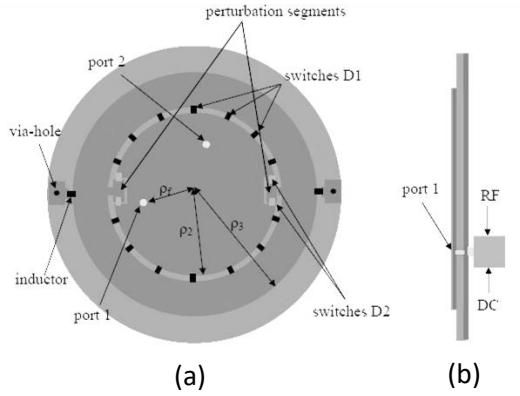

Figure 1.18. Pattern and polarization reconfigurable MSA [25]. Top and side views. Dimensions (mm): a= 130, *b* =160, c= 33, d=21.75, e=21.75, n=29, m=65.25, l=21.75, k=3.2.

1.1.2.7. Frequency/Pattern/Polarization Reconfigurable MSA using PIN Diodes Switches

The main challenge in today's antenna designs is to come up with a single microstrip antenna structure that is capable to produce reconfigurability in the three radiation properties all together.

Still, a modified structure of microstrip antenna which is capable of independently reconfigure the operating frequency, the radiation pattern and the polarization has been proposed **[26]**. The configuration, shown in **Fig. 1.19**, comprises two layers of Rogers RO4003 substrates. The first layer supports the driver element, which is a square patch which is fed coaxially. The second layer carries a parasitic metallic surface subdivided into pixels with their biasing control circuits. The parasitic pixels are interconnected by PIN diodes.

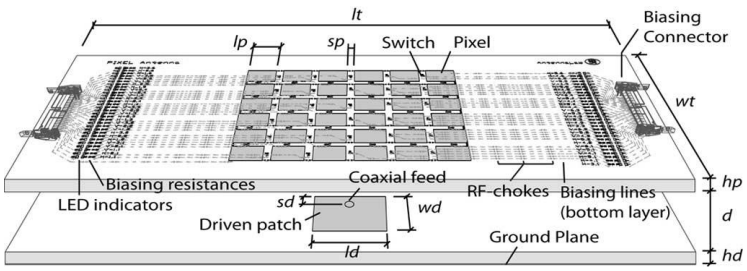

Figure 1.19. 3D view of the design of a microstrip antenna with reconfigurability of frequency, radiation pattern and polarization [26]. Dimensions (mm): lp= 12, sp=3, hp= 1.5, ld=wd=31, hd=3, lt=240, wt=120, d=variable.

The activation of a specific switch configuration of pixels generates the suitable geometry over the metallic surface to deliver the required reconfigurable antenna properties. The antenna simultaneously reconfigures its operation frequency over a 25% frequency range, steers the radiation pattern beam over E and H planes, and switches between four different polarizations

1.2 Conductive Polymers based Microstrip Antennas

A variety of antennas based on different types of conductive polymers have been reported in the literature, from optically transparent to opaque, rigid to flexible, and narrow-band to UWB. In this context, it is worth mentioning the very first antenna designs based on conductive polymers.

The earliest reported transparent polymeric antennas were presented by National Aeronautics and Space Agency (NASA) in 1997 **[27]**, namely including two antennas working at 2.3 and 19.5 GHz based on a transparent conductive dioxide polymer AgHT-8. This work has showed the feasibility of transparent and conformal antennas design based on polymeric materials, despite the fact that the antennas were not flexible.

A four-element crossed dipole direction-finding antenna assembly based on a fabric realized in S2 glass fibres with Polypyrrole (PPy) coating layer was reported in 1999 **[28]**. This design used PPy rather than metal to reduce the antenna radar cross section (RCS) to gain corrosion resistance and to exploit adjustable electromagnetic properties, by smartly taking advantage of the relative low conductivity (from 10 to 100 S/m) in the PPy coating. Avoiding metals in the design is due to two reasons.

- Firstly, metals are heavy and have a very high metallic conductivity leading to a large RCS due to the strong incident wave reflection;
- Secondly, low antenna efficiency is acceptable or can be compensated.

However, this concerned a very special application, and more generally highly conductive conductors are naturally a common requirement for the majority of antenna design, so as to achieve high antenna efficiency. Because of the relatively low conductivity and the process-limited thickness, antennas based on conductive polymers usually have low efficiencies. For instance, Cichos et al. **[29]** represented a performance study of polymer-based RFID antennas working at 13.56 MHz for a short communication range. The experimental results from this study demonstrated that antennas realized with conductive polymer pastes achieved approximately only half of the real range of its corresponding copper antenna. This can be straightforwardly

attributed to the higher ohmic losses, and it was also demonstrated that the read range can be improved by increasing the paste thickness and by using lamination.

Two dipole antennas based on PEDOT:PSS for RFID applications were proposed by Kirsch et al. **[30]**, shown in **Fig. 1.20**. These were realized on polyethylene terephthalate (PET) substrate using modified PEDOT:PSS ink patterned with screen printing and inkjet printing technologies. The antennas exhibited a light weight and an excellent mechanical flexibility, but a lower gain (2 to 6 dB lower) than the copper ones, due to the very limited achievable printed polymer thickness and the low film quality.

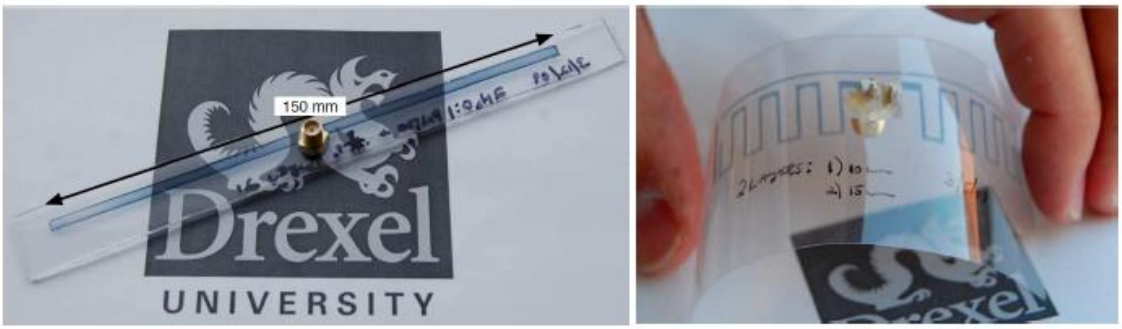

Figure 1.20. Two mechanically Flexible Antennas realized in PEDOT:PSS [30].

The same authors have also conducted a performance study of similar polymeric dipole antenna in multiple-input multiple-output (MIMO) systems. They concluded that the antenna yields approximately half of that of copper due to the relatively low conductivity **[31-32]**.

Verma et al. **[32]** and Kaufman et al. **[33]** investigated the effect of film thickness, respectively, on the radiation efficiency of 4.5 GHz PPy patch antenna and for an UWB antenna. They confirmed that sufficient film thickness is crucial for antenna efficiency. The efficiency of antenna based on lossy conductors like conductive polymer can be strongly dependent on the antenna radiation characteristics. For example, a resonant antenna such as slot antenna will have a lower antenna efficiency compared to a non-resonant antenna such as a leaky-wave antenna, since the resonance process will typically build up a higher current density and thus cause higher ohmic losses in the conductor. Especially when the conductor has a thickness well below a skin depth and a relatively low conductivity, the discrepancy between antenna types can be significant. As an example, an UWB antenna realized using a PPy film was reported by Kaufmann et al. yielding an antenna efficiency of nearly 80% **[34]**. The UWB antenna, shown in

Fig. 1.21(a), is of a three-layer structure in which a layer of Rogers Ultralam 2000 dielectric substrate is sandwiched between two patterned layers of 158 µm thick PPy. In contrast, a proximity patch antenna, shown in **Fig. 1.21 (b)**, made from sufficiently thick and conductive PANI films only had an efficient thickness of 56% **[35]**. A patch antenna made of a composite material based on polyaniline (PANI) and carbon nanotubes (MWCNTs) has been proposed **[36]**. This was designed to operate at the frequency of 4.5 GHz and is shown in **Fig. 1.21(c)**. A square ring circularly polarised microstrip antenna, shown in **Fig. 1.21(d)**, constituted of $SrTiO_3$/Polyolefin elastomer (POE) composite as a substrate material and Polypyrrole has been proposed gave a radiation efficiency around 62-65 % **[37]**. A compact, highly efficient and flexible ultra-wideband antenna operating from 3 to 20 GHz was also proposed **[38]**, shown in **Fig. 1.21(e)** giving a radiation efficiency of 85%.

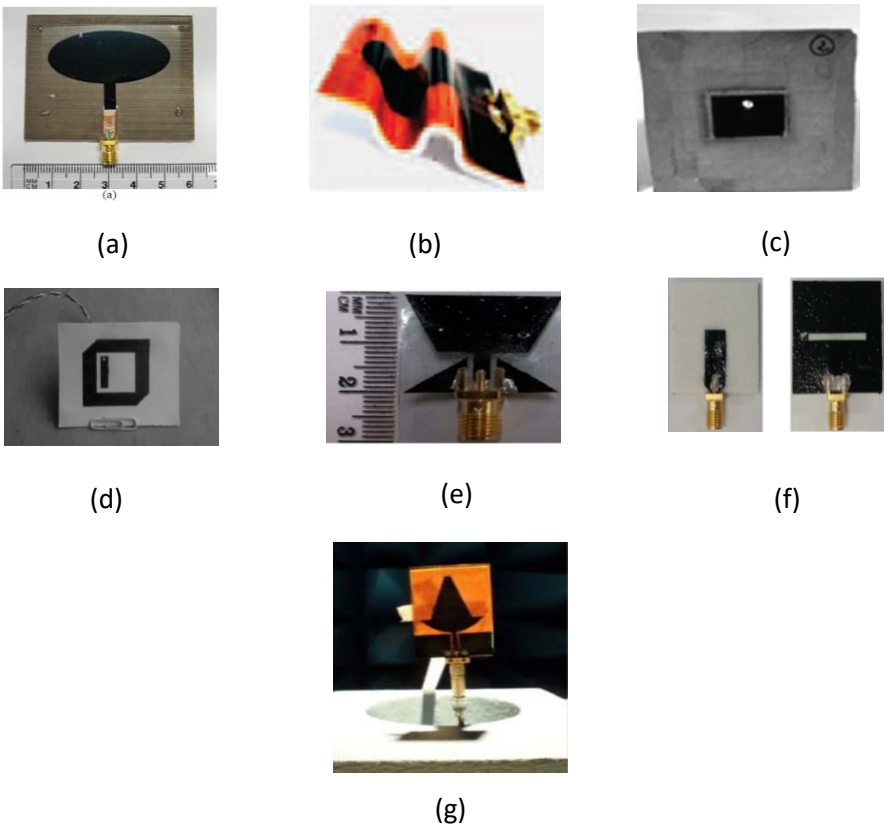

(a) (b) (c)

(d) (e) (f)

(g)

Figure 1.21. Recent published antennas based on conductive polymers.

The polymer PEDOT:PSS having a high electrical conductivity was used to fabricate a flexible antenna for 5.8 GHz applications, shown in **Fig. 1.21(f)**. It has achieved a radiation efficiency of about 82% **[39]**. A wideband flexible antenna made by covering a Kapton substrate

with a flexible magneto-dielectric polymer-based nanocomposite layer has also been proposed **[40]**, depicted in **Fig. 1.21(g)**. **Table 1.1** summarizes the state of the art for antennas based on conductive polymers found in the literature.

Table 1.1. Physical properties of some conductive polymers.

Materials	σ (S/m)	D (µm)	R_s (Ω/square)	Efficiency (%)	Flexibility	Year
PANI/CCo	7500	75	-	82 to 91	Excellent	2018
PEDOT:PSS	18000	110	0.5	82	Excellent	2016
PEDOT:PSS	9532	70	-	85 to 90	Excellent	2016
PPy	2000	90	-	62 to 65	None	2015
PANI/CNT	4500	75	2.9	-	Excellent	2015
PEDOT:PSS	2720	158	2.3	79.2	None	2012
PPy	2000	140	3.6	64.8	None	2010
PEDOT:PSS	10000	7	14.3	33.6	None	2010
PEDOT:PSS	500000	-	-	56	Excellent	2009
PANI	6000	100	1.6	56	None	2006

1.3 Conductive Polymers based Reconfigurable Microstrip Antennas

One potentially application of conductive polymers in antenna design is for reconfigurable devices in which the polymer adjustable conductivity can be used. A suggested configuration uses a patch antenna with two strips loaded on the patch edges **[41]**, as shown in **Fig. 1.22**. These two strips were made from conductive polymers with tuneable conductivity leading to the fact that the patch resonant frequency can be reconfigured by electrically tuning *ON* or *OFF* these stripes. However, this design was only experimentally verified by physically removing the two edges, raising doubts on the feasibility of practical realization.

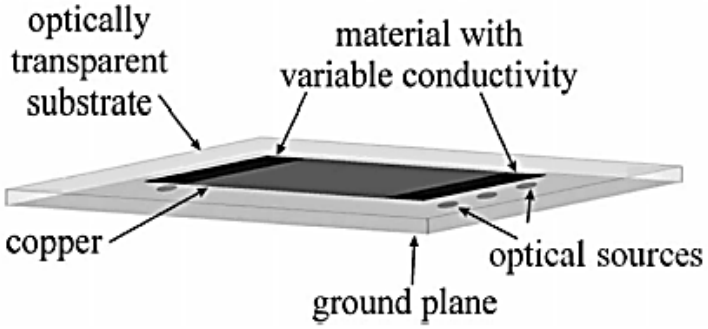

Figure 1.22. A reconfigurable planar antenna with two patch edges in conductivity-adjustable materials [41].

Recently, a new method in designing reconfigurable antennas based on conductive polymers has been proposed **[42]**, shown in **Fig. 1.23**. This includes an ion exchange material and at least one polymer member coupled to a communication circuit. The polymer member is configured to respond to receiving a bias voltage, interact with the ion exchange material to change its electrical conductivity. By varying the bias voltage, one or more polymer members of an electrically reconfigurable antenna can be activated (become conductive) or deactivated (become non-conductive). Varying the conductivity of one or more polymer members can be used to change an operating frequency of the electrically reconfigurable antenna.

1.4 Conclusion

In this chapter, we presented a review on state of the art of reconfigurable microstrip antenna based on copper and conductive polymers. Two main reconfiguration mechanisms have been discussed when implementing microstrip antennas with reconfigurable radiation properties. Altering the dielectric constant and the conductor dimensions were the keys to achieve reconfiguration in microstrip antennas.

Bibliography

[1] F. Yang and J.R. Sambles, “Determination of the permittivity of nematic liquid crystals in the microwave region”, *Liquid Crystals*, 30(5), pp. 599–602, 2003.

[2] F. Goelden, A. Gaebler, M. Goebel, A. Manabe, S. Mueller, and R. Jakoby, “Tunable liquid crystal phase shifter for microwave frequencies”, *Electron. Lett.*, 45(13), pp. 686–687, 2009.

[3] O.H. Karabey, S. Bildik, S. Bausch, S. Strunck, A. Gaebler, and R. Jakoby, “Continuously Polarization Agile Antenna by Using Liquid Crystal-Based Tunable Variable Delay Lines”, *IEEE Trans. Ant. Prop.* 61(1), pp. 70–76, 2013.

[4] O.H. Karabey, S. Bildik, S. Strunck, A. Gaebler, and R. Jakoby, “Continuously polarisation reconfigurable antenna element by using liquid crystal based tunable coupled line”, *Electron. Lett.*, 48(3), pp. 141–143, Feb. 2012.

[5] A.C. Polycarpou, M.A. Christou, and N.C. Papanicolaou, “Tunable Patch Antenna Printed

on a Biased Nematic Liquid Crystal Cell", *IEEE Trans. Ant. Prop.*, 62(10), pp. 4980–4987, 2014.

[6] G. Houzet *et al.*, "Dielectric dispersion of $BaSrTiO_3$ thin film from centimeter to submillimeter wavelengths", *J. Appl. Phys.*, 109(1), p. 014116, 2011.

[7] E. Mikheev, A.P. Kajdos, A.J. Hauser, and S. Stemmer, "Electric field-tunable $Ba_xSr_{1-x}TiO_3$ films with high figures of merit grown by molecular beam epitaxy", *Appl. Phys. Lett.*, 101(25), p. 252906, 2012.

[8] A.A.H. Azremi, N.A. Saidatul, P.J. Soh, M.A. Idris, and N. Mahmed, "A cylindrical barium strontium titanate (BST) dielectric resonator antenna for 5.0 GHz wireless LAN application", in *2008 Asia-Pacific Symp. Electromag. Comp. and 19th Int. Zurich Symp. Electromag. Comp.*, 2008, pp. 327–330.

[9] V.K. Palukuru, K. Sonoda, J. Hagberg, and H. Jantunen, "BST-Polymer Composite-Based Planar Inverted-F (PIFA) Chip Antenna for 2.4 GHz Wrist Applications", *Integrated Ferroelectrics*, 114(1), pp. 17–24, Nov. 2010.

[10] M. Sazegar et al., "Low-Cost Phased-Array Antenna Using Compact Tunable Phase Shifters Based on Ferroelectric Ceramics", *IEEE Trans. Microw. Theo. Techn.*, 59(5), pp. 1265–1273, 2011.

[11] N. Ni and A. H. Cardona, "Tunable 3.5 GHz and 1.5 GHz chip antennas based on thin-film $BaSrTiO_3$ capacitors", in 2011 *IEEE Radio and Wireless Symposium*, 2011, pp. 58–61.

[12] H. Jiang *et al.*, "Miniaturized and Reconfigurable CPW Square-Ring Slot Antenna Loaded with Ferroelectric BST Thin Film Varactors", *IEEE Trans. Ant. Prop.*, 60(7), pp. 3111–3119, 2012.

[13] Y. Wang *et al.*, "Design of an Instantaneous-Wideband Frequency Reconfigurable Microstrip Antenna Based on $(Ba,Sr)TiO_3MgO$ Composite Thin Films", *IEEE Trans. Ant. Prop.*, 62(12), pp. 6472–6475, 2014.

[14] Y. Wang *et al.*, "A Frequency Reconfigurable Microstrip Antenna Based on $(Ba, Sr)TiO_3$ Substrate", *IEEE Trans. Ant. Prop.*, 63(2), pp. 770–775, 2015.

[15] H.V. Nguyen *et al.*, "Miniaturized and reconfigurable notch antenna based on a BST ferroelectric thin film", *Mater. Res. Bull.*, 67, pp. 255–260, 2015.

[16] H.A. Majid, M.K.A. Rahim, M.R. Hamid, N.A. Murad, and M.F. Ismail, "Frequency-Reconfigurable Microstrip Patch-Slot Antenna", *IEEE Ant. Wireless Prop. Lett.*, 12, pp. 218–220, 2013.

[17] A. Mansoul, F. Ghanem, M.R. Hamid, and M. Trabelsi, "A Selective Frequency-Reconfigurable Antenna for Cognitive Radio Applications", *IEEE Ant. Wireless Prop. Lett.*, 13, pp. 515–518, 2014.

[18] S.-J. Shi and W.-P. Ding, "Radiation pattern reconfigurable microstrip antenna for WiMAX application", *Electron. Lett.*, 51(9), pp. 662–664, 2015.

[19] M. Jusoh, T. Aboufoul, T. Sabapathy, A. Alomainy, and M.R. Kamarudin, "Pattern-Reconfigurable Microstrip Patch Antenna With Multidirectional Beam for WiMAX Application", *IEEE Ant. Wireless Prop. Lett.*, 13, pp. 860–863, 2014.

[20] M.F.M. Yusoff, M.K.A. Rahim, H.A. Majid, M.R. Hamid, P. Gardner, and M.N. Osman, "An Electronically Reconfigurable Patch Antenna Design for Polarization Diversity with Fixed Resonant Frequency", *Radioengineering* 24(1), pp. 45-53, 2015.

[21] D. Seo and Y. Sung, "Reconfigurable square ring antenna for switchable circular polarisation", *Electron. Lett.*, 51(6), pp. 438–440, 2015.

[22] H.A. Majid, M.K.A. Rahim, M.R. Hamid, and M.F. Ismail, "Frequency and Pattern Reconfigurable Slot Antenna", *IEEE Trans. Ant. Prop.*, 62(10), pp. 5339–5343, 2014.

[23] W. Li, Z. Ren, X. Shi, and Y. Hei, "A frequency and pattern reconfigurable microstrip antenna using PIN diodes", in *2014 IEEE Ant. Prop. Soc. Int. Symp. (APSURSI)*, 2014, pp. 1449–1450.

[24] R.K. Singh, A. Basu, and S.K. Koul, "A Novel Reconfigurable Microstrip Patch Antenna with Polarization Agility in Two Switchable Frequency Bands", *IEEE Trans. Ant. Prop.*, 66(10), pp. 5608-5613, 2018.

[25] J. Hu, Z.-C. Hao, "Design of a Frequency and Polarization Reconfigurable Patch Antenna with a Stable Gain", *J. Eng. Appl. Sci., 37*(1), 2018. doi.org/10.25211/jeas.v37i1.2008

[26] D. Rodrigo, B.A. Cetiner, and L. Jofre, "Frequency, Radiation Pattern and Polarization Reconfigurable Antenna Using a Parasitic Pixel Layer", *IEEE Trans. Ant. Prop.*, 62(6), pp. 3422–3427, 2014.

[27] R.N.L. Simons, "Feasibility Study of Optically Transparent Microstrip Patch Antenna", Int. Symp. Radio Sci. Meet., Montreal, Canada, 1997.

[28] R.F. Solberg and P.J. Siemsen, "Development of a conductive polymer, composite, direction-finding antenna", in IEEE Ant. Prop. Soc. Int. Symp. 1999 Digest, vol. 3, pp. 1966–1969, 1999.

[29] S.Cichos, J. Haberland, and H. Reichl, "Performance analysis of polymer based antennas-coils for RFID", 2nd Int. IEEE. Conf. Polym. Adhes. Microelectron. Pontonics., pp.120-124, 2002.

[30] N.J. Kirsch, N.A. Vacirca, E.E. Plowman, T.P. Kurzweg, A.K. Fontecchio, and K.R. Dandekar, "Optically transparent conductive polymer RFID meandering dipole antenna", in 2009 IEEE Int. Conf. RFID, pp. 278–282, 2009.

[31] N.J. Kirsch, "Performance of transparent conductive polymer antenna in MIMO and Ad-Hoc network", in IEEE 6th Int. Conf. Wirel. Mob. Comput. Netw. Comm. IEEE, pp.9-14, 2010.

[32] A. Verma, C. Fumeaux, V. Truong, and B.D. Bates, "Effect of film thickness on the radiation efficiency of a 4.5 GHz polypyrrole conducting polymer patch antenna", in 2010 Asia-Pacific Microwave Conf., pp. 95–98, 2010.

[33] T. Kaufmann, A. Verma, S.F. Al-Sarawi, V. Truong, and C. Fumeaux, "Comparison of two planar elliptical ultra-wideband PPy conductive polymer antennas", in Proc. 2012 IEEE Int. Symp. Ant. Prop., pp. 1–2, 2012.

[34] T. Kaufmann, A. Verma, V.-T. Truong, B. Weng, R. Shepherd, and C. Fumeaux, "Efficiency of a Compact Elliptical Planar Ultra-Wideband Antenna Based on Conductive Polymers", Int. J. Ant. Prop., Article ID 972696, 11 pages, 2012.

[35] Z. Hamouda et al., "Dual-Band Elliptical Planar Conductive Polymer Antenna Printed on a Flexible Substrate," IEEE Trans. Ant. Prop., 63(12), pp. 5864–5867, 2015.

[36] H. Zahir et al., "Design fabrication and characterisation of polyaniline and multiwall carbon nanotubes composites-based patch antenna," *IET Microw. Ant. Prop.*, 10(1), pp. 88–93, 2016.

[37] N. Ehteshami, V. Sathi, and M. Ehteshami, "Experimental investigation of a circularly

polarised flexible polymer/composite microstrip antenna for wearable applications", *IET Microw. Ant. Prop.*, 6(15), pp. 1681–1686, 2012.

[38] S.J. Chen et al., "A Compact, Highly Efficient and Flexible Polymer Ultra-Wideband Antenna", *IEEE Ant. Wireless Prop. Lett.*, 14, pp. 1207–1210, 2015.

[39] S.J. Chen, C. Fumeaux, B. Chivers, and R. Shepherd, "A 5.8 GHz flexible microstrip-fed slot antenna realized in PEDOT:PSS conductive polymer", in 2016 *IEEE Int. Symp. Ant. Prop.* (APSURSI), 2016, pp. 1317–1318.

[40] Z. Hamouda, J. Wojkiewicz, A.A. Pud, L. Koné, S. Bergheul, and T. Lasri, "Magnetodielectric Nanocomposite Polymer-Based Dual-Band Flexible Antenna for Wearable Applications", IEEE Trans. Ant. Prop., 66(7), pp. 3271–3277, 2018.

[41] R.L. Haupt, "Reconfigurable patch with switchable conductive edges", Microw. Opt. Technol. Lett., 51(7), pp. 1757–1760, 2009.

[42] P.J. Kinlen, US Patent Application 15/349,769, filed May 17, 2018.

Chapter 2

Conductive Polymers Basics & Reconfigurable Antennas Concepts

Growing resources and much efforts are invested into conductive polymers research. Increasingly higher electrical conductivity, better mechanical resilience and tunability in resistance have been gradually reported in the literature. Conductive polymers are becoming of interest in antennas applications owing to their flexibility. This chapter reports not only the state of the art of conductive polymers-based antennas, but also on reconfigurable conductive polymers-based antennas. We end the chapter with the preliminary results of a design of a frequency reconfigurable antenna based on conductive polymers using the feature of tunable substrate permittivity.

2.1 Background

Since the initial report on their electrical conductivity in 1977 [1-2], conductive polymers have attracted significant attention from all over the world. Three scientists mainly contributed to this breakthrough: H. Shirakawa, A.J. Heeger and A.G. MacDiarmid, who jointly received the Noble Prize in Chemistry in 2000 for the discovery and development of electrically conductive polymers. With steadily growing resources and efforts invested into research on conductive polymers, increasingly higher electrical conductivity, better mechanical resilience and tunability in resistance have been gradually reported in the literature. For these reasons, conductive polymers have become very promising as antenna conductors especially in the view of achieving flexible and purely non-metallic flexible designs. Additionally, since the conductivity can be to some extent be controllable in some polymers [3], the realization of reconfigurable antennas becomes another potential aspect for research. As results, many antennas based on various conductive polymers have been reported recently.

2.2 Electrical and mechanical properties of conductive polymers

Polymers consist of large molecules or macromolecules which are formed by chains of many repeated carbon-based sub-units. They can be found in our body as fundamental building blocks, including for example in DNA, and are present in nearly everything around such as plastics and rubber. Generally, most natural and synthetic polymers are highly insulating. In contrast, polymers with electrical conductivity are referred to as conducting/conductive polymers, or more precisely as intrinsically conducting polymers. The chemical structures of some typical conductive polymers including polyacetylene ($(CH)_x$), polyphenylene vinylene (PPV), Polypyrrole (PPy), Polyaniline (PANI) and PEDOT are shown in **Fig. 2.1**, all demonstrating a conjugated molecular structure in the main chain with л-electrons delocalized. The unique electrical and optical properties are a result of this conjugate л systems [4].

One of the earliest conductive polymer references described the preparation of Polyaniline by the anodic oxidation of aniline was published by Henry Letheby, as early as 1862 [5]. The polymer reported in this reference was conductive and exhibited an electrochromic characteristic. Around 100 year later, description of polymers with much higher conductivity appeared in the literature. For example, in 1963, Australian scientists reported a series of highly conductive PPy,

which had a measured conductivity as high as 0.01 S/m. In 1968, R. De Surville et al. reported about a polymer PANI which possessed a similar conductivity of 0.013 S/m **[6]**. Even though these experimental values of polymer conductivity were much greater than the ones reported before, they were still not high enough for practical applications.

In late 1970s, the interest in conductive polymers started to grow significantly following the demonstration by researchers at IBM Research Laboratory that polythiazyl ($(SN)_x$) can be superconductive **[7]**. In 1977, the attention on these materials become even intense, when MacDiarmid's teams showed that the doping of polyacetylene films could achieve an unprecedented conductivity of 3800 S/m **[1]**. Since then, expectations in polymers conductivity have been raising continuously. As depicted in **Fig. 2.2**, the DC conductivity of conductive polymers can range from 10^{-10} to 10^{7} S/m. This is very close to that of silver, the most conductive metal.

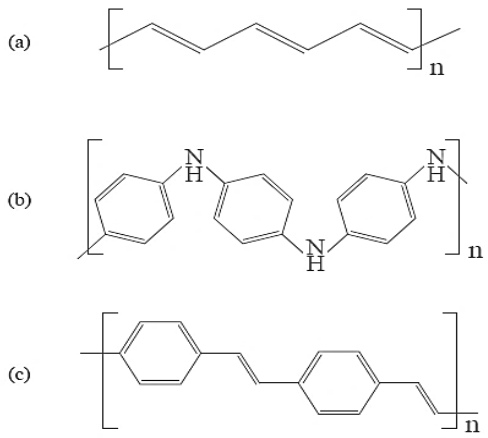

Figure 2.1. Chemical structures of typical conductive polymers. (a) polyacetylene ((CH)x); (b) polyphenylene vinylene (PPV); (c) Polyaniline (PANI).

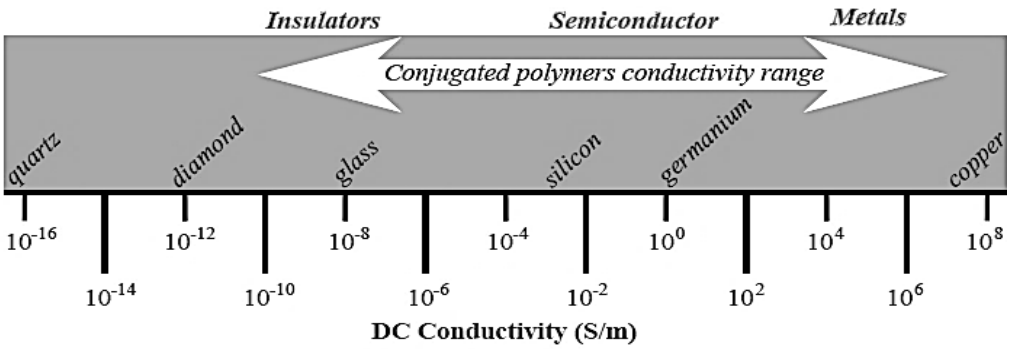

Figure 2.2. DC electrical conductivity range of some materials.

During the last few decades, many conductive polymers have been studied in details. These include Polyacetylen, PPV, PANI, Polypyrrole (PPy) and Poly(3,4-rthylenedioxythiophene) (PEDOT). Although, polyacetylen is probably the most conductive polymer investigated so far, the potential applications using this material are quite limited due to the difficulty in its processing and its inherent chemical instability. In contrast, PPy can have reasonably high conductivity and is environmentally stable due to its heteroaromatic and extended p-conjugated backbone structure **[8]**. The chemical structure of PPy is shown in **Fig. 2.3(a)**. By doping, which allows partial charge extraction from the chain, the electrical of neutral PPy can be dramatically increased from an insulating level to a metallic level. PPy has been intensively studied for many applications as electrodes in capacitors and rechargeable batteries, sensors, actuators and electromagnetic devices **[9]**. Another type of polymer namely Poly(3,4-ethylendioxythiophene) usually referred to as PEDOT, has drawn much attention recently, since it has excellent environmental and chemical stability combined with a high conductivity under doping **[10]**. These advantages have made it as a promising material for broad applications in solid states capacitors, electrodes materials and antistatic painting. Doping with poly(styrenesulfonate) (PSS), PEDOT becomes PEDOT:PSS which exhibits a high mechanical flexibility and an excellent thermal stability not to mention its high conductivity **[11-12]**.

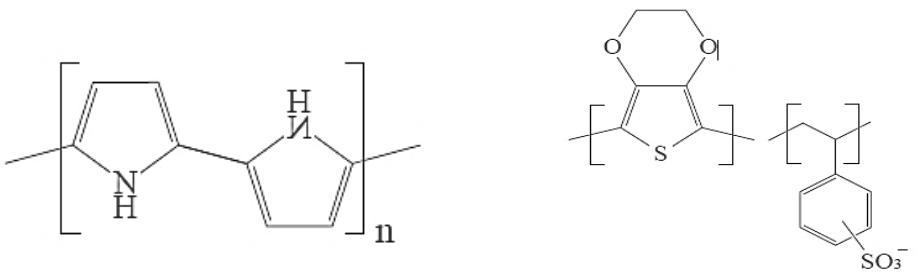

(a) (b)

Figure 2.3 Chemical structures of: (a) Polypyrrole (PPy); (b) Poly(3,4-rthylenedioxythiophene) (PEDOT).

2.3 Electromagnetic properties of conductive polymers

In regards to electromagnetic applications of conductive polymers, electromagnetic interference (EMI) shielding and antenna design in the microwave region have generally been the two key aims. This is because of the fact that conductive polymers have a certain desired feature, namely its high conductivity that can be easily controlled in the fabrication process. For

instance, metals or metal-coated materials are suitable for EMI shielding by wave reflexion. However, they cannot be adopted for EMI shielding that is based on absorption due to their very shallow skin depth which is a direct consequence of their extremely high conductivity. In contrast, because of the comparatively low conductivity, conductive polymers not only can reflect but also absorb electromagnetic waves, and thus they hold a critical advantage over metallic materials.

In designing antennas, a high conductivity is of course one of the major criteria for assessing the suitability of a polymeric material. It is known that a conductivity that is high is one of the two most crucial conditions guaranteeing a high efficiency antenna. The other crucial condition lies in the thickness of the polymer owing to latter importance. It has been proven that it is not easy to simultaneously synthesize a highly conductive polymer and has sufficient thickness. Therefore, the process-limited thickness of conductive polymers determines the cross section area in the material where RF circuit is flowing which is inversely proportional to the effective resistance. If the polymer thickness is too thin, for instance, much less than a skin depth, this will lead to a significant increase in the effective surface resistance by confining the RF currents in an insufficient cross-sectional area.

A better understanding of the concept of skin depth is fundamental here. We assume that a harmonic plane wave with an angular frequency of ω is propagating in a conductive medium having the permittivity, permeability and conductivity ε, μ, and σ, respectively. The governing Maxwell's equations in phasor form are:

$$\nabla \times \underline{E} = -j\omega\mu\underline{H} \tag{1}$$

$$\nabla \times \underline{H} = \sigma\underline{E} + j\omega\mu\underline{E} \tag{2}$$

Then the corresponding wave equation for the electrical field vector $\underline{E}$ is:

$$\nabla^2\underline{E} + \omega^2\mu\varepsilon\left(1 - j\frac{\sigma}{\omega\varepsilon}\right)\underline{E} = 0 \tag{3}$$

where the propagation constant γ for the plane wave in the medium is defined as:

$$\gamma^2 = \omega^2\mu\varepsilon\left(1 - j\frac{\sigma}{\omega\varepsilon}\right) \tag{4}$$

Then, the complex γ can be seen as a combination of the attenuation constant α and the phase constant β which are its real and imaginary parts, respectively:

$$\gamma = \alpha + j\beta = \sqrt{\omega^2\mu\varepsilon\left(1 - j\frac{\sigma}{\omega\varepsilon}\right)} = j\omega\sqrt{\mu\varepsilon}\sqrt{1 - j\frac{\sigma}{\omega\varepsilon}} \tag{5}$$

A non-zero attenuation constant α indicates that the field amplitude has an exponential decay in the medium along the propagation direction. Since those conductive polymers that could be suitable for use in antenna technology are chosen with a high conductivity, meaning that σ >> ωε. The propagation constant can be simplified then to:

$$\gamma = \alpha + j\beta \approx (1+j)\sqrt{\frac{\omega\mu\sigma}{2}} \tag{6}$$

The skin depth δ for good conductors then can be defined as

$$\delta = \frac{1}{\alpha} = \sqrt{\frac{2}{\omega\mu\sigma'}} \tag{7}$$

This describes the depth for which the field amplitude in the conductor will decay by a factor of $e^{-1}(36.8\%)$. Based on the skin depth concept discussed above, it is noted that when electromagnetic waves at microwave frequencies flow in a good conductor, the skin depth is very small. For instance, in **[12]**, a five-layer spin-coated PEDOT:PSS thick film had one of the highest conductivity reported, namely 2.35×10^5 S/m, but with a thickness of only 109 nm, which is approximately a one hundredth of the skin depth at 10 GHz. As a results, even with a very high conductivity, PEDOT:PSS thin films are not appropriate for microwave antenna design due to the very limited thickness. Consequently, to justify whether a sub-skin-depth-thick thin film material is suitable or not for microwave antenna designs, a quantity called sheet resistance which is dependent on both the conductivity and the thickness can be conveniently adopted. Sheet resistance R_s, in $\Omega/square$, is defined through the following relationship:

$$R_s = \frac{1}{\sigma d'} \tag{8}$$

where σ and d are the film conductivity and thickness, respectively. To quantitatively illustrate this measure, a copper thin film having $5.8 \times 10^7\ S/m$ at the working frequency of 10 GHz, the skin depth ($661\ nm$) the calculated sheet resistance is $0.026\ \Omega/square$, whereas for the film of PEDOT:PSS **[12]** Rs is 39 $\Omega/square$. It is noted that generally the highest achievable thickness for polymers with satisfactory conductivity is about $100\ \mu m$.

2.4 Frequency Reconfigurable MSA with CP radiators

A single antenna is adopted which should operate in the multiple narrow frequency bands of mobile networks in Algeria. These includes global system monitoring (GSM) frequency bands 1.8 and 1.9 GHz, Universal Mobile Telecommunications Service (UMTS) frequency bands 2.1 and 2.6 GHz, the Wireless Local Area Network (WLAN) frequency band 2.4 GHz. We assume

in this simulation a microstrip antenna with patch made of conductive polymer **(CP)** film of conductivity 5×10^8 S/m and a thickness of 35 μm. Herein, we assume that the permittivity of the substrate is tunable. By assuming so, the basics of frequency reconfigurable conductive polymer microstrip antenna are built.

An important parameter that requires consideration in designing conductive polymer-based antennas is the thickness of the CP sheets (patch and ground plane). This issue has been assessed **[13]**, and as a result, it was shown that the thickness of the conductor element made of PPy affects strongly the gain and the radiation efficiency of the antenna as shown in **Fig. 2.4**.

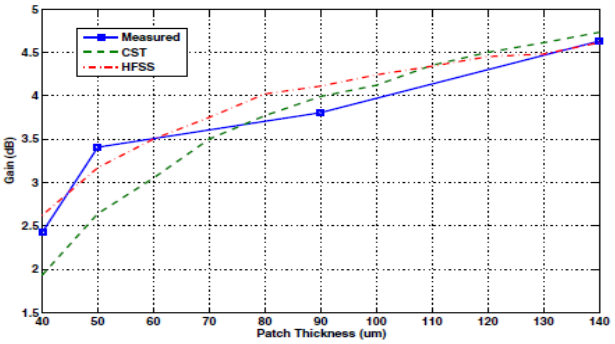

(a)

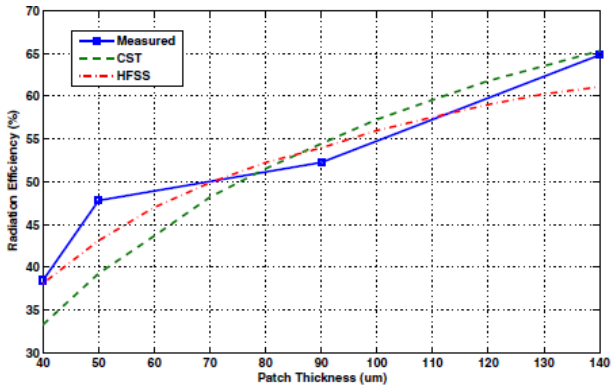

(b)

Figure 2.4. Effect of PPy sheet thickness on the gain and radiation efficiency of microstrip antenna [13]. (a) Effect on gain; (b) effect on radiation efficiency.

2.4.1 Reconfiguration Principles

The dielectric constant or permittivity determines the resonant frequency of a microstrip rectangular patch as it is given by **[13]**:

$$\varepsilon_r = \left(\frac{c}{2 \cdot L \cdot f_r}\right)^2 \quad (9)$$

ε_r is the dielectric constant of the substrate and which is assumed to be controllable in the present design, c is the light velocity, f_r is the resonant frequency of the patch and L is the patch length. The relationship between frequency and dielectric constant of the substrate is illustrated in **Fig. 2.5**. It is well observed that the dielectric constant decreases linearly with the increase in the resonance frequency.

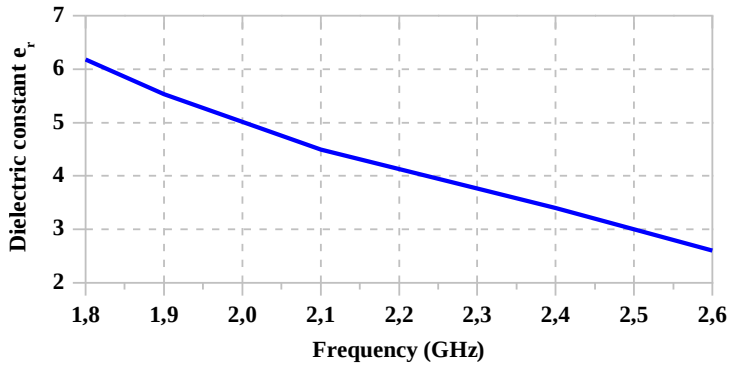

Figure 2.5. Frequency variation in accordance with the tuning dielectric constant [13].

2.4.2 Design in CST

To introduce conductive polymer in the present design as conductor material, two sheets of thickness 0.035 mm having a conductivity close to that of copper 5.80×10^7 S/m were assumed as patch and ground plane respectively. The design concept is shown n **Fig. 2.6** with the final dimensions presented in **Table 2.1**.

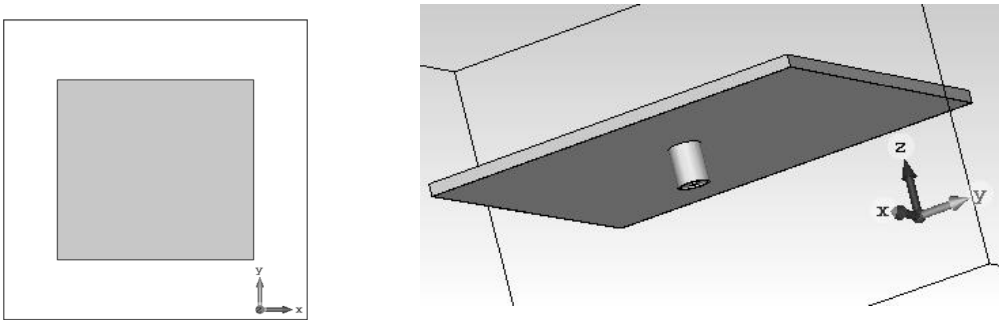

Figure 2.6. Design concept of conductive polymer and tunable substrate based microstrip antenna. (a)Top view; (b) Bottom view in 3-D.

Table 2.1 Dimensions of the rectangular Microstrip Antenna

Patch width (*mm*)	Patch length (mm)	Substrate thickness (*mm*)	Patch thickness (*mm*)
30	32.45	1.57	0.035

2.4.3 Simulation results

After going through the simulation process using the commercial software Computer Simulation Technology CST, we spent a lot of time optimizing the antenna dimensions, and carefully adjusting the dielectric constant ε_r in order to achieve the resonance at the five desired frequencies.

- **Simulated results of the reflexion coefficient |S11|**

The reflexion coefficient results are shown in **Fig. 2.7**. By altering the dielectric constant of the substrate, the antenna resonance frequency can be controlled easily. The antenna reflexion coefficient is observed to vary accordingly for GSM frequency bands (1.8 and 1.9 GHz), UMTS of the frequency bands (2.1 and 2.6 GHz) and for the WLAN for the frequency band 2.4 GHz.

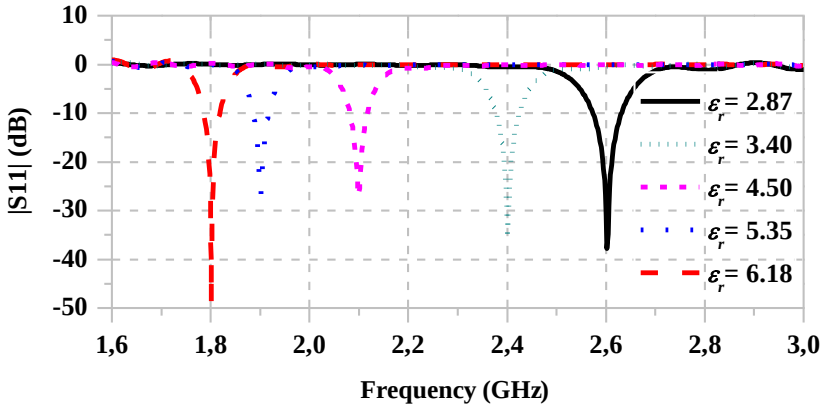

Figure 2.7. Reflexion coefficient for different values of the dielectric constant.

- **Simulated results of the radiation efficiency**

The radiation efficiency is the ratio of the total power radiated by the antenna to the total power accepted by the antenna at its input terminals during radiation **[14]**. The radiation efficiency can also be defined, using the direction of maximum radiation as a reference, as:

$$radiation\ efficiency = \frac{gain}{directivity} \tag{10}$$

where directivity and gain, imply that they are measured or computed in the direction of maximum radiations **[14]**. As illustrated in **Fig. 2.8**, the radiation efficiency of the simulated reconfigurable antenna increases with the increasing frequencies. These results suggest that

change in dielectric constant affects not only the resonance frequency of a microstrip antenna but radiation efficiency is significantly considered.

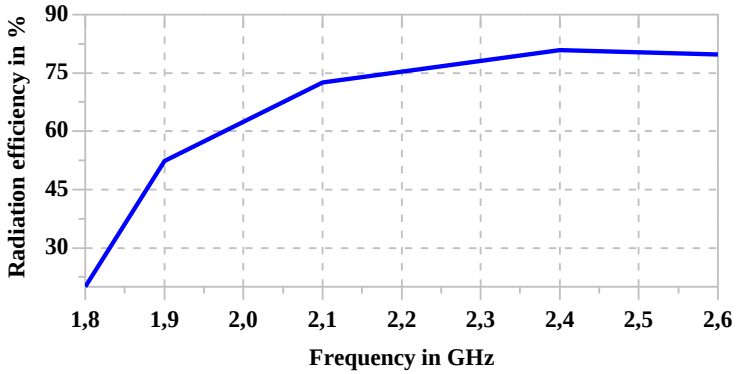

Figure 2.8. Relationship between the radiation efficiency and MSA resonance frequency.

The radiation patterns of the microstrip antenna are unidirectional in E-plane and H-plane for all frequencies as illustrated in **Fig. 2.9**.

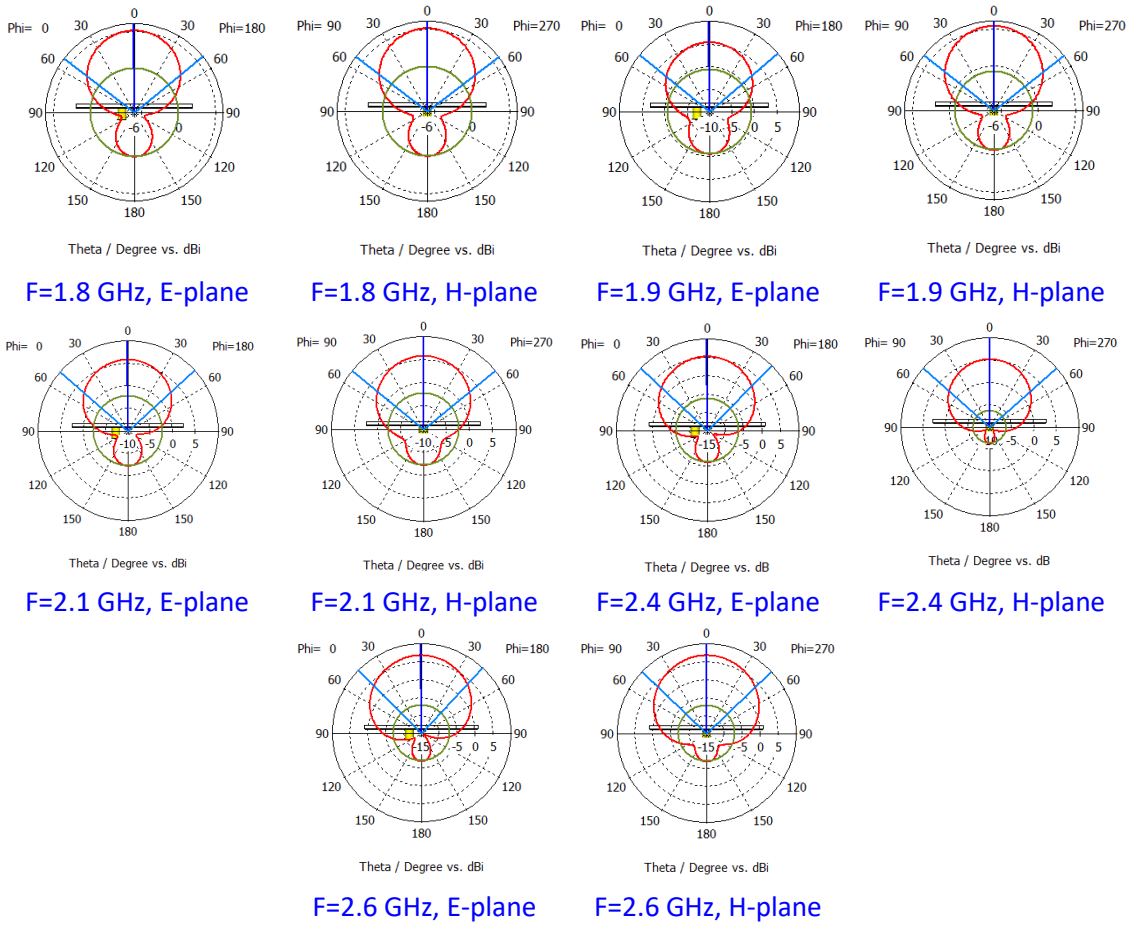

Figure 2.9. Simulated radiation patterns in E and H planes at various frequencies.

2.5 Conclusion

In summary, a brief review on the development, the features and the state of the art of conductive polymer and their applications in antenna designs has been presented here. Preliminary results of an antenna design based on conductive polymers using the commercial software CST at varying dielectric constant of the polymer, and which is intended to applications in GSM frequency bands (1.8 and 1.9 GHz), UMTS of the frequency bands (2.1 and 2.6 GHz) and the WLAN for the frequency band 2.4 GHz have been discussed. These results are very promising.

Bibliography

[1] H. Shirakawa, E.J. Louis, A.G. MacDiarmid, C.K. Chiang, and A.J. Heeger, "Synthesis of electrically conducting organic polymers: halogen derivatives of polyacetylene, (CH)x", *J. Chem. Soc. Chem. Commun.*, 0(16), pp. 578–580, 1977.

[2] C.K. Chiang *et al.*, "Electrical Conductivity in Doped Polyacetylene", *Phys. Rev. Lett.*, 39(17), pp. 1098–1101, 1977.

[3] R.L. Haupt, "Reconfigurable patch with switchable conductive edges", *Microw. Opt. Technol. Lett.*, 51(7), pp. 1757–1760, 2009.

[4] T.A. Skotheim, J. Reynolds, and J. Reynolds, Conjugated Polymers : Theory, Synthesis, Properties, and Characterization, CRC Press, 2006.

[5] H. Letheby, "XXIX.-On the production of a blue substance by the electrolysis of sulphate of aniline," *J. Chem. Soc.*, 15(0), pp. 161–163, 1862.

[6] R. De Surville, M. Jozefowicz, L.T. Yu, J. Pepichon, and R. Buvet, "Electrochemical chains using protolytic organic semiconductors", *Electrochim. Acta*, 13(6), pp. 1451–1458, 1968.

[7] Y. Li, Organic optoelectronic materials, ser. Lecture Notes in Chemistry, Y. Li (Ed.), *Springer*, vol. 91, 2015.

[8] R.L. Greene, G.B. Street, and L.J. Suter, "Superconductivity in Polysulfur Nitride $(SN)_x$", *Phys. Rev. Lett.*, vol. 34, no. 10, pp. 577–579, 1975.

[9] M.-Z. Yang, C.-L. Dai, and D.-H. Lu, "Polypyrrole Porous Micro Humidity Sensor Integrated with a Ring Oscillator Circuit on Chip", *Sensors*, 10(11), pp. 10095–10104,

2010.

[10] G. Heywang and F. Jonas, “Poly(alkylenedioxythiophene)s-new, very stable conducting polymers”, *Adv. Mater.*, 4(2), pp. 116–118, 1992.

[11] U. Lang, E. Müller, N. Naujoks, and J. Dual, “Microscopical Investigations of PEDOT:PSS Thin Films”, *Adv. Func. Mater.*, 19(8), pp. 1215–1220, 2009.

[12] Y. Xia, K. Sun, and J. Ouyang, “Solution-Processed Metallic Conducting Polymer Films as Transparent Electrode of Optoelectronic Devices,” *Adv. Mater.*, 24(18), pp. 2436–2440, 2012.

[13] A. Verma, C. Fumeaux, V.T. Truong and B.D. Bates, “Effect of film thickness on the radiation efficiency of a 4.5 GHz polypyrrole conducting polymer patch antenna”, in 2010 Asia-Pacific Microwave Conf., pp. 95–98, 2010.

[14] R. Garg, P. Bhartia, I.J. Bahl, and A. Ittipiboon, Microstrip Antenna Design Handbook, *Artech House*, 2001.

Chapter 3

Reconfigurable Monopole UWB Antenna with Triple Filtering Functions

THE frequency band that extends from 3.1 to 10.6 GHz and referred as the Ultra-Wide Band (UWB) attracts interests since its free utilization which was announced by the International Telecommunications Union (ITU) in 2002. This band allows high transmission rate, low power consumption, low-cost, less obstacles penetration and so on. However, due to the increasing number of users in this band, it has started to suffer from multiple problems such as congestions and interference. Consequently, antennas designers in the UWB community have been attempting to develop new UWB antennas configurations that are capable to handle interference obstacles. The present chapter presents the simulation results of a reconfigurable microstrip UWB monopole antenna design capable to overcome some of the interferences known to be an obstacle in UWB development. The obtained results obtained from well-known software (CST and HFSS) are analysed in the light existing published data.

3.1 Literature Review

Many works have been published lately demonstrating different shapes of UWB antennas with the ability to filter out up to five interfering bands from the UWB frequency spectrum **[1]**. A tapered-slot UWB antenna with a single band-notched printed using liquid crystal polymer (LCP) as a substrate of a permittivity of 2.9 and a thickness of 0.05 mm was proposed in **[2]**. The antenna operated over the UWB spectrum ranging from 3.1 to 10.6 GHz while it was capable to suppress the wireless local area network (WLAN) at 5.25 GHz band through a H-shaped slot at the middle of the radiating element as shown in **Fig. 3.1(a)**. In **[3]**, an ultra-wideband antenna has been proposed with triple notched bands. Its structure involved a U-shaped monopole radiating patch and an adapted rectangular ground plane printed on the opposite sides of a low-cost Rogers 5880 substrate (with a thickness of 0.5 mm and a relative permittivity of 2.2). As shown in **Fig. 3.1(b)**, the notch performance was implemented by designing a pair of I-shaped and L-shaped stubs inside the square slots of the ground plane in addition to two resonant open-circuited stubs being positioned on both sides of the radiating patch. The antenna operating bandwidth was from 2.77 to 11.38 GHz. The proposed antenna rejected the three bands 3.27–3.75 GHz, 5.51–5.96 GHz and 6.95–7.65 GHz. Up to five notched bands have been provided by the ultra-wide band antenna proposed in **[4]**. It consists of a modified circular monopole and a trapezoidal ground plane with curved corners, as shown in **Fig. 3.2**.

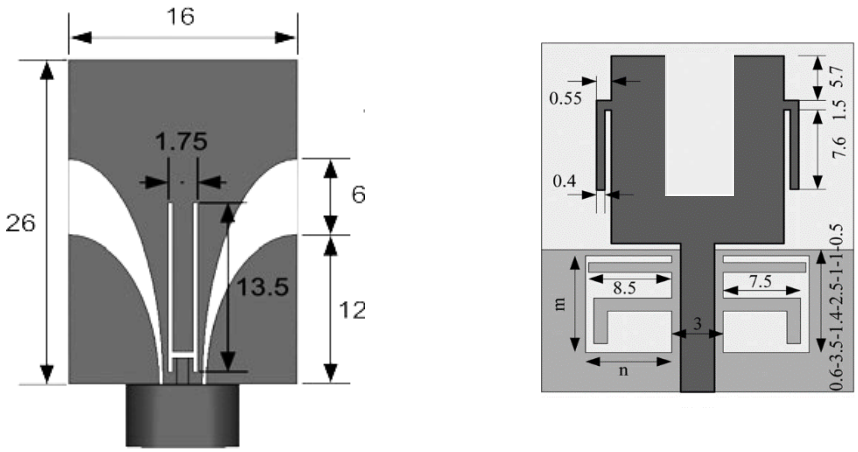

Figure 3.1. Perpetual notching UWB antennas. (a) single notch proposed in **[2]**; (b) triple notch proposed in **[3]**.

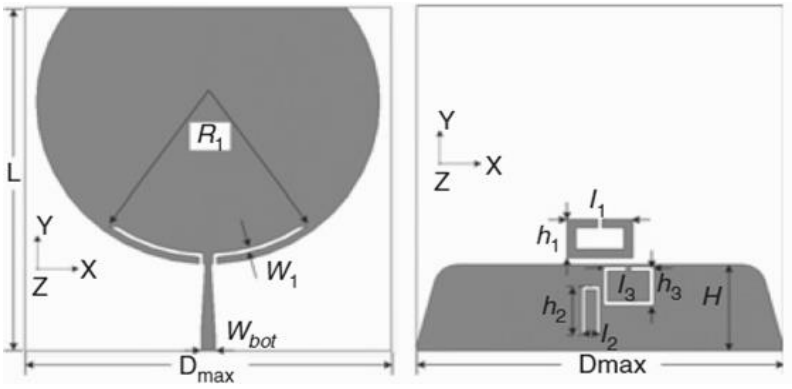

Figure 3.2. Five perpetual notches UWB antenna [4]. (a)Top view; (b) bottom view; Dimensions (mm): D_{max} = 80.00; $R1$= 37.50; W_{bot}= 1.55; w_1= 0.2; l_1 = 14.40; h_1= 9; l_2= 1; h_2= 1; l_3= 11; h_3= 9.

The ground plane and the monopole are etched on the back and front sides of a Rogers RT 5870 substrate with a permittivity of 2.33 and a thickness of 0.508 mm. Two notched bands at 2.4 and 7.5 GHz are generated by introducing symmetric arc-shaped open slots on the patch. Another two notched bands at 3.3 and 5.2 GHz are achieved by designing a complimentary slit ring resonator (CSRR) and a U-shaped CSRR in the ground plane. Besides, the fifth notch at 5.8 GHz is produced by placing a metallic open loop next to the upper border of the ground plane.

The filtering functions provided by those designs are perpetual, which means that a significant part of the spectrum is permanently out of work. This is an undesirable drawback particularly in case the interferences are not active. Instead, it is worthwhile if one can design an UWB antenna that is capable of controlling its filtering functions. Unlike perpetual filtering, the filtering in this case can be activated only if the interference is present and otherwise it is deactivated. This could strongly help to efficiently exploit the UWB spectrum. The procedure is referred to as "reconfigurable filtering" and it has been an active topic of current.

The UWB antenna proposed in **[5]** provides two reconfigurable notched bands of 3.12–3.84 GHz wireless interoperability medium access (WiMAX) and 5–6.07 GHz WLAN. On the top of Flame Retardant (FR)-4 substrate of permittivity 4.4 and a thickness of 0.8 mm. The modified rectangular radiated patch is designed with a circular and three rectangular-shaped slots etched on, while the ground plane is on the bottom side, as shown in **Fig. 3.3**. To reconfigure the notched bands, two PIN diodes D1 and D2 are placed across the circular slot to control its effect.

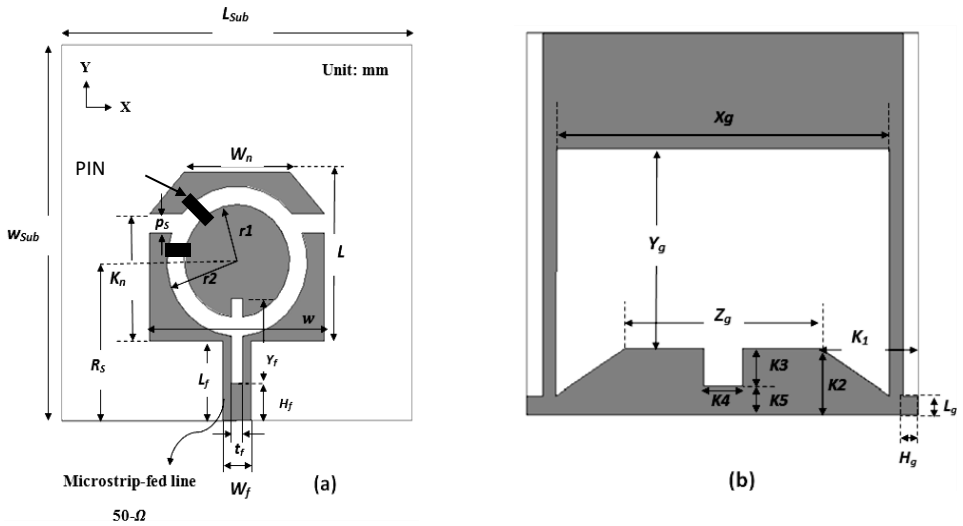

Figure 3.3. Dual reconfigurable notched band [5]. (a)Top view; (b) bottom view; Dimensions (mm): *r1*= 3; *r2* = 4; W_n= 6; K_n= 6.75; *L*= 9; *W*= 10; p_s= 1; R_s= 8.5; Y_f= 4.5; L_f= 4.25; H_f= 2; t_f= 0.6; Y_g= 10.5; X_g= 17; Z_g= 10; L_g= 1; H_g= 0.8; K_1= 5; *K2*= 3.5; *K3*= 2; *K4*= 2; *K5*= 1.5.

Another two notched bands reconfigurable microstrip antenna was proposed in **[6]**. It consists of slot rectangular patch fed by a microstrip line printed on the top face of FR-4 substrate with the ground plane on the lower one as shown in **Fig. 3.4**. By etching two resonant slots on the patch and controlling them by placing a PIN diode across each one, the two reconfigurable notches at WLAN 5.43–6.1 GHz and WiMAX 3.15–3.85 bands were achieved.

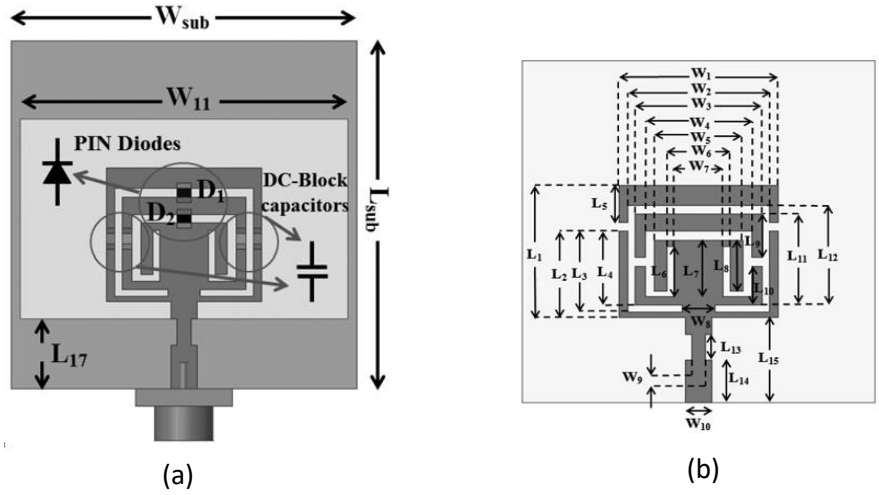

Figure 3.4. Compact dual notched band reconfigurable UWB antenna [6]. (a)Top view; (b) bottom view; Dimensions (mm): Ws_{ub}= 20; W_1= 9; W_2= 8; W_3= 7.2; W_4= 6; W_5= 5; W_6= 3.6; W_7= 2.8; W_8= 1.9; W_9= 0.8; W_{10}= 1.5; W_{11}= 19; L_{sub}= 20; L_1= 7.7; L_2= 5; L_3= 4.7; L_4= 4.3; L_5= 2.2; L_6= 2.9; L_7= 3.3; L_8= 2.95; L_9= 2.5; L_{10}= 2.3; L_{11}= 5.3; L_{12}= 5.8; L_{13}= 1.5; L_{14}= 2.5; L_{15}= 5; L_{16}=11.5; L_{17}= 4.

The published work in [7] gave a new structure of UWB antenna with reconfigurable dual notched bands. It lied on Rogers RT/Duroid 5880 of 2.2 permittivity and 0.8 mm thickness. As shown in Fig. 3.5, the proposed structure comprises a square ring patch with two parasitic elements joined on its both sides to enhance the bandwidth. An inverted L-shaped parasitic element is positioned inside the ring patch to notch at WLAN 5.1–5.7 GHz band.

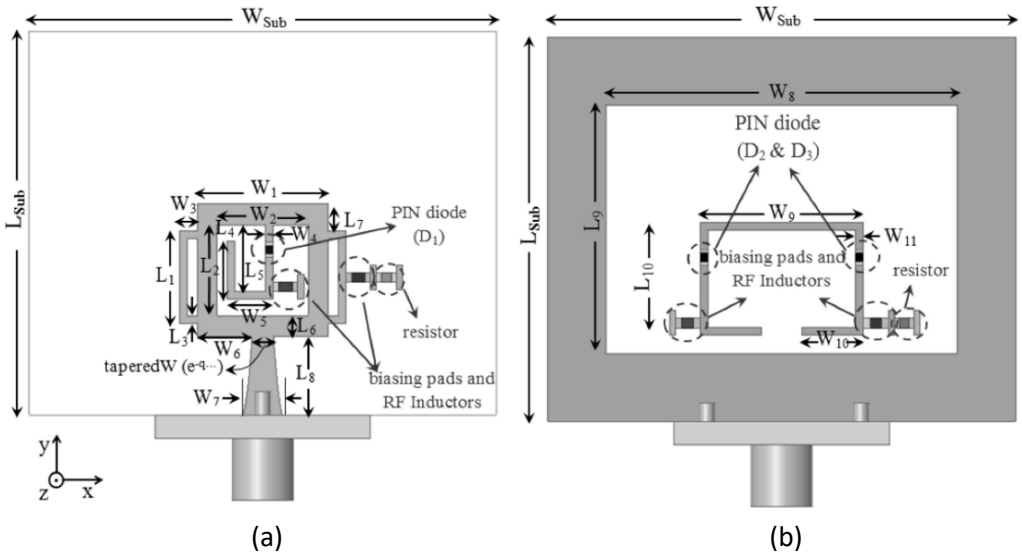

Figure 3.5. Dual notched band reconfigurable UWB antenna [7]. (a)Top view; (b) bottom view; Dimensions (mm): W_{Sub}= 30.3; W_1= 8.5; W_2= 5.9; W_3= 1.2; W_4= 0.5; W_5= 3; W_6= 3.6; W_7= 2.5; W_8= 22.8; W_9= 10.6; W_{10}= 4; W_{11}= 0.5; L_{sub}= 24.8; L_8= 5.1; L_9= 16.; L_{10}= 7.3; q= 1.7; tapered W=1.4.

In addition, a split ring resonator is located inside the square ring ground plane on the bottom side of the substrate helping to produce a notch at downlink X-band for satellite communication systems (7.2–7.8 GHz). The reconfiguration of the notch is acquired by controlling the L-shaped parasitic element and the split ring resonator (SRR) using two PIN diodes. The antenna proposed in [8] offers the highest operational notching modes. The geometry consists of microstrip fed patch and ground plane printed on opposite sides of a substrate of a 2.65 permittivity and 1.6 mm thickness. A three notched bands are produced by inserting a defected microstrip structure (DMS) feed line and an inverted π-shaped slot on the patch. The notch performance is controlled by placing four ideal switches (metallic stubs) across the two slots as shown in Fig. 3.6.

The operating bandwidth of this antenna extends from 3.1 to 14 GHz. It provides six operating modes with regards to the three notched bands at 5.5, 6.8 and 11.5 GHz. Little attention has been paid in this research to the excessive usage of switches (ideal stubs), since experimentally more switches adds more components to the biasing circuit, and hence complicates further the design, enlarges the size and affects the radiation efficiency. An optimal design is highly desirable. This should contain less switches and ensure a high operational notch performance.

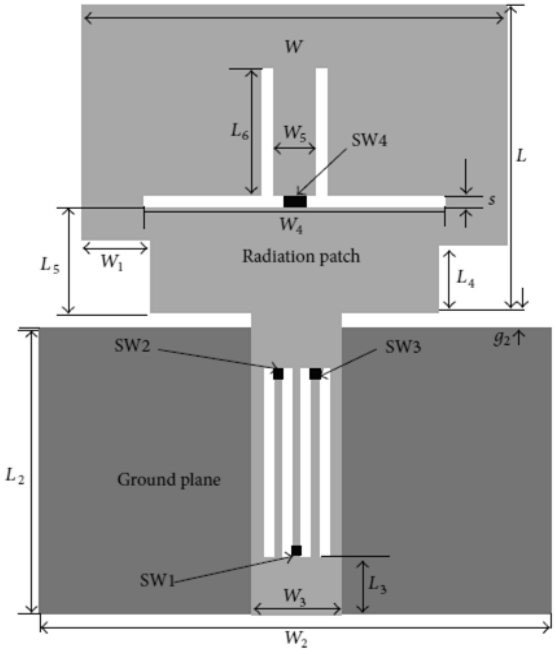

Figure 3.6. Triple notched bands reconfigurable UWB antenna with ideal switches [8]. (a)Top view; (b) bottom view; Dimensions (mm): W= 16; L= 15; W_1= 2; W_2= 30; W_3= 4.7; W_4= 9; W_5= 3.2; L_1= 6; L_2= 16.2; L_3= 3.7; L_4=2.2; L_5= 4.1; L_6= 6.2; g_2= 0.8; s= 0.4. Ideal switches: SW1, SW2, SW3 and SW4.

3.2 Design of the Basis Monopole Structure

The printed monopole UWB configuration is chosen as basis for the proposed reconfigurable filtering system structure. The requirements for UWB applications are satisfied by monopole designs in terms of wide bandwidth, omnidirectional radiation pattern, higher gain, implementation low-cost **[9]**. The proposed structure, shown in **Fig. 3.7**, consists of a circular patch with radius R fed by a 50 Ω microruban line of width W_f printed on the upper face of the FR-4 substrate (the permittivity ε_r = 4.4, the thickness of 1.5 mm). The ground plane of length Lg is printed on the bottom face of the substrate. The overall dimension is $W \times L$. Using the

software of CST (Computer Simulation Technology) [10] in time domain solver calculations, the design was optimized through careful parametric refinements. A particular attention was given to the parameter *d* in order to obtain the characteristics of UWB.

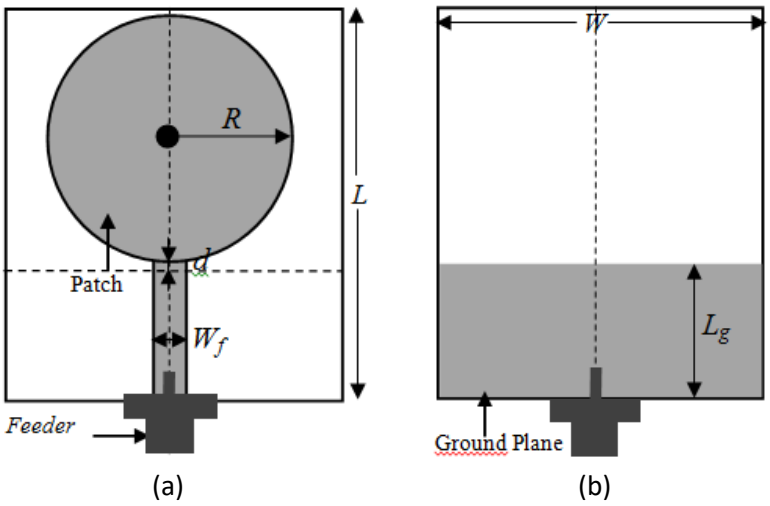

Figure 3.7. First designed antenna basis structure. (a)Top view; (b) bottom view; dimensions (mm): *W*= 35; *L*= 40; *R*= 12; *d*= 1; W_f = 3; *Lg*= 12.

3.3 Filtering Implementation

The antenna resonance and radiation properties are due to a certain current distribution within the geometry. Filtering functions can be introduced by driving new current paths in the patch and ground planes, which would mismatch the antenna resonance at particular frequencies within the UWB spectrum (i.e. 3.1 to 10.6 GHz). Upon this, a parametric study has been performed in which three slots *S1*, *S2*, *S3* of 0.5 mm width were introduced into the patch and the ground planes as depicted in **Fig. 3.8**. In order to determine the primary slot's length, we have used the following relations [11]:

$$\lambda_g = \frac{c}{f_c \times \sqrt{\varepsilon_{eff}}} \; ; \quad l = \frac{\lambda_g}{4} \; ; \; l_{eff} = \frac{\lambda_g}{2} \tag{11}$$

in which λ_g is the guided wavelength, c is the light speed, f_c is the central frequency of the filtered band and ε_{reff} is the effective dielectric constant. Afterwards, several parametric calculations have been performed in CST software in order to refine the positions and the lengths of each one of the separate slots.

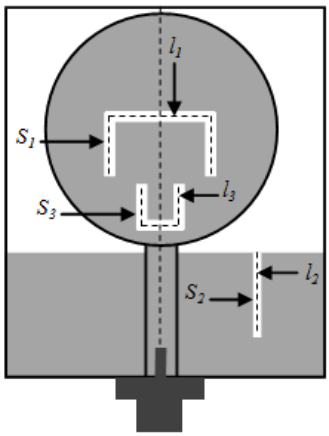

Figure 3.8. Design of the slots (S1, S2 and S3) to produce the filtering functions. Top and bottom views together with the dielectric being transparent; S1 of length l_1 *and* S_3 of length l_3 are created on the patch; S_2 of length l_2 is created on the ground plane.

Parametric optimization of the slot S1 is shown in **Fig. 3.9(a)**. It is very well observed that the length of S1 controls heavily the notch properties around the notch of the band 3.5 GHz.

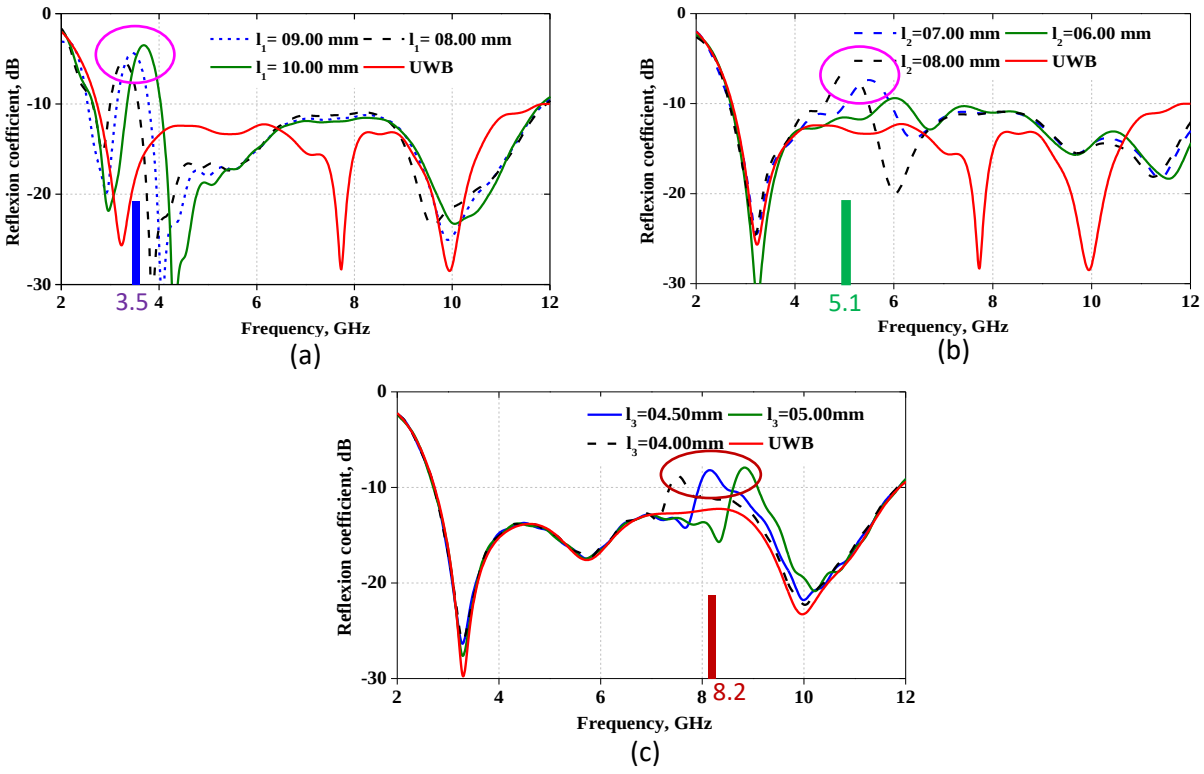

Figure 3.9. Impact of slots parameters optimization on the notch performance. (a) S1 around 3-4 GHz; (b) S2 around 4.5-5.5 GHz; (c) S3 around 7-9 GHz.

Fig. 3.9(b) illustrates the contribution of the length of S2. As it can be observed, l_2 controls the notch level and the bandwidth nearby 5.1 GHz. Meanwhile, the length of S3 controls the notch level and the bandwidth around the frequency 8.2 GHz, as it is observed in **Fig. 3.9(c)**. The optimum filtering at the three frequencies 3.5, 5.1 and 8.2 GHz of interest is obtained with the optimum lengths l_1=12 mm, l_2= 7 mm and l_3= 4.70 mm.

3.4 Filtering Control with Ideal Switches

In order to reconfigure the filtering system, an ideal switching procedure has been carried out. As shown in **Fig. 3.10**, the flow of the current around the slots is controlled by adding four ideal switches. Let's name A1 and A2 the two ideal switches for the slot S1, A3 for S2 and A4 for the slot S3. From the simulation in HFSS, it has been observed that when the switches are closed (*OFF*) the function of the slots is deactivated. An indication is by observing the simulated current distribution around the slots, shown in **Fig. 3.11**.

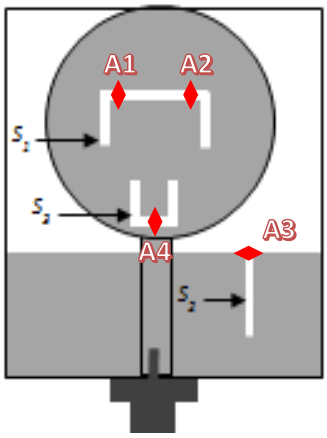

Figure 3.10. Insertion of ideal switches to control current circulation around the slots.

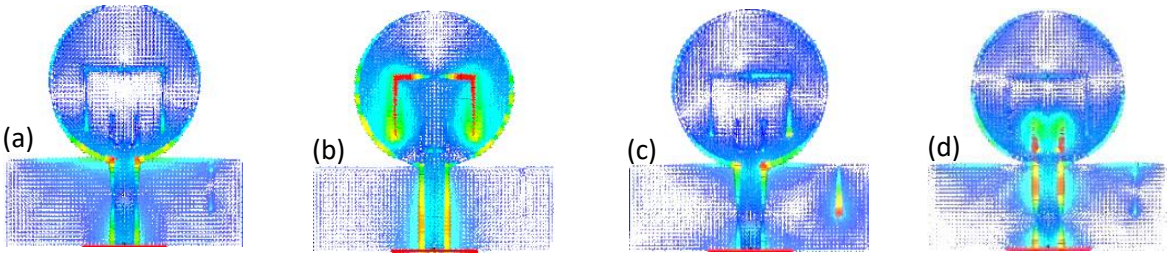

Figure 3.11. Surface current distributions with ideal switches. (a) A1, A2, A3 & A4 *ON* at 3.5 GHz. (b) A1, A2 *OFF,* A3 & A4 *ON* at 3.5 GHz; (c) A1, A2 & A3 *ON,* A4 OFF at 5.10 GHz; (d) A1, A2 & A4 *ON,* A3 *OFF* at 8.2 GHz.

3.5 Control of the Filtering using Real Switches

Just to confirm, and even if possible, improve the results obtained from HFSS, the antenna design was relaunched in the well-known software CST. The simulation results of the optimized design are depicted in **Fig. 3.12**. Four cases were separately simulated. Unlike HFSS, CST provides an easy tool feature that allows the user not only to include switching control circuits but also simulate their impact on the antenna performance. Commonly used in control mechanisms in reconfigurable microstrip antennas are radio frequency (RF) PIN diodes. Furthermore, CST microwave studio offers the possibility to include S-parameters of PIN diodes. So, four diodes called D_1, D_2, D_3 and D_4 substituted for the ideal switches.

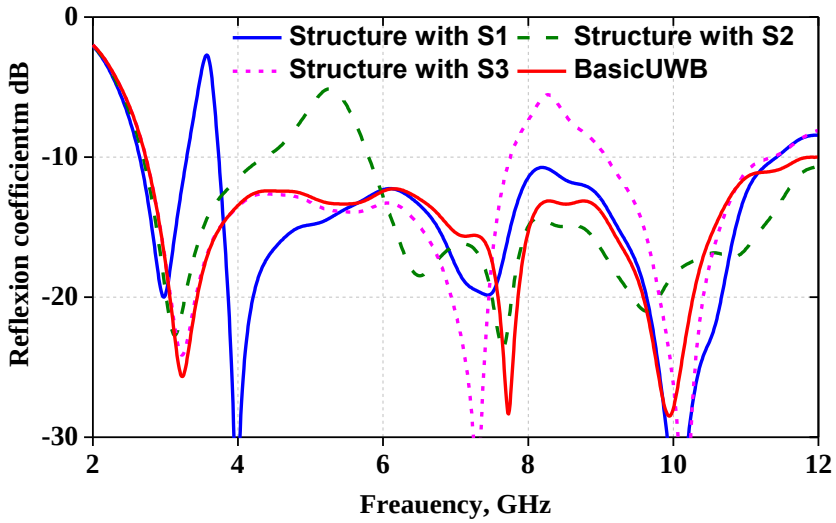

Figure 3.12. Modification of the initial structure for filtering functions purposes.

An analytical model is provided to express the functionality of the diodes as switches *ON*/*OFF*. The transmission line circuit that includes the equivalent RLC model of the diode is depicted in **Fig. 3.13**. The filtering functions are governed by controlling the effects of the slots, across which, four PIN diodes D_1, D_2, D_3 and D_4 are placed as shown in **Fig. 3.14(a)**. In order to make PIN diodes in switching modes, a biasing circuit is required to simulate the practical working conditions of the control circuit. As a result, the biasing circuit that was designed and included in the simulation of the antenna is given in **Fig. 3.14(b)**. This is consisting of separation slots and biasing lines. The PIN diodes, usually biased by a DC voltage, a separation between the positive and negative terminals of each diode is necessary. The PIN diode switching mode can be performed through the following mechanism:

- When a DC biasing power is applied forwardly to the diode and by gradually varying the amount of power, the diode acts as a variable resistor and allows the passage of RF signals (surface currents) at a certain value of DC power (100 mA). So, in this case the diode is at ON state (notch is deactivated).
- When zero or reversely biasing power is applied to the diode, the later looks like a very low capacitance and therefore it represents a very high impedance towards RF signal (surface currents). In this case, the PIN diode is at *OFF* state (notch active).

In CST, S-parameters of BAR50-02V PIN diodes **[13]** are used to represent the *ON* and *OFF* states of the diode.

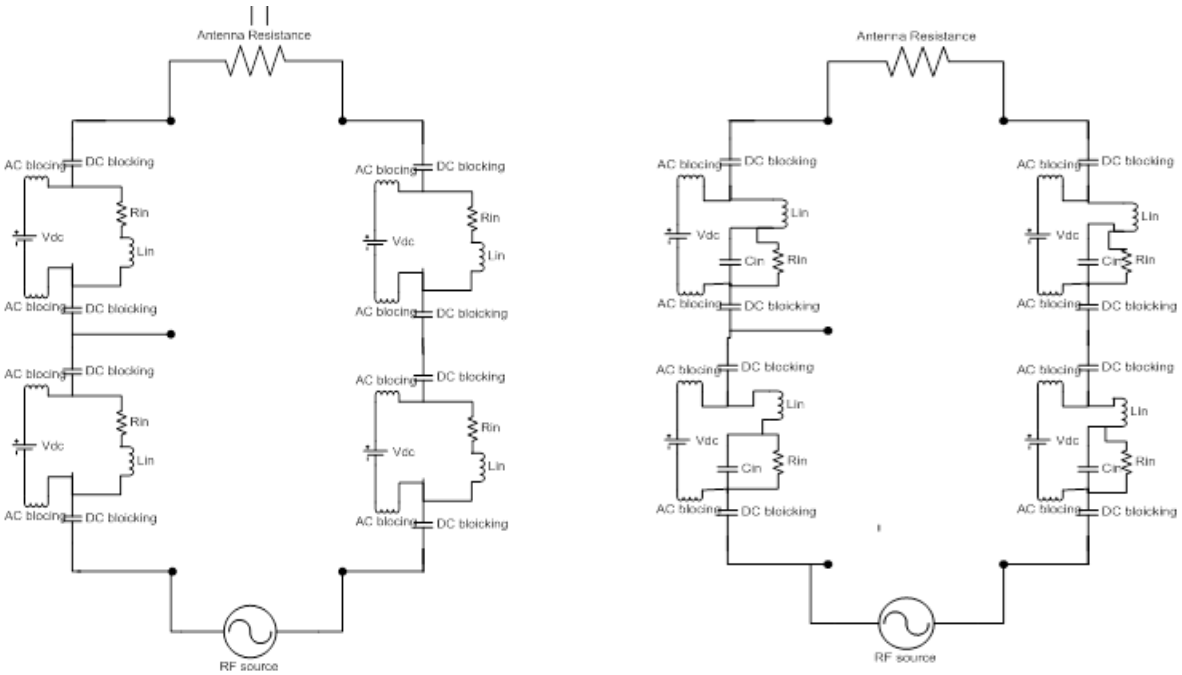

Figure 3.13 Transmission line model of the antenna including the diodes equivalent RLC circuit. (a) forward biasing; (b) reverse biasing.

To ensure the continuity of RF signals in the antenna across the separation slots, capacitive lumped components are inserted in the simulation model as RF capacitors with the value of C = 22 pF, as shown in **Fig. 3.14 (b)**. Additionally, inductive lumped components of the value L = 27 nH are introduced as Choke inductors to connect the biasing lines to the antennas. The role of the inductors is to isolate high frequency alternative and DC signals. Simulation of the antenna that includes diodes, capacitors, inductors, separation slots and biasing lines is carried out in

CST. The filtering functions were optimized through parametric refining the slots dimensions. Switching the diodes *ON* and *OFF*, the antenna provided eight operational states. **Table 3.1** summarizes these operating states together with the antenna filtering performances.

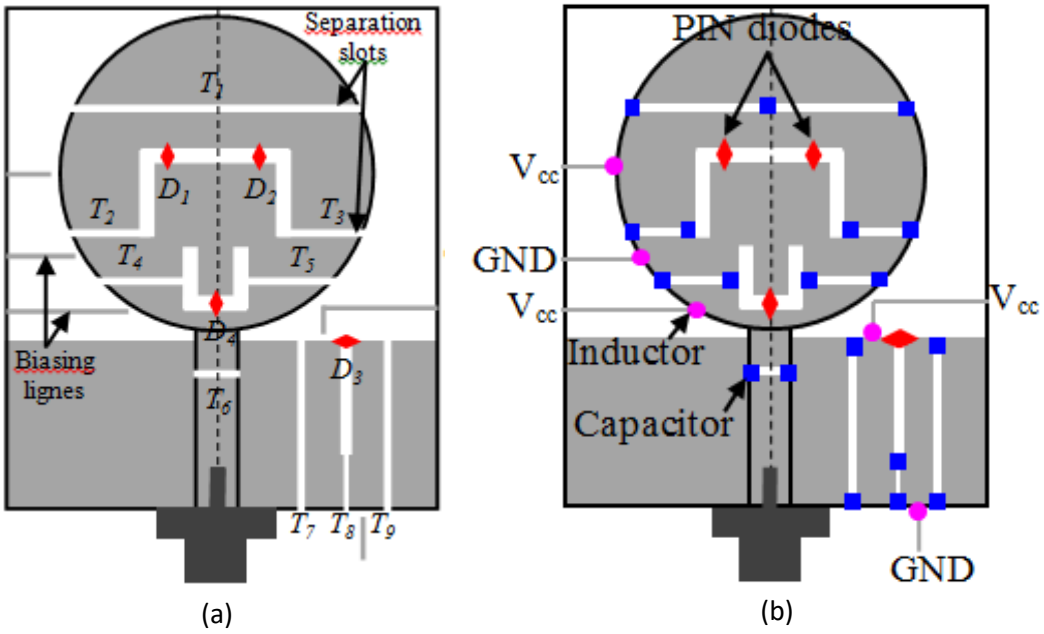

Figure 3.14. Design of the separation slots at the radiating patch and ground plane. (a) Slots: T_i (i = 1 to 9); Biasing lines; (b) RF components.

Table 3.1. Summary of the eight operational states of the antenna.

Antenna operating states		Diode switching states				Filtering performances		
		D_1	D_2	D_3	D_4	WiMAX (3.4-3.7) GHz	WLAN (5.0-5.3) GHz	ITU (8.0-8.4) GHz
Mode 1	State 1	*ON*	*ON*	*ON*	*ON*	-	-	-
Mode 2	State 2	*OFF*	*OFF*	*ON*	*ON*	x	-	-
	State 3	*ON*	*ON*	*OFF*	*ON*	-	x	-
	State 4	*ON*	*ON*	*ON*	*OFF*	-	-	x
Mode 3	State 5	*OFF*	*OFF*	*OFF*	*ON*	x	x	-
	State 6	*OFF*	*OFF*	*ON*	*OFF*	x	-	x
	State 7	*ON*	*ON*	*OFF*	*OFF*	-	x	x
Mode 4	State 8	*OFF*	*OFF*	*OFF*	*OFF*	x	x	x

3.6 Simulation Results

Simulating the final configuration in the platform of CST, the results showed that the proposed antenna can be reconfigured to work in eight distinct operational states which can be classified into four modes:

- Mode 1 includes state 1;
- Mode 2 includes state 2, state 3 and state 4;
- Mode 3 includes state 5, state 6 and state 7;
- Mode 4 includes state 8.

The first mode, from the reflexion coefficient curves shown in **Fig. 3.15(a)**, the antenna operational bandwidth covers completely the UWB spectrum (from 3 to 12 GHz) with reflexion coefficient being below -10 dB all over without filtering actions.

The second mode illustrated in **Fig. 3.15(b, c and d)** indicates that the operational bandwidth of the antenna covers the UWB spectrum in the range 3 to 11 GHz with the reflexion coefficient being less than -10 dB. However, three bands are filtered in each case of the three states. The filtering is achieved with the reflexion coefficient equals or greater than -5 dB. At state 2, the antenna is seen to filter the WiMAX band (3.4 - 3.7 GHz), **Fig. 3.15(b)**. At state 3, the antenna afects the WLAN band (5 - 5.3 GHz), **Fig. 3.15(c)**. At state 4, the antenna filters the ITU band (8 - 8.4 GHz), **Fig. 3.15 (d)**.

The third mode is illustrated in **Fig. 3.15(e, f and g)**. The antenna operational bandwidth covers the UWB spectrum from 3 to 11.9 GHz with the reflexion coefficient being less than -10 dB. However, the antenna is observed that it is filtering out simultaneously two bands when at the states 5, 6 and 7. At state 5, the antenna filters the two bands WiMAX at 3.5 GHz and WLAN at 5.1 GHz, as depicted in **Fig. 3.15(e)**. At state 6, the antenna filters the two bands WiMAX at 3.5 GHz and ITU at 8.2 GHz, see **Fig. 3.15(f)**. At state 7, the antenna filters the two bands WLAN at 5.1 GHz and ITU at 8.2 GHz, **Fig. 3.15(g)**.

The fourth mode which includes state 8 is given in **Fig. 3.15(h)**. The antenna operational bandwidth covers from 3 to 12 GHz, and it is seen that it filters the three bands simultaneously: WiMAX at 3.5 GHz, WLAN at 5.1 GHz and ITU at 8.2 GHz.

CST is based on the Finite Integration Technique (FIT), whereas HFSS is based on the Finite Element Method (FEM). Even though HFSS software simulation were carried out using

only ideal switches, HFSS results showed a little agreement with those obtained from CST. The lower performance obtained from HFSS is due to the use of ideal switches.

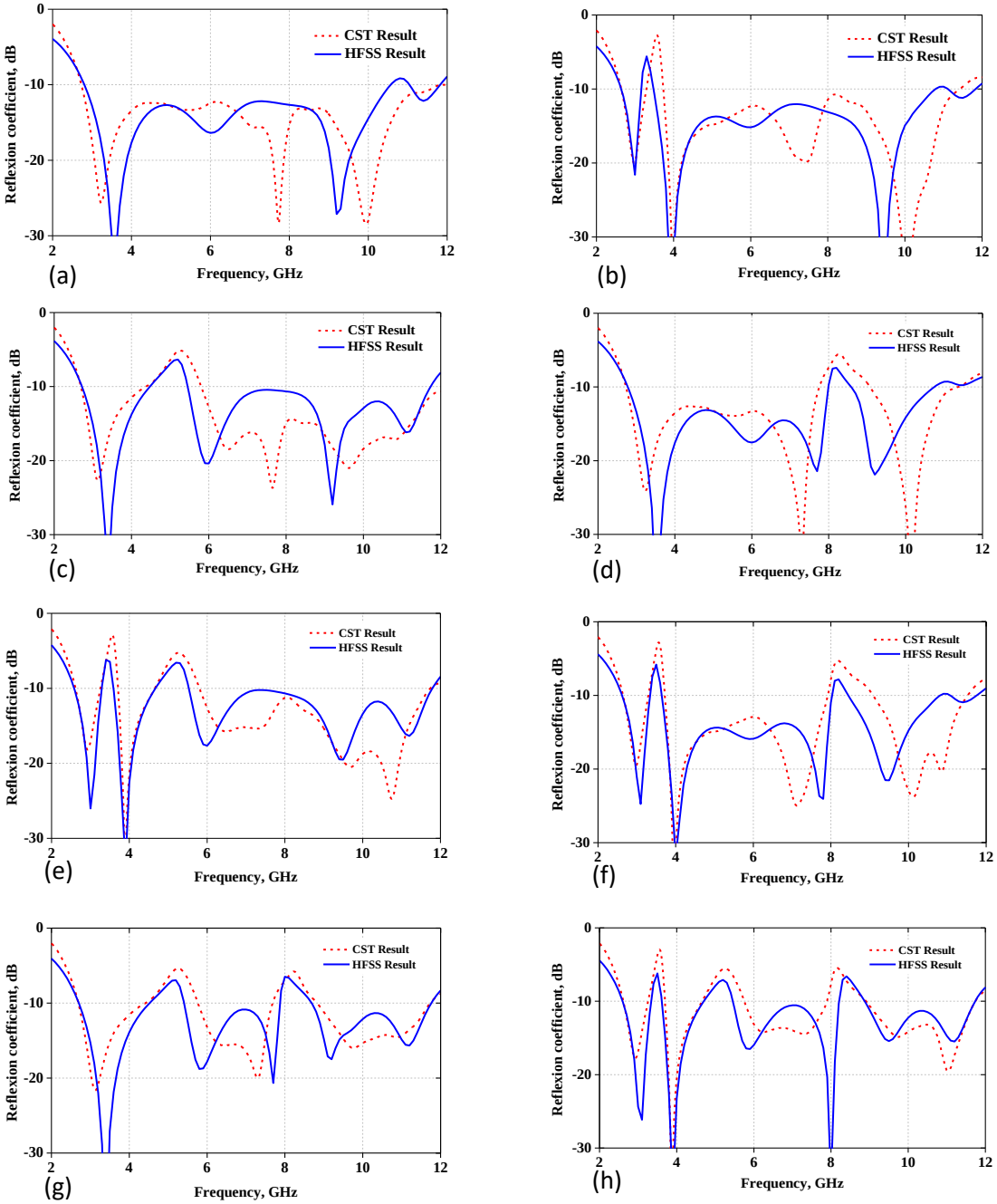

Figure 3.15. Simulation results of reflexion coefficients. (a) State 1 with UWB; (b) State 2 with notch at 3.5 GHz; (c) State 3 with notch at 5.1 GHz; (d) State 4 with notch at 2.8 GHz; (e) State 5 with notches at 3.5 and 5.1 GHz; (f) State 6 with notches and 3.5 and 8.2 GHz; (g) State 7 with notched at 5.1 and 8.2 GHz; (h) State 8 with notches at 3.5, 5.1 and 8.2 GHz.

To check on the contribution of the slots in the working mechanisms of the antenna, we visualized simulated surface current distribution of the final proposed antenna disposition in Mode 1 and Mode 2, shown in **Fig. 3.16**. As it can be seen, at Mode 1 (State 1), a uniform current distribution all over the structure is observed. This confirms the deactivation of the slots when the switches are set *ON*, that is the notch is deactivated. Meanwhile, strong current surround the slots at Mode 2 (State 2, State 3 and State 4). This confirms the role of the slots in generating the notch when the correspondent switches are set *OFF*.

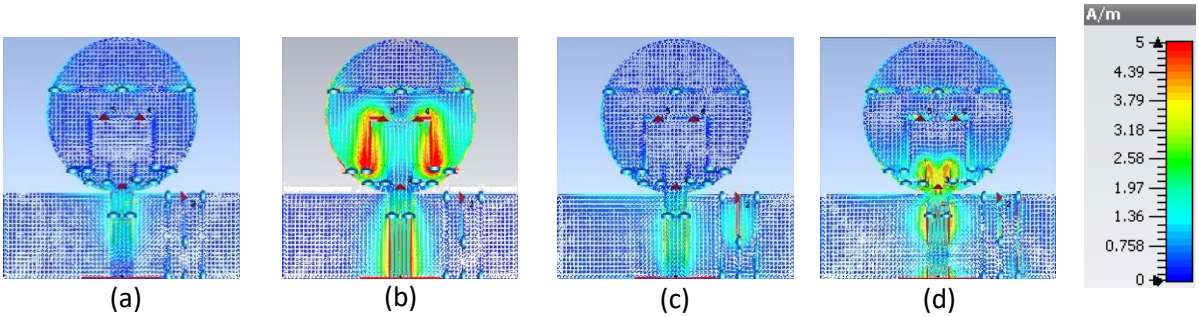

Figure 3.16. CST Surface current distributions of the antenna with real switches and the biasing circuit being considered. (a) State 1 with not notch; (b) State 2 with notch at WiMAX at 3.5 GHz; State 3 with notch at WLAN at 5.1 GHz; State 4 with notch at ITU at 8.2 GHz.

The simulated radiation pattern of the antenna with real switches at State 1 and State 8 are chosen to discuss the radiation performance of our proposed antenna. The radiation pattern polar plots given in **Fig. 3.17** and **Fig. 3.18**. These give information about the antenna radiation shapes and the maximum gain for the main lobes.

Firstly, at the three central notched frequencies 3.5, 5.1 and 8.2 GHz, the antenna shows omnidirectional radiation features at both E and H planes, as shown in **Fig. 3.17**. However, it is very important to mention the significant decrease of the gain at the notched frequencies for State 8 in comparison with that of State 1. The E-plane and H-plane radiation patterns are almost alike for State 1 and State 8. A very similar radiation pattern shape and almost the same maximum gain for State 1 and State 8 at the frequencies out of the notched bands 4.2, GHz and 9.5 GHz, as shown in **Fig. 3.18**.

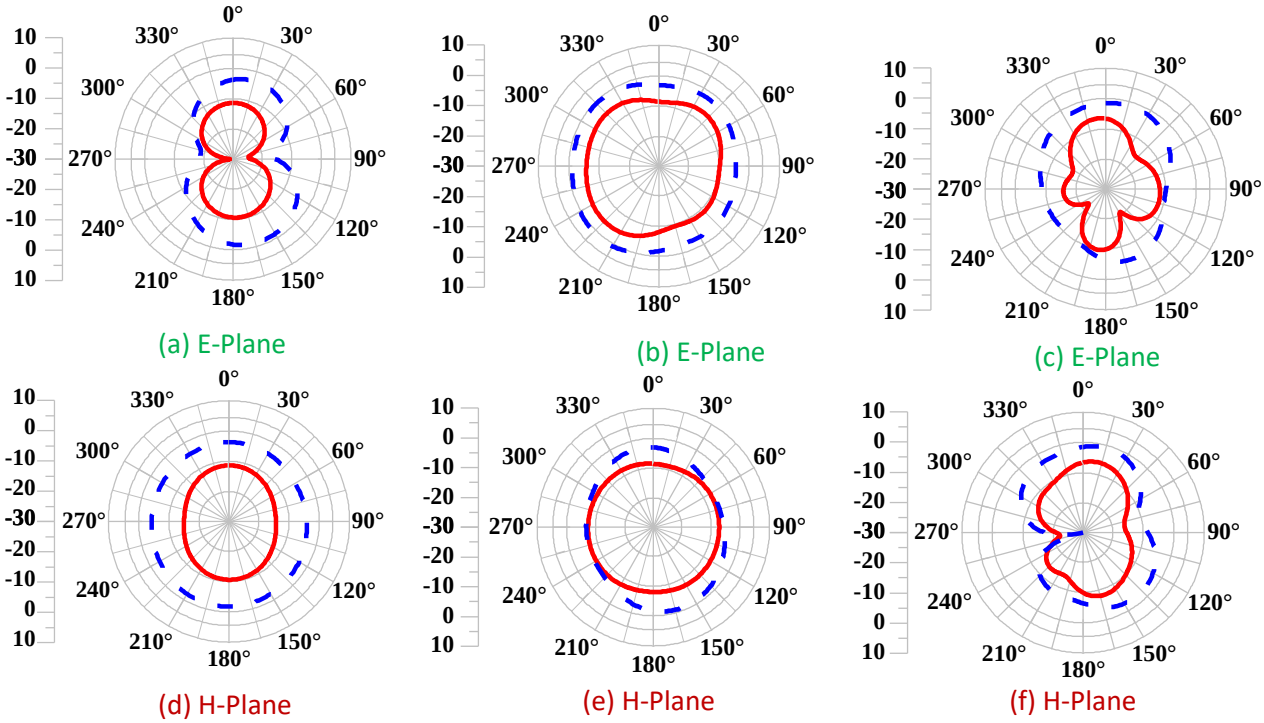

Figure 3.17. Radiation patterns as simulated in CST. (a and b) WiMAX 3.5 GHz; (c and d) WLAN 5.1 GHz; (e and f) ITU 8.2 GHz. E-plane=> ϕ=0° and θ [0° ; 360°], H-plane=>ϕ=90° and θ [0° ; 360°].

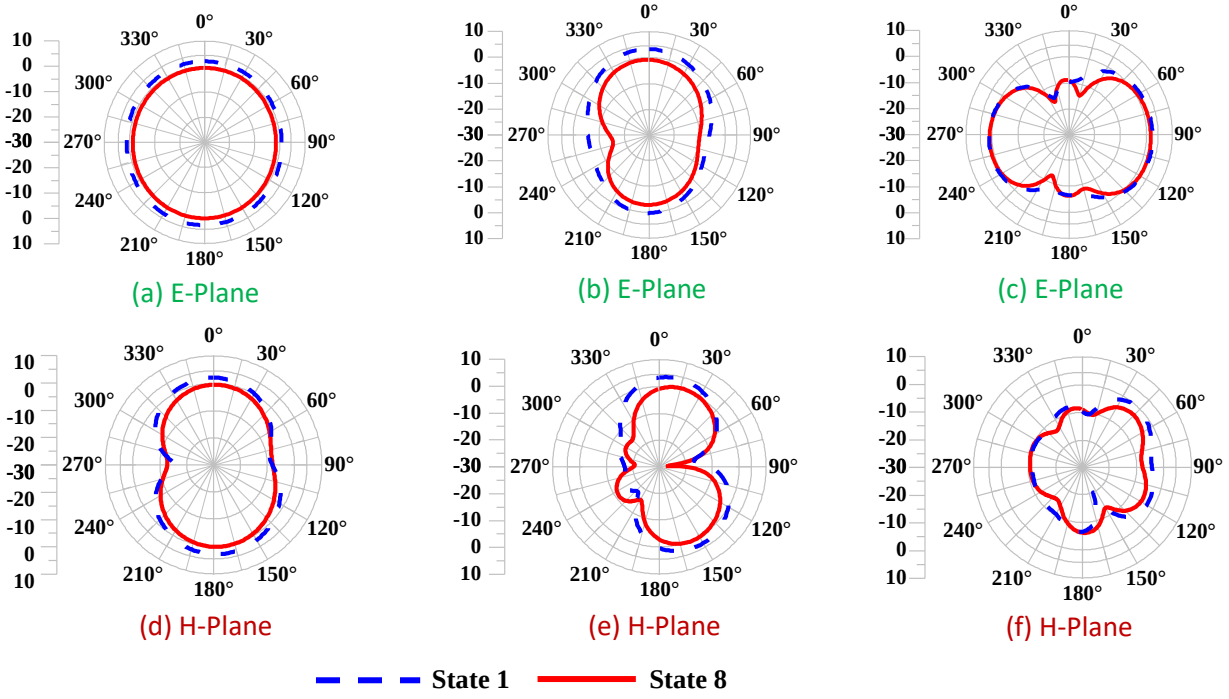

Figure 3.18 Radiation patterns simulated in CST (a and b) *at* 4.2 GHz; (c and d) at 6.7 GHz; (e and f) at 9.5 GHz. H-plane=>ϕ=90° and θ [0° ; 360°], H-plane=>ϕ=90° and θ [0° ; 360°].

It is worth noting the difference in the antenna gains when notches are activated (State 8) and deactivated (State 1). As shown in **Fig. 3.19**, at State 1, the antenna provides a positive gain that varies between 2 and 3 dBi. Whereas, at State 8, the antenna gain varies between 0 and 5 dBi at the frequencies outside the notched bands, and falls sharply at the notched frequencies 3.5, 5.1 and 8.2 GHz to the values -16, -4 and -8 dBi, respectively. This significant decrease in antenna maximum gain indicates that when notches are active, the antenna does not transmit or receive power at any of the three notched frequencies.

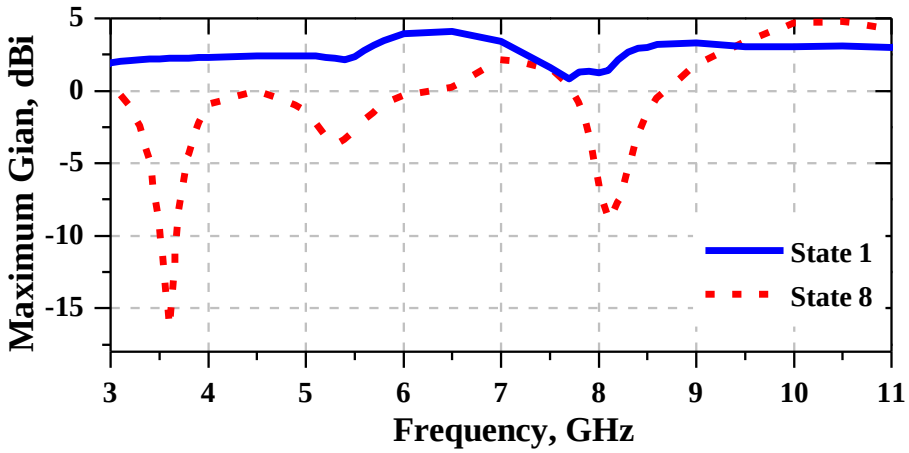

Figure 3.19. Frequency dependence of obtained antenna gain.

3.7 Comparison to Previous Designs

Our modest contribution has also been compared to data that have recently been published in the scope of this work. **Table 3.2** presents a summary of this comparison, where four key parameters were considered:

- ✓ The operating modes;
- ✓ The number of the switches (*n*);
- ✓ The dimensions of the design;
- ✓ The substrate.

In summary, the proposed antenna in **[6]** has the smallest size and used the lowest number of switches ($n = 2$), but offering only 4 operational modes. The proposed antennas in **[5]** and **[7]** have a larger size as compared to, have used more switches ($n = 3$), and offered the same number of operation modes, that is 4. The antenna of **[6]** showed the highest performance as compared

to the others [5,7]. The proposed antenna in [8] had additional operational modes (6) but at the expense of switches (it required *n*=4) and to some extent a larger size.

Our antenna, which has been designed on the low-cost substrate FR-4, has the same number of switches (*n*=4) in comparison to [8] and required a slightly larger size (30% extra), happily, it offers the highest number of operational modes, that is 8. This is the key feature of our design.

Table 3.2. Comparison of performance to literature.

Antenna	Number of operational modes	Number of switches (*n*)	Size in mm^3	Used substrate
Ref. [5]	1- UWB. 2- UWB with notch at 3.5 GHz. 3- UWB with notch at 5.5 GHz. 4- UWB with notch at 3.5 and 5.5 GHz.	3	40×30×0.8	FR-4
Ref. [6]	1- UWB 2- UWB with notch at 3.5 GHz. 3- UWB with notch at 5.7 GHz. 4- UWB with notch at 3.5 and 5.7 GHz.	2	25×25×0.8	FR-4
Ref. [7]	1- UWB. 2- UWB with notch at 5.3 GHz. 3- UWB with notch at 7.5 GHz. 4- UWB with notches at 5.3 and 7.5 GHz.	3	30.3×24.8×0.8	Rogers RT/Duroid 5880
Ref. [8]	1- UWB. 2- UWB with notch at 6.8 GHz. 3- UWB with notch at 8.7 GHz 4- UWB with notches at 6.8 and 8.7 GHz. 5- UWB with notches at 5.5 and 11.5 GHz. 6- UWB with notches at 5.5, 6.8 and 11.5 GHz.	4	30×31×0.8	Uknown
This work	1- UWB. 2- UWB with notch at 3.5 GHz. 3- UWB with notch at 5.1 GHz 4- UWB with notch at 8.2 GHz. 5- UWB with notches at 3.5 and 5.1 GHz. 6- UWB with notches at 3.5 and 8.2 GHz. 7- UWB with notches at 5.1 and 8.2 GHz. 8- UWB with notches at 3.5, 5.1 and 8.2 GHz.	4	35×35×1.6	FR-4

3.8 Conclusion

This chapter has discussed the design, the simulation and the optimization of a monopole microstrip UWB reconfigurable antenna. The study has shown the integration of a triple notched band into the monopole antenna. A detailed description was presented on the design and simulation processes undertaken on the basis of two well-known commercial softwares (CST

and HFSS). The obtained results showed promising performances. It remains to validate these results by an experimental work.

Bibliography

[1] A.H. Nazeri, A. Falahati, and R.M Edwards, "A novel compact fractal UWB antenna with triple reconfigurable notch reject bands applications", AEU-Int. J. Electron. Commun., 101, pp.1-8, 2019.

[2] M. Ur-Rehman, Q.H. Abbasi, M. Akram, and C. Parini, "Design of band-notched ultra wide band antenna for indoor and wearable wireless communications", *IET Microw. Ant. Amp. Prop.*, 9(3), pp. 243–251, 2014.

[3] K. Luo, W.-P. Ding, and W.-Q. Cao, "Compact monopole antenna with triple band-notched characteristics for UWB applications", *Microw. Opt. Technol. Lett.*, 56(4), pp. 822–827, 2014.

[4] J.J. Liu, K.P. Esselle, S.G. Hay, and S.S. Zhong, "Planar ultra-wideband antenna with five notched stop bands", *Electron. Lett.*, 49(9), pp. 579–580, 2013.

[5] N. Tasouji, J. Nourinia, C. Ghobadi, and F. Tofigh, "A Novel Printed UWB Slot Antenna with Reconfigurable Band-Notch Characteristics", *IEEE Ant. Wireless Prop. Lett.*, 12, pp. 922–925, 2013.

[6] B. Badamchi, J. Nourinia, C. Ghobadi, and A.V. Shahmirzadi, "Design of compact reconfigurable ultra-wideband slot antenna with switchable single/dual band notch functions", *IET Microw. Ant. Amp. Prop.*, 8(8), pp. 541–548, 2014.

[7] H. Oraizi and N.V. Shahmirzadi, "Frequency- and time-domain analysis of a novel UWB reconfigurable microstrip slot antenna with switchable notched bands", *IET Microw Ant. Amp. Prop.*, 11(8), pp. 1127–1132, 2017.

[8] Y. Li, W. Li, and Q. Ye, "A Reconfigurable Triple-Notch-Band Antenna Integrated with Defected Microstrip Structure Band-Stop Filter for Ultra-Wideband Cognitive Radio Applications", *Int. J. Ant. Prop.*, 2013.

[9] D. Valderas, Ultrawideband Antennas: Design and Applications, World Scientific, 2011.

[10] CST, Computer Simulation Technology software, www.cst.com.

[11] T.D. Nguyen, D.H. Lee, and H.C. Park, “Design and Analysis of Compact Printed Triple Band-Notched UWB Antenna”, *IEEE Ant. Wireless Prop. Lett.*, 10, pp. 403–406, 2011.

[12] ANSYS-HFSS, High Frequency Electromagnetic Field Simulation Software, www.ansys.com/products/electronics/ansys-hfss.

[13] I.T.AG, BAR50-02V - Infineon Technologies, www.infineon.com/cms/en/product/rf-wireless-control/rf-diode/rf-pin-diode/antenna-switch/bar50-02v/.

Chapter 4

Reconfigurable UWB CPW-Antenna with Two Notched Bands

IN the previous chapter, reconfigurable filtering functionality is implemented in conventional monopole UWB antennas, in which changes were acquired in both the ground and radiating patch planes. It is undesirable to alter the basic configuration of radiating patch for being the main source of the whole antenna radiations. Herein, we describe a compact and single layered UWB antenna with reconfigurable filtering functions. By aiming to save the geometry of the radiating patch, the biasing circuit has been implemented solely in the ground plane.

4.1 Literature Review

Due to the increasing number and variety of wireless systems sharing the frequency range 3.1- 10.6 GHz, and due to co-existence of narrow-bands wireless systems, in particular the WiMAX band (3.3-3.7 GHz) and the WLAN band (5.15-5.35 GHz), the ultra-wide band (UWB) systems usually suffer from major interferences obstacles. The implementation of reconfigurable coplanar waveguide (CPW) structure with reconfigurable filtering of WiMAX and WLAN has become an interesting research subject in view of how compactness and integration capabilities CPW design would offer to future antenna structure.

During this decade, a lot of work has been published on the subject. Symeon Nikolaou et *al.* **[1]** proposed two symmetrical prototypes of coplanar waveguide reconfigurable UWB antennas with notch functions at the band 5-6 GHz. In the first antenna, a U-slot was designed on the patch and controlled by micro-electro-mechanical system (MEMS) switch. In the second antenna, shown in **Fig. 4.1(a)**, two L-shaped λ/4 stubs are placed next to right and left edges of the patch where their connections to the patch are ensured by two MEMS switches, as shown in **Fig. 4.1(b)**. Both designs provide a satisfactory reconfigurable notching performance but at the expenses of the size and the notching frequency.

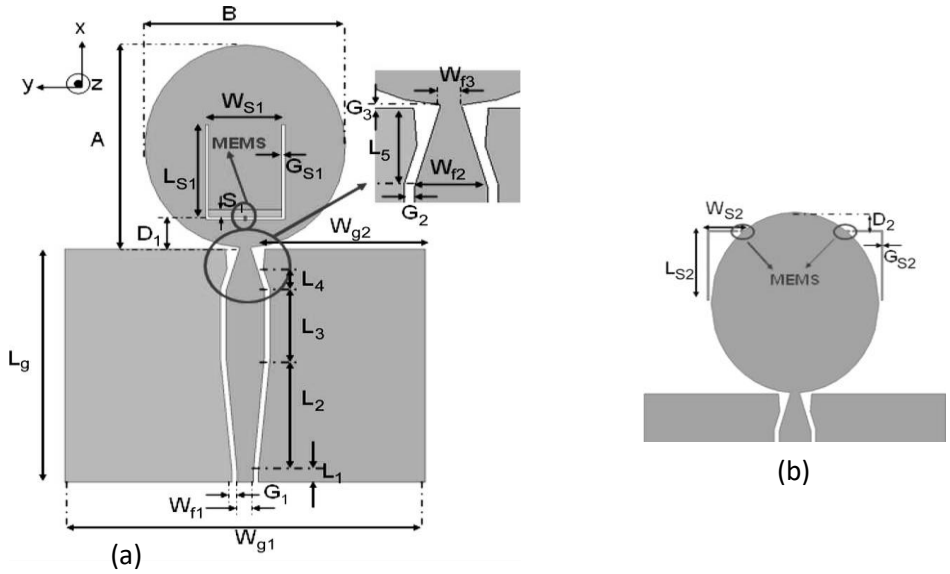

Figure 4.1. Single layer monopole UWB reconfigurable antennas [1].

(a) U-shaped slot-based antenna; (b) L-shaped stub-based antenna. Dimensions (mm): L_1= 1; L_2= 10; L_3= 6; L_4= 1.93; L_5= 3.7; W_{s1}= 5.6; G_{s1}= 0.2; L_{S1}= 8.8; D_1= 2.6; W_{S2}= 3.41; G_{S2}= 0.2; L_{S2}= 6.8; D_2= 1.8; W_{g1}= 26.8; W_{g2}= 12.25; W_{f1}= 1.28; W_{f2}= 2.97; W_{f3}= 0.85; S_1= 0.7; G_1= 0.05; G_2= 0.1; G_3= 0.11; L_g= 20; A= 18; B=15.3.

UWB CPW antenna proposed by Dimitris Anagnostou *et al.* [2] was a reconfigurable antenna that rejects the WLAN band 5-6 GHz. Its schematic view is shown in Fig. 4.2. It consists of CPW single sided structure printed on SiO_2 substrate. The WLAN band-notched behaviour is generated through the adoption of two λ/4 open-circuited stubs added to the edges of the antenna. To tune the notch, MEMS switches *ON* and *OFF* the notch and therefore, provided an efficient tunable rejection. However, MEMS controlling is difficult practically owing to the fact these are expensive and difficult to be integrated, in addition, the final prototype is usually vulnerable mechanically.

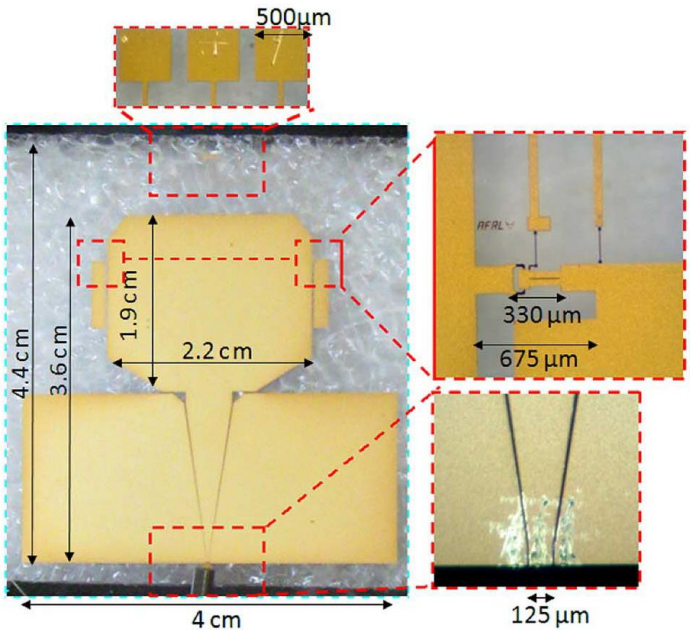

Figure 4.2. Single layer UWB MEMS reconfigurable antenna [2].

More filtering functions were successfully implemented in the coplanar waveguide UWB antennas proposed in [3] and [4]. In the first one, shown in Fig. 4.3, a single slot is implemented on the patch and five optical switches are positioned across this slot to control the current flow at their edges. The switching is controlled by an external light source fixed above the antenna surface. Four distinct notching functions could be produced at WLAN 2.4 GHz, WiMAX 3.5 GHz, WLAN 5 GHz and ITU 8 GHz.

The same control technique was undertaken in the UWB antenna proposed in [4], shown in Fig. 4.4, however, with less notching performance, since only two narrow bands can be filtered independently. In this design, complementary split ring resonators (CSRR) were designed on the circular radiating patch to generate the two notched bands at WiMAX 3.5 GHz and WLAN 5.1

GHz. The two notch functions are then controlled by two optical switches positioned at the external slot of each CSSR. Both designs offer a potent notching performance, however, the integration of source of light to control the switch is not usually easy.

It is worth mentioning that the notches and their reconfigurations were implemented in the patch. It is not a good thing since it is undesired to affect the antenna radiation characteristics which are mainly ensured by the radiation patch [5]. Herein; we propose a better way that takes advantage from the CPW-design and by bringing changes to the ground plane rather than the radiating patch which made our design outperform those cited in the literature.

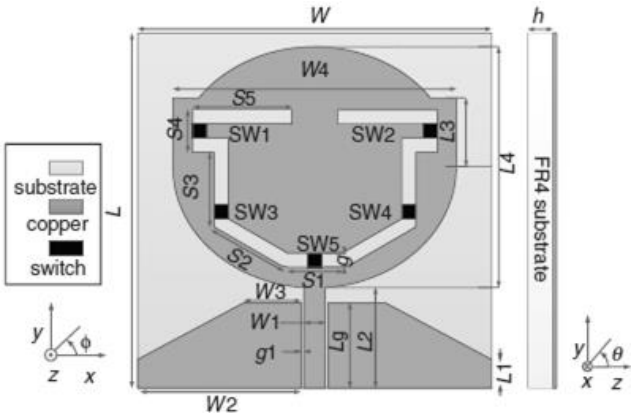

Figure 4.3. Single layer UWB optically reconfigurable antenna [3].

Dimensions (mm): TW= 25; W1= 1.5; W2= 11.5; W3= 4.05; W4= 20; L= 25; Lg= 6; L1= 2; L2= 7; L3= 5; L4= 17; S= 3.8; S2= 6.3; S3= 5.4; S4= 3; S5= 7; g = 1; g1= 0.25.

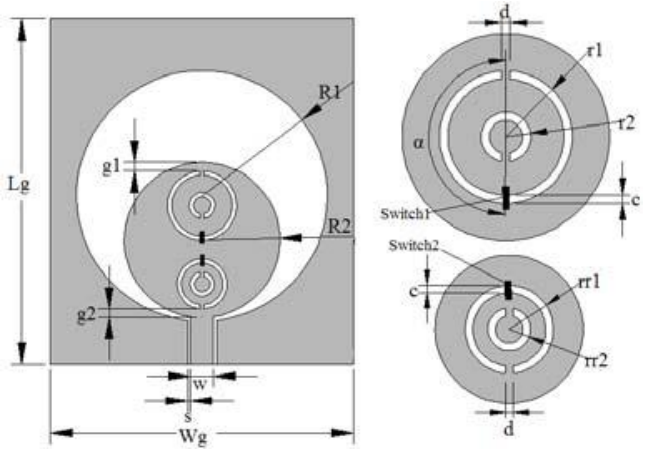

Figure 4.4. Single layer UWB optically reconfigurable antenna [4].

Dimensions (mm): Lg= 40; Wg= 35; w= 2.7; s= 0.3; g1= 1; g2= 1; R1= 14.5; R2= 9; r1= 4; r2= 1.5; rr1= 2.9; rr2= 1.4; c=0.5; d=0.5.

4.2 Basis structure of the proposed design

The basis structure we started with is shown in **Fig. 4.5**. The disposition was inspired from that proposed in **[6]**. A significant change was brought to their proposal. In fact, we replaced the originally microstrip feed line by a coplanar waveguide feed line. As such, the present antenna is compact and single layered. It consists of rectangular patch with a surrounding ground plane, both of which are printed on FR-4 substrate of thickness 1.57 mm, a permittivity of 4.3 and a loss tangent of 0.018. The initial dimensions of the disposition are 20×25 mm^2. We aim to keep the size as compact as possible. The SMA connector is included in the simulation from the start, in order to include its effect as in real environment. To obtain a good resonance in the spectrum region of UWB (3 to 11 GHz), significant changes were brought to the structure. To optimize the antenna response performance (S_{11} < -10 dB) at higher frequencies, the interior edges of the ground plane were modified. Their effect on the resonance frequencies are displayed in **Fig. 4.6(a)**. Meanwhile, at the lower frequencies the resonance is enhanced by changing the patch dimensions. This is done by introducing on it a slot which has controllable dimensions (the length and the width). The slot allows browsing over the optimal contribution of the patch dimensions, as shown in **Fig. 4.6(b)**.

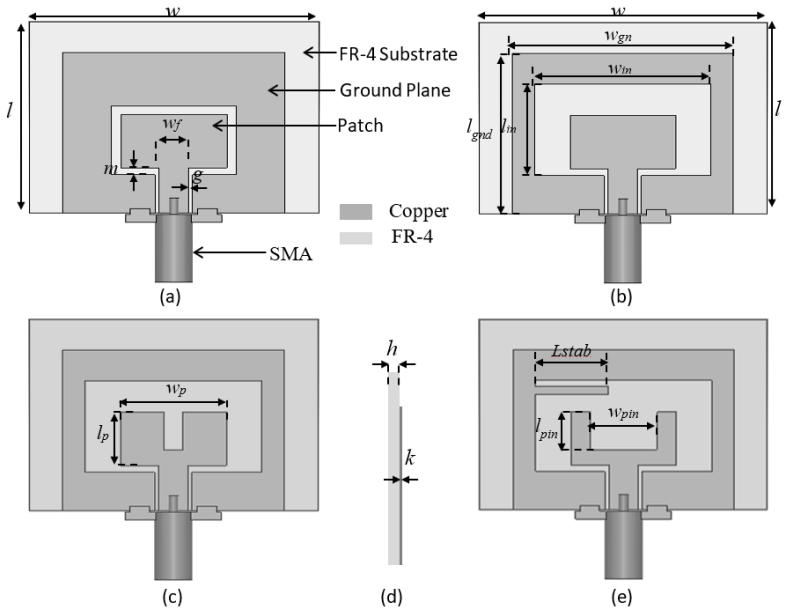

Figure 4.5 Design and modification of the basis UWB single layer structure.

(a) basic CPW UWB design; (b) Optimization of the interior edges of GND; (c) patch optimization; (d) side view of the structure; (e) combined optimization of the patch and GND. Final dimensions (mm): l= 25; w= 30; w_f=3; m=9; g=0.43; w_{gnd}=24; l_{gnd}=20; w_{in}=19.2; l_{in}=12; l_p=7; h= 1.57; k=0.035; w_p=12.5; l_{pin}=5; w_{pin}=9; $Lstab$=4.9.

In order to adjust finely the resonance at mid-band frequencies, a stub is added inside the ground plane, and thus allowing us to get a compromise between the radiating patch and the ground plane, as shown in **Fig. 4.6 (c)**. CST has been used in the simulation.

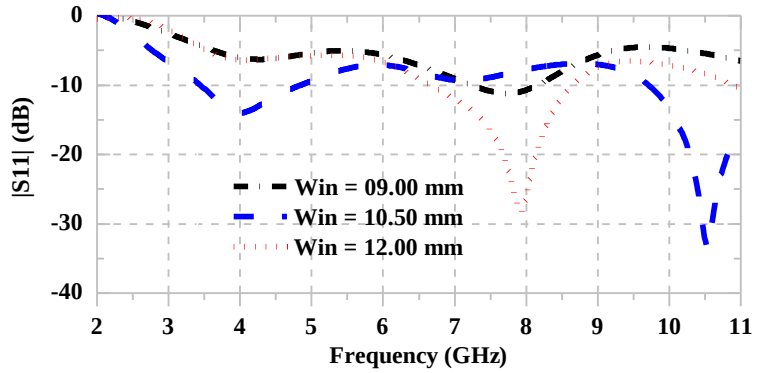

(a)

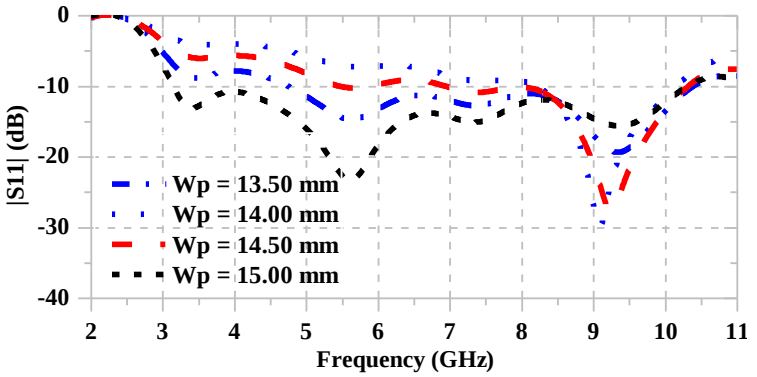

(b)

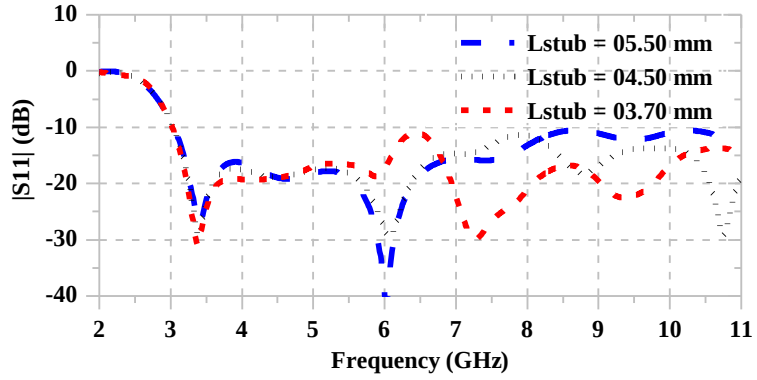

(c)

Figure 4.6. Optimization of the slots' dimensions.

(a) Optimization of the slot S_{WiMAX}; (b) Optimization of the slot S_{WLAN}; (c) Combined S_{WiMAX} and S_{WLAN}.

4.3 Implementation of the Notches

The concept of the λ/2 slot, discussed previously is used to design and optimize the dimensions of two open-ended slots introduced to our final design. This filtering design method is appropriate in our case since it does not require an extension to the size of the basis structure.

We aim first to generate a notch for WiMAX 3.5 GHz band. Consequently, an open-ended slot named S_{WiMAX} is etched in the ground plane as shown in **Fig. 4.7(a)**. The notch has been obtained after searching for the optimal position and dimensions of the slot S_{WiMAX}. A demonstration of such a process from CST results is depicted in **Fig. 4.8**. The same process was followed in order to introduce another open-ended slot named S_{WLAN} as illustrated in **Fig. 4.7(b)**, to be able to generate the notch around the WLAN 5.1 GHz band. By visualizing current distribution variations in accordance to those of the impedance bandwidth of the antenna, the slots S_{WiMAX} and S_{WLAN} were positioned on the left wing and on the right wing of the ground plane, respectively.

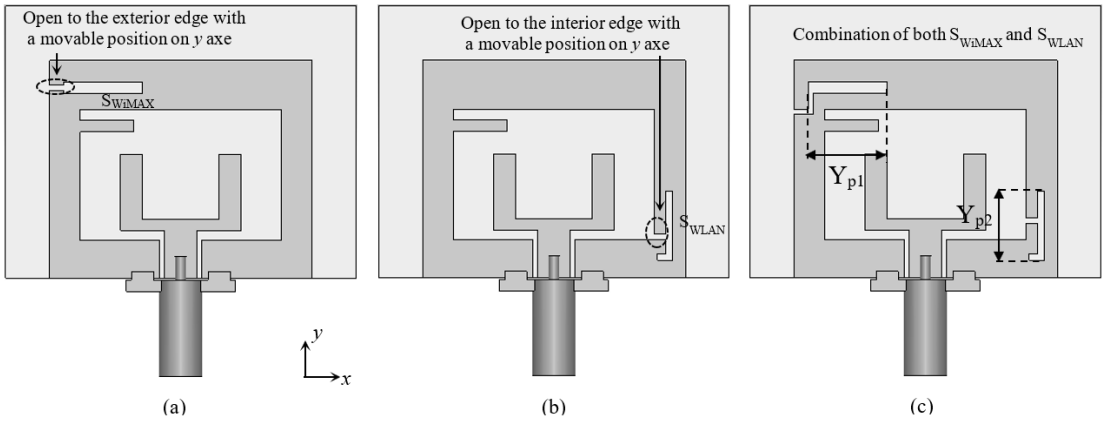

Figure 4.7. Implementation of the slots in the basis UWB structure.

(a) Slot design for WiMAX filtering, (b) Slot design for WLAN band filtering, (c) Combined design for WiMAX and WLAN filtering.

Then, the lengths of the slots are altered carefully till notch actions started to take effect by observing the antenna resonance. Thus, as shown in **Fig. 4.8(a and b)**, the filtering notches level and the central frequency was seen to vary in response to changes in the slots' lengths. Obviously, the best notch performance is obtained when the length of each slot is equal to the λ/2 at each central frequency of the two bands WiMAX (3.30-3.70 GHz) and WLAN (5.00-5.30 GHz). The

two slots, optimized in their dimensions, were inserted together in the structure as depicted in **Fig. 4.7(c)**. Combining the slots aims to take into consideration the effect of each slot on the other. The obtained simulated result is shown in **Fig. 4.8(c)**.

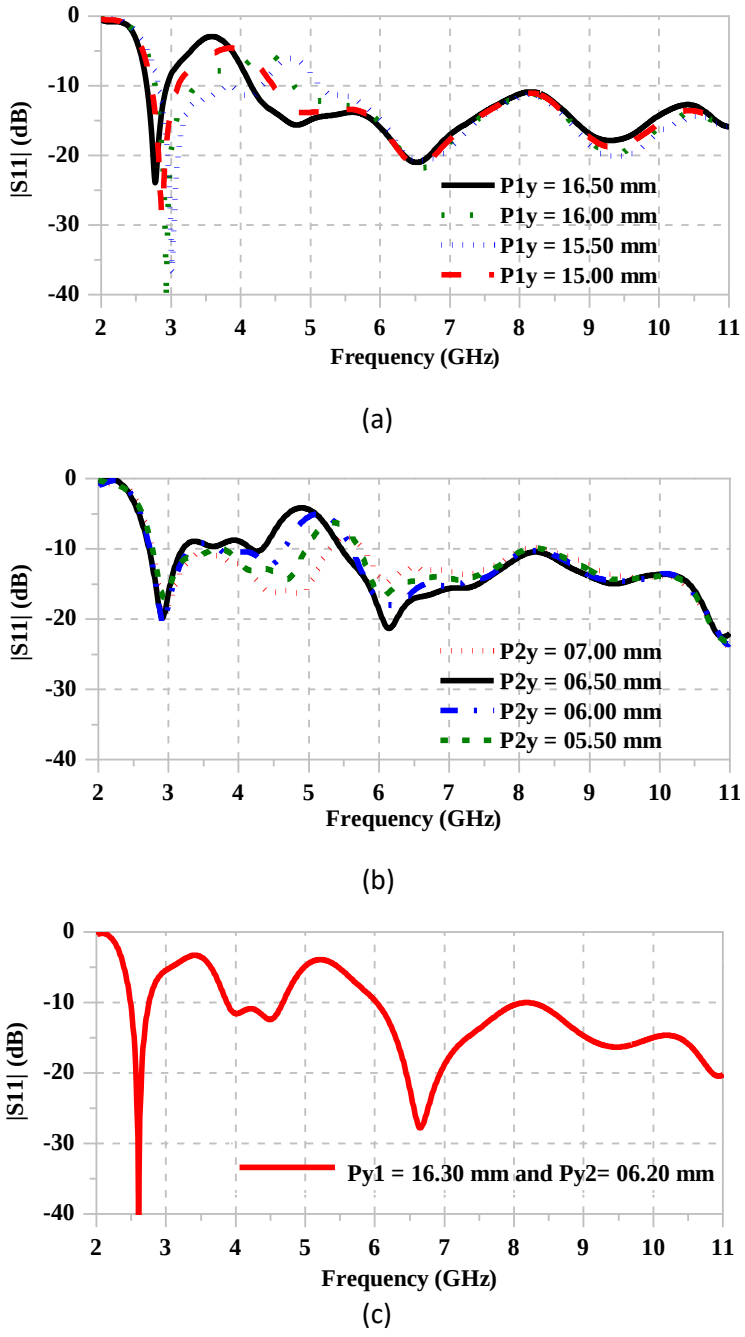

Figure 4.8. CST simulations show the optimization process of the slots' dimensions.

(a) Optimization of S_{WiMAX}, (b) optimization of S_{WLAN}, (c) Both slot combination resonance.

4.4 Reconfiguration with Ideal Switches

Herein, we implement the filtering reconfiguration. Such a process is controlled via activating and disactivating the slot effect, whose monitoring is followed through looking at the current distribution. By closing the slots at their open ends, which is done via the setting a metallic stub across them, the current flows through the stubs and affects the latter distribution around the slot. In order to represent the closed state of the slots, two metal stubs are placed across the open end of each slot. Assuming that the stub are ideal switches, four switching configuration cases may occur. These cases are depicted in **Fig. 4.9**.

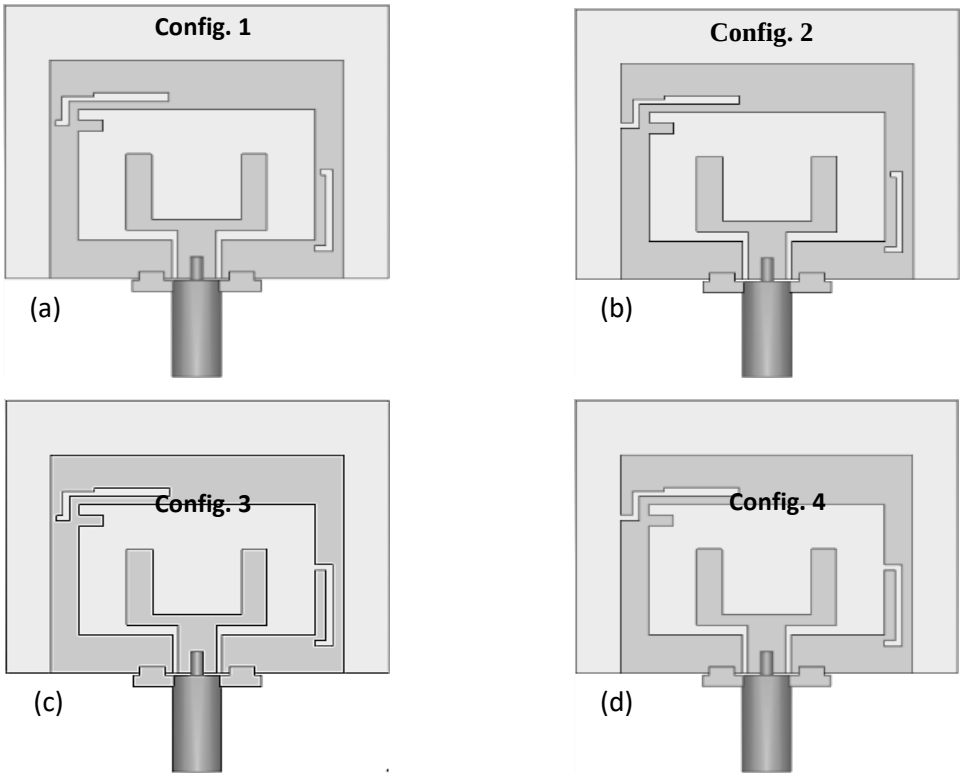

Figure 4.9. Switching configuration cases of the antenna.

Config. 1: *ON*/*ON*; Config. 2: *ON*/*OFF*; Config. 3: *OFF*/*ON*; Config. 4: *OFF*/*OFF*.

The switches serve to activate and disactivate the slots' effect which in turn controls the current flow around the slots' edges which in turn allows a control over the filtering functions. The current distribution of the antenna assuming an ideal switching control is depicted in **Fig. 4.10**. Our analysis is focalised particularly onto the two interesting frequencies 3.5 and 5.1 GHz in dependence on the switches S_{WiMAX} and S_{WLAN}. **Table 4.1** presents the switching cases in relation to the four possible configurations. Accordingly, every time a slot is closed (*OFF*), there

is a normal current flow around the slot edges (Config. 1 at 3.5 and 5.1 GHz), (Config. 2 at 5.1 GHz), (Config. 3 at 3.5 GHz). When a slot is open (*ON*), there is a strong current flow around the slots' edges, represented by the cases (Config. 2 at 3.5 GHz), (Config. 3 at 5.1 GHz) and (Config. 4 at 3.5 and 5.1 GHz). Hence, the current distribution around the slots can be easily controlled through ideal s witches. In other words, an ideal reconfigurable filtering is implemented in the basic UWB antenna structure. A simulation of this design which includes ideal switches has been carried out using CST microwave studio for the four configuration cases. **Fig. 4.11** shows the simulation results. It indicates that in Config. 1 there is no filtering action. While, in Config. 2 and Config. 3 the bands WiMAX at 3.5 GHz and WLAN at 5.1 GHz are filtered out. Meanwhile, in Config. 4, both bands are filtered simultaneously.

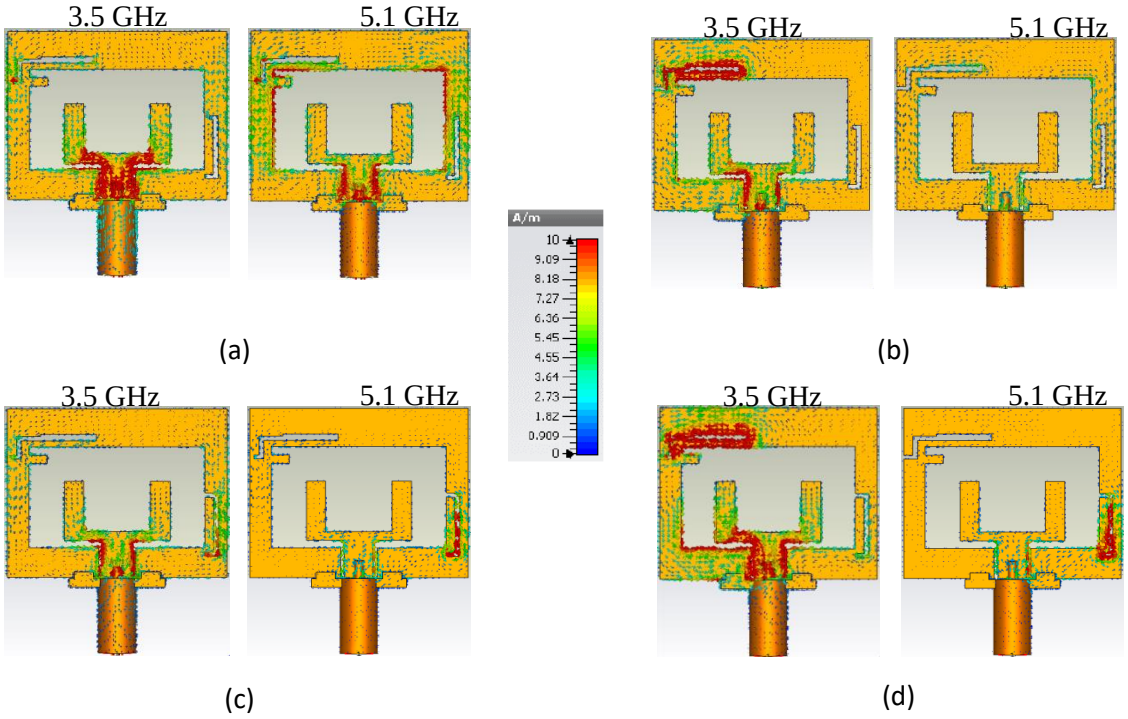

Figure 4.10. Surface current distribution at the notched frequencies.

(a) Config. 1; (b) Config. 2; (c) Config. 3; (d) Config. 4.

Table 4.1. Ideal switching configuration cases.

Configurations	Ideal slot control	
	S_{WiMAX}	S_{WLAN}
Config. 1	*OFF*	*OFF*
Config. 2	*ON*	*OFF*
Config. 3	*OFF*	*ON*
Config. 4	*ON*	*ON*

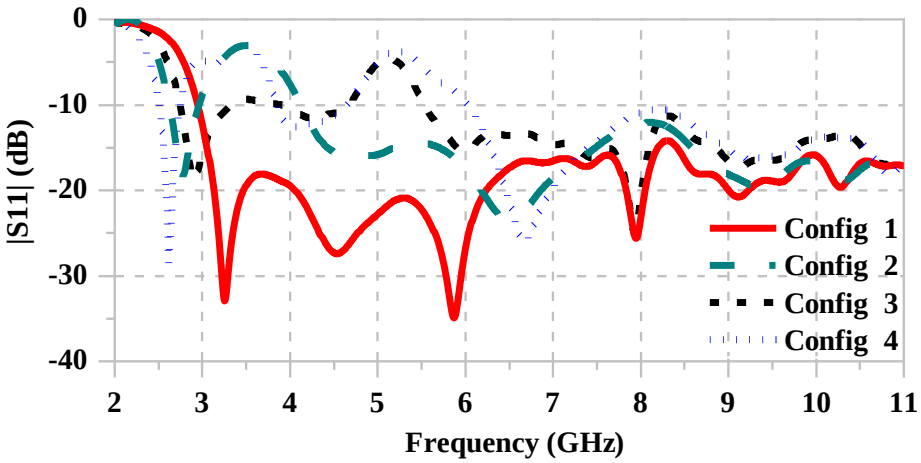

Figure 4.11. Simulation results of the antenna according to an ideal switching case.

4.5 Reconfiguration with Real Switches using PIN Diodes

Herein, real switches are implemented the design simulation. The ideal switches, the stubs, have been replaced with discrete ports represented by PIN diodes, BAR 50-02V PIN diode, with their circuit diagram shown in **Fig. 4.12**. In the Appendix B, a brief description on the PIN diode is provided. It is possible to switch from a state *ON* to a state *OFF* using BAR 50-02V PIN diode to control the current flow at the open end of the slots.

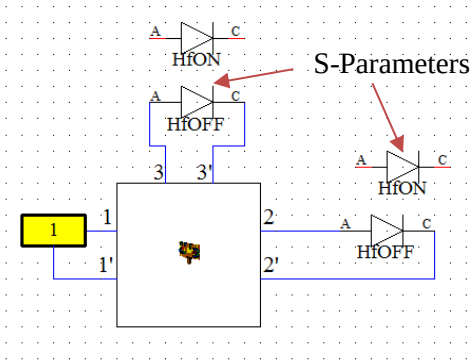

Figure 4.12 The insertion of S-parameter files using CST design studio.

Prior to the experimental fabrication, an extensive optimization has been undertaken that even included taking into consideration of any undesirable effect due to the switching control circuit. As shown in **Fig. 4.13**, the filtering monitoring was conceived for each slot separately. The black spots at the open end of each slot represents the discrete port where the PIN diode

should be inserted. The continuity through the separations slots is ensured by the use of capacitors of 22 pF. The simulated and finally optimized results of the slots' dimensions for the real switches case are shown in **Fig. 4.14**.

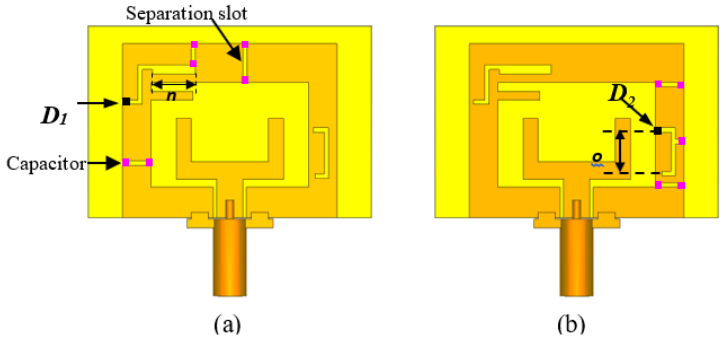

Figure 4.13. Antenna schematic assumed in the ca se of real control circuit of the two filtering functions. (a) Control design of S_{WiMAX}, (b) Control design of S_{WLAN}.

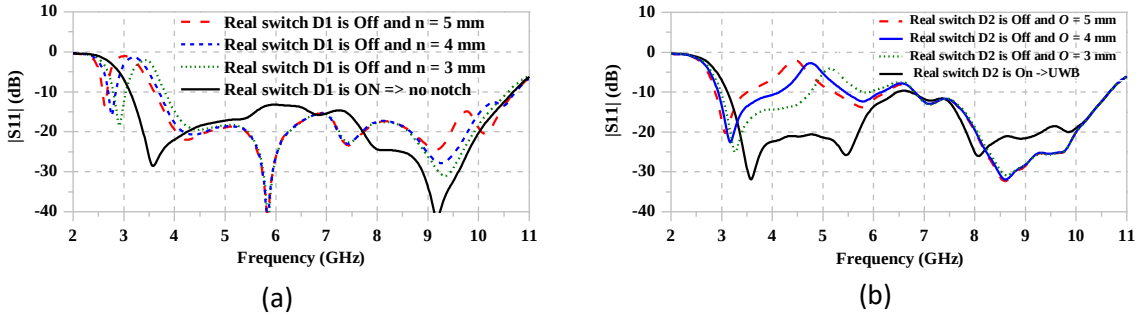

Figure 4.14. Simulated results obtained assuming real switches. (a) Optimization of S_{WiMAX}; (b) Optimization of S_{WLAN}.

Thereafter, combining the biasing circuits of S_{WiMAX} and S_{WLAN} has been performed in the configuration as depicted **Fig. 4.15**. Four arms were added to the design facilitating the connexion of the external biasing source to the structure. However, to prevent AC signals from reaching DC sources, inductive contacts were required between the biasing arms and the structure. This was done by inserting an inductive lumped element at each of the four contacts, as shown in the figure as indicated by the blue spot.

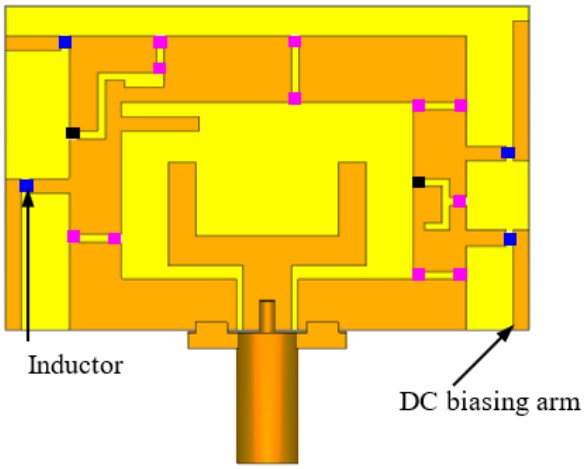

Figure 4.15. Antenna schematic after the insertion of the filtering control slots and the biasing arms.

Simulation of such a disposition in CST design studio assuming the four possible states gave the results depicted in **Fig. 4.16**.

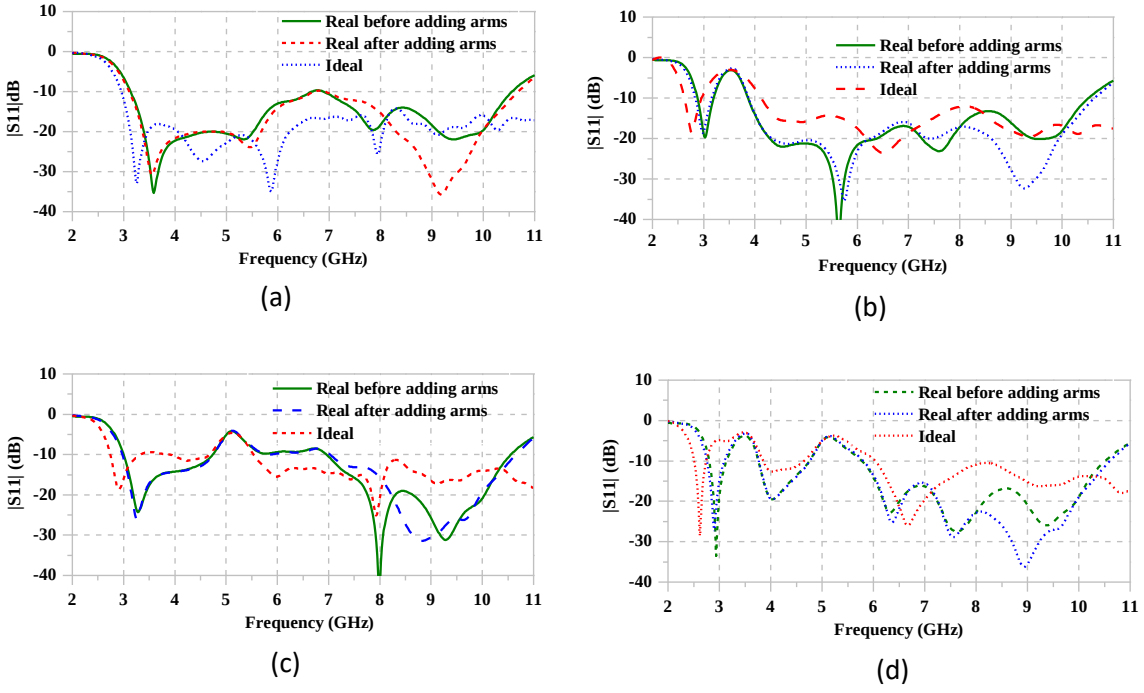

Figure 4.16. Comparative performances between ideal and real switches. (a) *ON/ON*; (b) *OFF/ON*; (c) *ON/OFF*; (d) *OFF/OFF*.

Surface current distributions simulated of the final antenna disposition are shown in **Fig. 4.17**, where we give a particular attention to the frequencies of interest: 3.5 and 5.1 GHz. **Table 4.2** presents the four operational states of the antenna with the resulting notching functions.

- In State 1, it is clear that the current distribution is barely uniform, an indication that the slots are not functional while both diodes are in ***ON*** state. This does not bring any notching action at both frequencies of interest.
- In state 2, it shows a high current density near the slot S_{WiMAX} at the frequency 3.5 GHz, but not that important at 5.1 GHz. Thus, the notch is obtained at 3.5 GHz which confirms the impact of S_{WiMAX}.

Table 4.2. Notching functions as related to switching states.

Antenna states	Diodes switching states		Notching function	
	Diode 1	Diode 2	WiMAX	WLAN
State 1	*ON*	*ON*	-	-
State 2	*OFF*	*ON*	X	-
State 3	*ON*	*OFF*	-	X
State 4	*OFF*	*OFF*	X	X

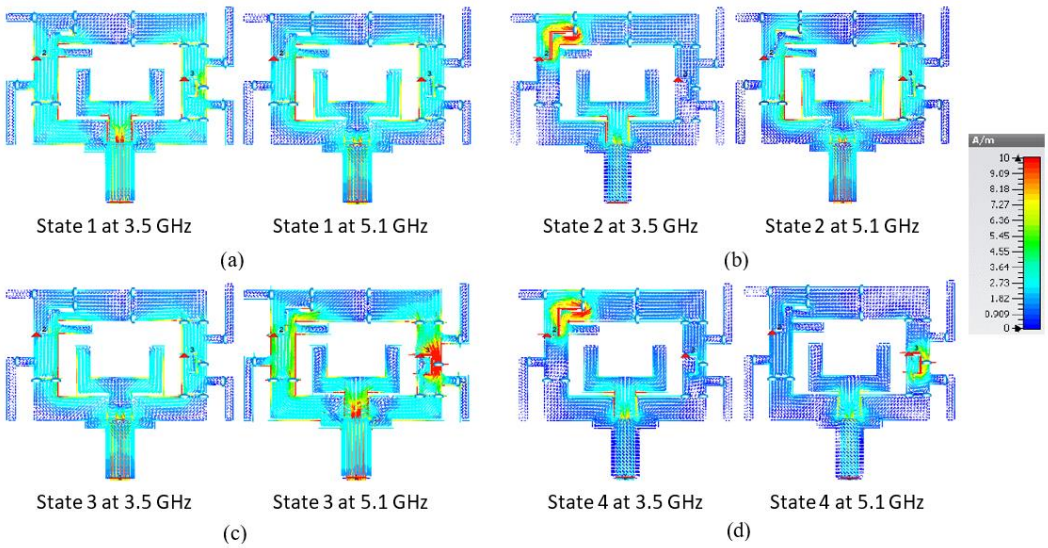

Figure 4.17. Simulated current distribution assuming real switches.

- In state 3, Diode 1 set ***ON*** and Diode 2 is ***OFF***, a notch at 5.1 GHz has occurred. A high current density is observed around the slot S_{WLAN} at 5.1 GHz and a normal distribution is observed at 3.5 GHz.

- In state 4, both frequencies 3.5 and 5.1 GHz are notched with both diodes being at the state ***OFF***. A high current density is observed around both slots S_{WiMAX} and S_{WLAN}.

4.6 Prototyping

As shown in **Fig. 4.18**, a prototype of the final design, which was fabricated using a single faced copper clad FR-4 substrate of the thickness of 1.57 mm and a permittivity of 4.3. The copper clad was 0.035 mm thick. BAR 50-02V PIN diodes were employed as switches in the antenna. Their operating frequency ranges from 10 MHz up to 6 GHz. This kind of diodes is suitable in mobile communication antenna as a switch. This diode in particular offers a very low capacitance at zero volt (0.15 pF). It has a low forward resistance and a very low harmonic distortion. Its reverse voltage (V_r) can be risen up to 50 V and its forward current (I_f) is 100 mA. The capacitors are used to match RF connectivity through the slots, and as such, the capacitance should be of high values according to $X_C = 1/(2\pi fC)$. The RF Choke inductor of 27 nH was used. Inductors are used to block RF signals in which low inductive reactance is required to stop reverse bias AC signals $X_L = 2\pi fL$ at frequencies above 1 GHz.

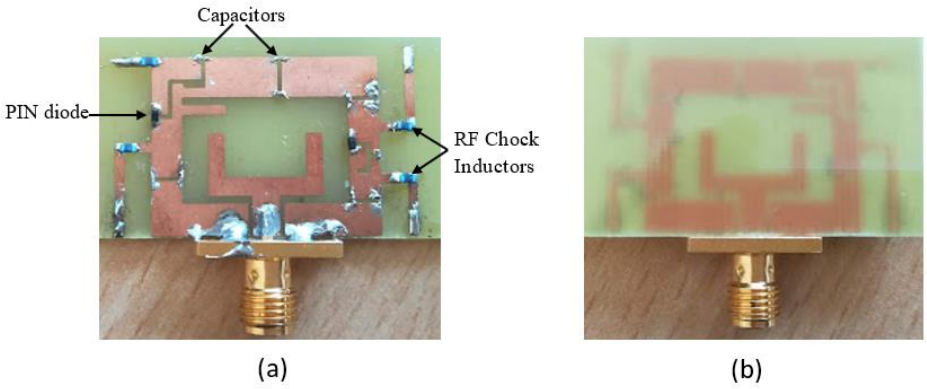

Figure 4.18. The fabricated prototype with RF components and SMA. (a) Top view (b) Bottom view.

4.7 Measurements and Discussion

The reflexion coefficient $|S_{11}|$ at the antenna port was gauged using Aritsu® 37397C (0.04–65 GHz) vector network analyser (VNA). The FR-4 substrate is made intentionally larger in order to allow adding the arms as well as soldering the external biasing wires. DC voltage source with two output channels is used to provide DC signals to bias the PIN diodes.

4.7.1 Measurements of the Reflexion Coefficient $|S_{11}|$

The experimental setup to measure the reflexion coefficient $|S_{11}|$ is pictured in **Fig. 4.19**. The results of the measurement are depicted in **Fig. 4.20** along with those of the simulation in dependence on the four switching states according to **Table 4.2**. It can be seen that the measured and simulated results agree well in all the switching states. Accordingly, the antenna is seen to offer a broad bandwidth extending from 3 to 10.5 GHz, thus includes the UWB range, and a reflexion coefficient that is less than -10 dB. Furthermore, it is able to filter WLAN (5.1 to 5.3 GHz) when it is configured in state 2 and WiMAX (3.3 to 3.6 GHz) when it is reconfigured in state 3. Moreover, it is able to filter simultaneously the two bands when it is configured in state 4.

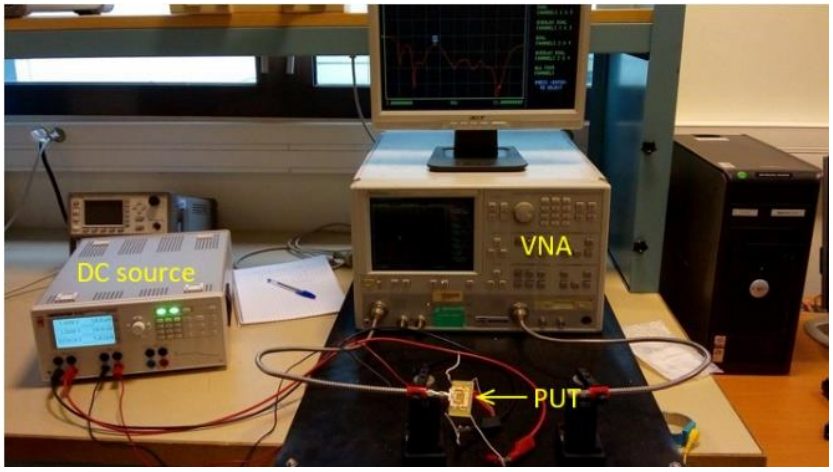

Figure 4.19. Reflexion coefficient Measurement using a vector network analyser (VNA).

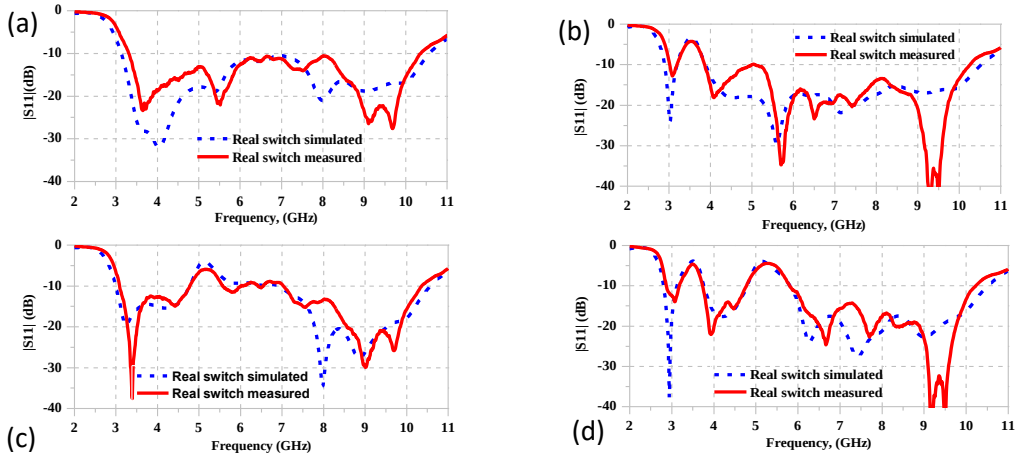

Figure 4.20. Measured and simulated Frequency dependence of $|S_{11}|$.

(a) State 1; (b) State 2; (c) State 3; (d) State 4.

4.7.2 Radiation Performance Measurements

The measured radiation patterns of the antenna in both E- and H- planes were carried out in anechoic chamber, its setup is shown in **Fig. 4.21**.

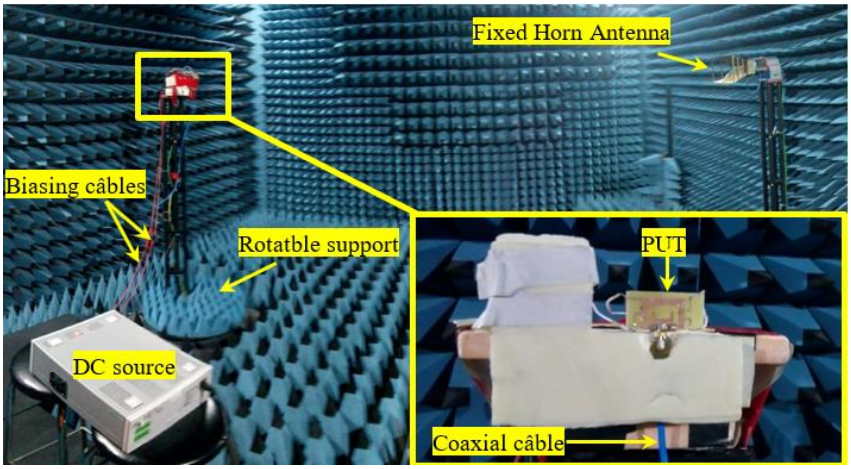

Figure 4.21. Radiation performance measuring setup in the anechoic chamber.

The measured and simulated results of the radiation patterns are presented together for comparison reasons in **Figs. 4.22** and **4.23**. The radiation pattern of both state 1 and 4 are gathered in the same figure in order to enhance discrepancies between the two states. **Fig. 4.22** shows the radiation pattern at the filtered frequencies 3.5 and 5.1 GHz. As it can be noticed, omnidirectional radiation patterns are a shared feature in this design which is ideal for UWB systems. It is worth noting that a gain reduction by more than -10 dBi is observed of the radiation patterns at the filtered frequencies 3.5 and 5.2 GHz. This actually illustrates the successful filtering process. The same properties are obtained at frequencies out of the notches 4.2 and 6.7 GHz for E- and H-planes as shown in **Fig. 4.23**. However, the patterns are almost similar for both states 1 and 4 at these frequencies. For checking reasons, the dependence of the maximum gain on the frequency at the four switching was measured and is depicted in **Fig. 4.24**. As it can be observed, a maximum average gain lying between 2 and 5 dBi is attained in the four switching cases. However, the minimum gain, which is about -10 dBi, is observed in state 2 at 3.5 GHz, state 3 at 5.2 GHz and State 4 at simultaneously 3.5 and 5.2 GHz.

These considerable reductions in the maximum gain are a clear indication on the successful implementation of the two filtering functions at 3.5 and 5.2 GHz in the present proposed antenna.

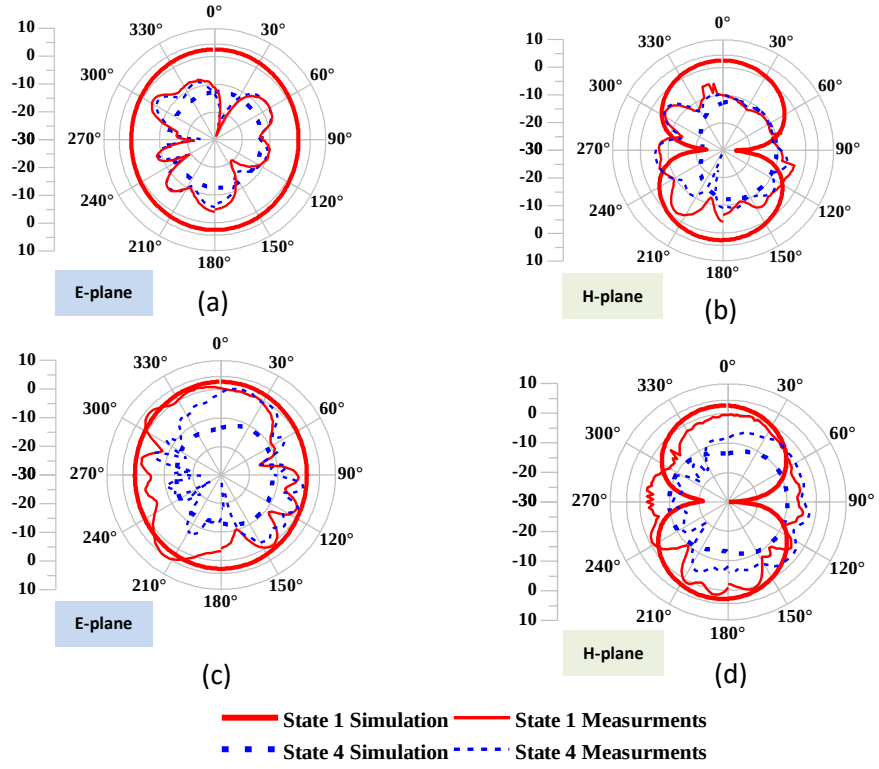

Figure 4.22. Radiation patterns at notch frequencies. (a and b) 3.5 GHz; (c and d) 5.1 GHz. E-plane=>ϕ= 0° and θ= [0°-360°]. H-plane=>Phi=ϕ° and θ= [0°-360°].

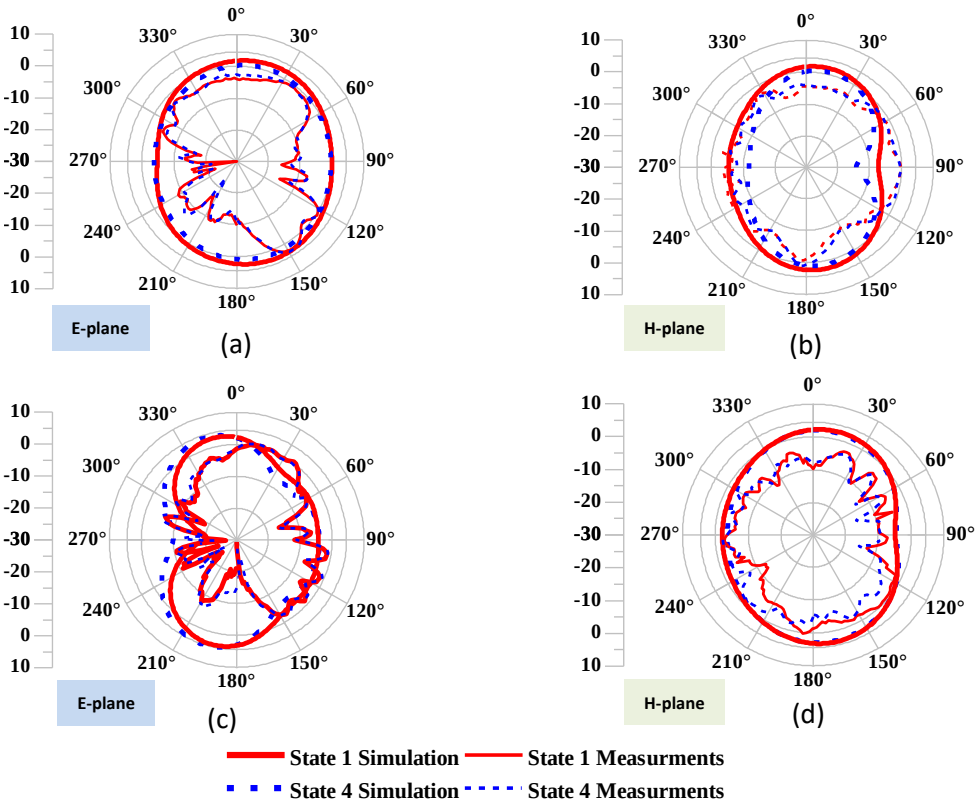

Figure 4.23. Radiation patterns out of the notch frequencies. (a and b) 4.2 GHz; (c and d) 6.7 GHz.

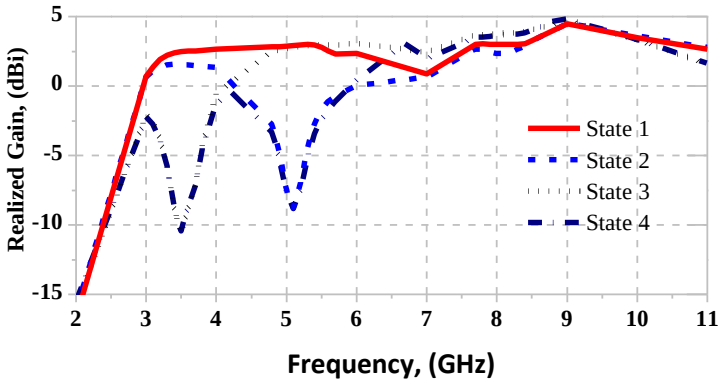

Figure 4.24. Simulated distribution of the gain as function of the frequency for the four switching states.

4.8 Conclusion

This chapter presented the design, the fabrication and the measurement processes undertaken of a low-profile and compact UWB antenna with reconfigurable filtering properties. The filtering was achieved by conceiving two particular slots, while the reconfigurability was achieved by switching two PIN diodes, which were integrated into the configuration to monitor the slots, in four distinct states.

Comparative analysis undertaken between simulated and measured results revealed certain discrepancies requiring further future work to be done. Yet, the obtained performances are promising and represent a sufficient solution for the interference problem. The reconfigurable filters were successfully implemented in a limited space within the ground plane.

The proposed antenna has been checked and validated through experimental fabrication and measurements. Such antenna is suitable for UWB applications where interferences of wireless interoperability medium access and wireless local area network are present.

The proposed antenna could be used in low-power UWB systems minimizing interferences within nearby receivers. The on-demand rejection of WiMAX and WLAN interfering signals can lead to UWB and WLAN links with increased ratio, higher capacity and throughput, and thus can improve the quality, the efficiency and the ratio of UWB communication links.

Bibliography

[1] S. Nikolaou, N.D. Kingsley, G.E. Ponchak, J. Papapolymerou, and M.M. Tentzeris, "UWB Elliptical Monopoles with a Reconfigurable Band Notch Using MEMS Switches Actuated Without Bias Lines", *IEEE Trans. Ant. Prop.*, 57(8), pp. 2242–2251, 2009.

[2] D.E. Anagnostou, M.T. Chryssomallis, B.D. Braaten, J.L. Ebel, and N. Sepúlveda, "Reconfigurable UWB Antenna with RF-MEMS for On-Demand WLAN Rejection", *IEEE Trans. Ant. Prop.*, 62(2), pp. 602–608, 2014.

[3] S.H. Zheng, X. Liu, and M.M. Tentzeris, "Optically controlled reconfigurable band-notched UWB antenna for cognitive radio systems", *Electron. Lett.*, 50(21), pp. 1502–1504, 2014.

[4] D. Zhao, L. Lan, Y. Han, F. Liang, Q. Zhang, and B. Wang, "Optically Controlled Reconfigurable Band-Notched UWB Antenna for Cognitive Radio Applications", *IEEE Photon. Technol. Lett.*, 26(21), pp. 2173–2176, 2014.

[5] A. Mansoul, F. Ghanem, M.R. Hamid, E. Salonen, and M. Berg, "Bandwidth reconfigurable antenna with a fixed lower and a variable upper limit", *IET Ant. Prop. Microw.*, 10(15), pp. 1725–1733, 2016.

[6] G. Sorbello, M. Pavone, and L. Russello, "Numerical and experimental study of a rectangular slot antenna for UWB communications", *Microw. Opt. Technol. Lett.*, 46(4), pp. 315–319, 2005.

Thesis Conclusion

In this thesis, we have reported on new designs of reconfigurable conductive polymers based planar and microstrip/planar antennas. We have provided state of the art of both types of antennas. Prior to implement practically one selected type of antennas, we carried out a lot of simulation work using two commercial software CST and HFSS. A lot of effort and time have been deployed and spent in order to optimize the different parameters for enhanced performances of different designs.

We reported on a simulation analysis carried out on a microstrip frequency reconfigurable antenna, built on a conductive polymer as substrate with the characteristic that allows tunable permittivity. The results were very promising.

We have also described the design of low-cost and low-profile reconfigurable antennas with the capability to filter interferences in the UWB range of the spectrum.

Finally, we described another design of single layer CPW antenna with two reconfigurable filtering functions dedicated for MMIC integration.

The solution of reconfigurable antennas proposed in this thesis is intended to overcome the problem of interference in the ultra-wide band spectrum by taking advantage of the reconfiguration concept. The proposed antennas have high capability to be embedded in small size UWB systems. The reconfigurable designs are of planar microstrip structures which are easy and low-cost to implement.

- The first antenna was a monopole structure characterized by its compact size while it was capable of filtering three interferences from the UWB spectrum. In another word, the antenna can be set to work in eight filtering cases. The reconfigurations were achieved by introducing significant changes to the basis monopole structure from which we started. This antenna offers the highest filtering capabilities in comparison to previously reported ones.
- A second UWB reconfigurable single-sided antenna was proposed. Though, it has a small sized structure, two reconfigurable filtering functions were successfully implemented. The electrical reconfiguration was integrated only in the ground plane in order not to affect the radiation efficiency of the antenna at the expenses of less filtering capabilities

as compared to the first antenna. Its performance was verified experimentally and good agreement was found.

Future tasks to be undertaken:

- **Filtering quality enhancement:**
  The filtering quality of the proposed antenna can be further enhanced in terms of filtering level and interference bandwidth.
- **Experimental fabrication and performance measurements:**
  The proposed reconfigurable monopole UWB antenna is awaiting practical validation. Measurements of the performance of the second proposed single-sided reconfigurable UWB antenna could be improved through adjustments of various parameters.
- **Synthesis, characterization of a conductive polymer suitable for reconfigurable antennas; design and fabrication of reconfigurable polymer-based antennas.**

Appendixes

A. Antenna Parameters

B. PIN Diode

C. Scientific Production

D. Paper

Appendix A

Antenna Parameters

An antenna is defined by the following main characteristics: input impedance, operating frequency and bandwidth; radiation characteristics: directivity, gain, radiation pattern and polarization.

1. Input impedance

An antenna generally behaves like a resonant circuit whose central resonant frequency depends on the values of an inductance L and a capacitance C related to its structure, dimension and any other associated component. In a real system, the antenna is connected to a transmitter or a receiver through a transmission line (like coaxial cable) which generally has an impedance of 50 or 75 Ω. It is the value for which the input impedance of the antenna must be matched to in order to allow the maximum conversion of electrical signal to waves or waves to an electrical signal. The complex input impedance Z_{in} follows:

$$Z_{in}|\omega| = R|\omega| + j.X|\omega|$$

where $\omega=2\pi f$, R is the antenna resistance due to ohmic or resistive heating, X is the antenna reactance and f is the resonance frequency.

2. Resonance frequency

The antenna resonance frequency expresses the measure of the input impedance in frequency. It is the frequency where the input impedance of the antenna is matched to the impedance of the transmission line.

3. Reflexion coefficient *Γ*

is a parameter that describes how much of an electromagnetic wave is reflected by an impedance discontinuity in the transmission medium. It is equal to the ratio of the amplitude of the reflected wave to the incident wave. It depends on the characteristic impedance of the transmission line Z_0 and the input impedance of the antenna $Z_{in}|\omega|$.

$$\Gamma = \frac{Z_{in}|\omega| - Z_0}{Z_{in}|\omega| + Z_0}$$

4. Voltage standing wave ratio (VSWR)

is a measure of impedance matching of loads to the characteristic impedance of a transmission line or waveguide. Impedance mismatches result in standing waves along the transmission line, and SWR is defined as the ratio of the partial standing wave's amplitude at an antinode (maximum) to the amplitude at a node (minimum) along the line.

$$VSWR = \frac{1 + \Gamma}{1 - \Gamma}$$

5. Bandwidth

Antenna bandwidth is the portion of frequency where the antenna input impedance is matched. Practically, it is defined as the frequency band where the reflexion coefficient is lower than -10 dB which corresponds to VSWR lower than 2.

6. Radiation pattern

Radiation pattern is a graphical representation of the far-field radiation properties of the antenna. It is quantification of an antenna ability to transmit/receive power in a particular direction. Radiation pattern is generally presented as the radiation intensity (equal to the radiated power for a solid angle unit) normalized (in dB) as a function of the direction.

7. Directivity

is defined as the ratio between the power density radiated in a given direction and the power density radiated by an isotropic source. The directivity gives information on the directional properties of an antenna without taking into account its efficiency η. Efficiency reflects the performance of the antenna and depends on the radiation resistance and the loss resistance.

8. Gain

is defined as the ratio of the radiation intensity in a given direction if the power accepted in the antenna was radiated isotropically in condition the losses related to mismatch and biasing are not considered. The gain of a directional antenna is expressed in decibels isotropic “dBi” with respect to the isotropic antenna.

9. Polarization

The polarization of an antenna refers to the orientation of the electric field (E-plane) of the radio wave with respect to the Earth's surface and is determined by the physical structure of the antenna and by its orientation. A simple straight wire antenna will have one polarization when mounted vertically, and a different polarization when mounted horizontally.

The polarization of a radiated wave is called linear if the vector of the electric field *E* is always in the same direction and plane. Linear polarization can be horizontal or vertical. In the other hand, the polarization is called circular or elliptic when the vector E of the electric field travels away by describing a circle or ellipse. Hence, it said right-hand circular polarization when the vector *E* turns to right and left-hand circular polarization when it turns to left.

Appendix B

PIN Diode

PIN diode is a semiconductor component composed of three layers: A *P*-layer where holes are the majority carriers, the *I*-layer is an intrinsic layer of a pure semiconductor and a *N*-layer which has electrons as majority carriers.

A *PIN* diode is a diode with a wide, undoped intrinsic semiconductor region between a *P*-type semiconductor and an *N*-type semiconductor region. The *P*-type and *N*-type regions are typically heavily doped because they are used for ohmic contacts.

The wide intrinsic region is in contrast to an ordinary *P–N* diode. The wide intrinsic region makes the *PIN* diode an inferior rectifier (one typical function of a diode), but it makes it suitable for attenuators, fast switches, photodetectors, and high voltage power electronics applications.

In the case of a *PIN* diode, the width of the intrinsic region W_i is small and the space charge area of the P^+-*I* and *I*-N^+ regions can be considered to extend over the entire width of the intrinsic region.

PIN diodes in reverse mode the leakage current is independent of the polarization and is directly related to the width of the intrinsic region. They behave like a plane capacitor. It is independent of the polarization level.

If biased forward, the diode *PIN* is equivalent to a resistance which decreases with the direct current which crosses it, whatever the dynamic level.

PIN diodes can be used either as variable resistors or as electronic switches for RF signals. In the latter case, the diode is basically a two-valued resistor, with one value being very high and the other being very low. These characteristics open several possible applications.

When used as switches, *PIN* diodes can be used to switch devices such as attenuators, filters, and amplifiers in and out of the circuit. It has become standard practice in modem radio equipment to switch dc voltages to bias *PIN* diodes, rather than directly switch RF/IF signals. In some cases, the *PIN* diode can be used to simply short out the transmission path to bypass the device.

Another application for PIN diodes is as voltage-variable attenuators in RF circuits. Because of its variable-resistance characteristic, the PIN diode can be used in a variety of attenuator circuits. Perhaps the most common is the bridge circuit, which is similar to a balanced mixer/modulator.

Appendix C

- **Scientific Production**

Scientific Production

Published Paper

- **Hicham Medkour**, Ameur Zegadi, Erika Vandelle, Imed Edin Djadour, Tan Phu Vuong,“ Quasi-Real Scenario of Reconfigurable Filtering Functions Antenna for UWB Communications”, *Elektronika ir Elektrotechnika*, vol. 24, no. 5, pp. 86-91, October 2018. DOI: http://dx.doi.org/10.5755/j01.eie.24.5.21849.

International Communications

- **Hicham Medkour** and Ameur Zegadi, “Compact MIMO Antenna with Reconfigurable Impedance Bandwidth”, International Conference on Electronics and New Technologies (ICENT-2017) 14-15 November 2017, M’sila -Algeria.
- **Hicham Medkour** and Ameur Zegadi, “Design of reconfigurable filtering based UWB antenna dedicated for radar applications”, In *Seminar on Detection Systems Architectures and Technologies (DAT)* 2017 pp. 1-4). IEEE, February 2017, Algiers Algeria. DOI: 10.1109/DAT.2017.7889162.
- **Hicham Medkour** and Ameur Zegadi, “A Compact Reconfigurable Ultra Large Band Antenna for Breast Cancer Detection Systems”, *International Conference on Technological Advances in Electrical Engineering (ICTAEE’16.),* October 2016, Skikda Algeria.
- **Hicham Medkour** and Ameur Zegadi, “Design and Simulation of UWB Antenna with Rejection of WiMAX, WLAN and ITU Bands”, *International Conference on Technological Advances in Electrical Engineering (ICTAEE’16.),* October 2016, Skikda Algeria.

Appendix D

- **Paper**

Quasi-Real Scenario of Reconfigurable Filtering Functions Antenna for UWB Communications

Hicham Medkour[1], Ameur Zegadi[1], Erika Vandelle[2], Imededdin Djadour[3], Vuong Tan Phu[2]
[1]*LCCNS, Department of Electronics, Ferhat Abbas University of Setif 1, Compus El-Maabouda, 19000 Setif, Algeria*
[2]*IMEP-LAHC, Grenoble INP – MINATEC, 3, Parvis Louis Neel - CS 50257 - 38016 Grenoble Cedex 1, France*
[3]*ETA, Department of Electronics, University of Mohamed El Bachir El Ibrahimi, El-Annasser, 34030, BBA, Algeria*
medkour_h19@univ-setif.dz

***Abstract*—In this paper, an Ultra Wide Band antenna with reconfigurable filtering-characteristic is proposed to overcome interferences problems in the frequency range 3.1 GHz–10.7 GHz. With dimensions of 35 x 35 mm^2, the structure is simple, low–cost and possesses an operating bandwidth from 3 GHz to 12 GHz. Besides, it is easy to reconfigure this antenna to filter one, two or three interferences, in which the filtering is achieved by three slots of half wavelength created in the geometry, while the reconfiguration is achieved through four PIN diodes used to control the three slot's effect. Considering the filtering action, this antenna can switch between eight distinct operational modes, which is the highest number compared to previous works. Design and analysis of the proposed configuration are done by two simulation software which are CST and HFSS. The acceptable agreement between the results obtained by both simulations proves the realistic working performance of the proposed structure. The present antenna is suitable for UWB communication applications, particularly; the which are suffering from interference issues with WiMAX 3.3 GHz–3.7 GHz, WLAN 5 GHz–5.3 GHz or ITU band 8 GHz–8.4 GHz.**

***Index Terms*—Filtering; Interference; PIN diodes; Reconfiguration; UWB antenna.**

I. INTRODUCTION

Recently, the frequency band from 3.1 GHz to 10.7 GHz, called Ultra-Wide Band (UWB) spectrum has been of great interest, since it is the band where data can be transmitted with high rate, low power consumption, low-cost, less obstacles penetration and so on [1], [2]. Because of these attractive properties, the number of applications performing in these bands is increasing rapidly these days, which unfortunately led to crowd this interesting part of spectrum and undesirable problem of interferences has emerged. Interferences that have been caused by some narrow bands considerably disturb the functionality of UWB systems and lower their performance.

For this reason, implementation of a filtering function into UWB systems is crucial to overcome interference issues; however, it is preferable not to introduce additional size into the UWB system circuitry, because miniaturization of today's wireless communication systems is strongly needed. Instead, it is much better if one can assign the filtering function to the antenna since the latter is a vital element for any wireless communication system; hence the antenna can perform the filtering operation without the need for integrating filtering circuits. This can help to get rid of additional size and complexity. Many papers have been published lately to propose different shapes of UWB antennas with the ability to filter up to five interfering bands from the UWB spectrum as in [3]–[6]. The filtering provided by those designs is perpetual, which means a significant part of the spectrum is always out of work (filtered). This is a clear drawback particularly once interferences are not active. Alternatively, it is worthwhile if one can design an UWB antenna that is capable of controlling its filtering action, like activating and deactivating the filtering or shifting its frequency. Unlike perpetual filtering, this could strongly help to efficiently exploit the UWB spectrum. This procedure is referred to as "reconfigurable filtering" and it has been a topic of many active researches in the last period.

In the literature, different shapes of UWB antennas with reconfiguration of single filtered bands have been reported in [7]–[10]. Then, it has been the goal to increase the number of filtering bands like in [11]–[14], in which UWB antennas with reconfiguration of two interferences are successfully implemented. Furthermore, UWB antennas with up to four reconfigurable interfering bands have been reported in [15] and [16]. A key mechanism to achieve filtering reconfiguration has been followed in these works, in which various kinds of switches, including PIN diodes, MEMS, FET transistors, Shotcky diode and optical switches have been used. However, less attention has been paid to the effect of the quantity of switches on the antenna size and functionality. As it is known, the more switches the antenna has, the bigger its size is. Here lies the weakness of the previous works, since more switches have been used to produce less filtering operational modes. Typically, n switches can contribute to 2^n operational filtering modes. For this reason, the present work has come to limit this drawback. Actually, a part of this work has been initiated and published in [17]. The objective is to design a compacted size UWB antenna capable of producing more

Manuscript received 5 February, 2018; accepted 17 July, 2018.

filtering operational modes, while using a smaller number of switches. As presented in the subsequent sections, the proposed antenna is thoroughly studied using two simulation software CST and HFSS. The results gotten are discussed while performance is presented and compared to that of previous works.

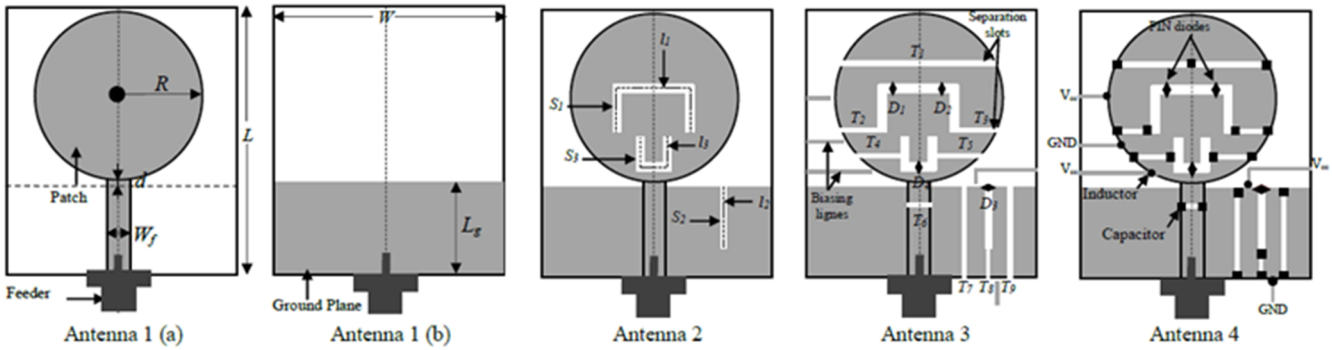

Fig. 1. Design and optimization steps: (a) top view; (b) lower view.

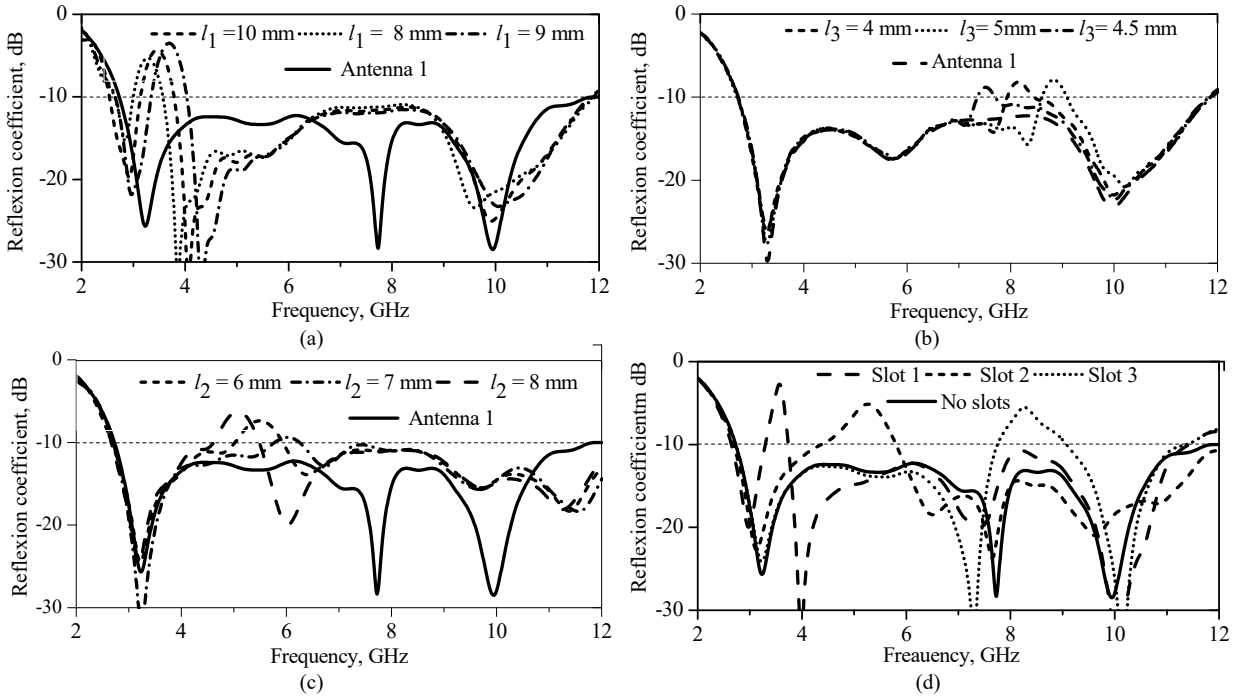

Fig. 2. Design and optimization step: a) Optimization of l_1, b) Optimization of l2, c) Optimization of l3, d) The individual effect of each slots.

II. DESIGN METHODOLOGY

In order to investigate the proposed reconfigurable filtering system, the printed monopole UWB structure is chosen. Because it satisfies the requirements for UWB applications such as wide bandwidth, omnidirectional radiation pattern, high gain and low-cost of implementation and so on [2]. As shown in Fig. 1 (Antenna 1), the proposed structure consists of a circular patch with radius R fed by a 50 Ohm micro-strip line of width W_f printed on the upper face of the FR-4 substrate with permittivity ε_r = 4.4 and thickness 1.5 mm. The ground plane with the length L_g is printed on the lower face of the substrate. The latter has overall dimensions of $W \times L$. Using Computer Simulation Technology software [18] through time domain solver calculations, the basic structure design and optimization are done while a careful parametric refinement is owned particularly to the parameter d in order to obtain an ultra-wide band characteristic. Given the fact that, the antenna resonance and radiation properties are due to a certain current distribution within the geometry, filtering functions can be created by occurring new current paths in the patch and ground plane, which will mismatch the antenna resonance at particular frequencies within the UWB spectrum 3.1 GHz–10.6 GHz. Based on that, a parametric study is carried out in which three slots S_1, S_2, S_3 of width 0.5 mm each are created in the patch and the ground plane as shown in Fig. 1 (Antenna 2). The concept followed to predict the primary slot's length is shown by equation under [19]

$$\lambda_g = \frac{c}{f_c \times \sqrt{\varepsilon_{reff}}}. \quad (1)$$

in which λ_g is the guided wavelength in m, c is the light speed in m/s. f_c is the central frequency of the filtered band in GHz and ε_{reff} is the effective dielectric constant. Hence, the filtering functions are obtained at l_1 = 12 mm, l_2 = 12 mm and l_3 = 10.39 mm. Afterwards, several parametric calculations have been performed using CST in order to refine the positions and the lengths of each slot separately. The influences of l_1, l_2 and l_3 on the filtering actions can be well observed in Fig. 2, in which the behaviours of the antenna with and without slots are presented for comparison.

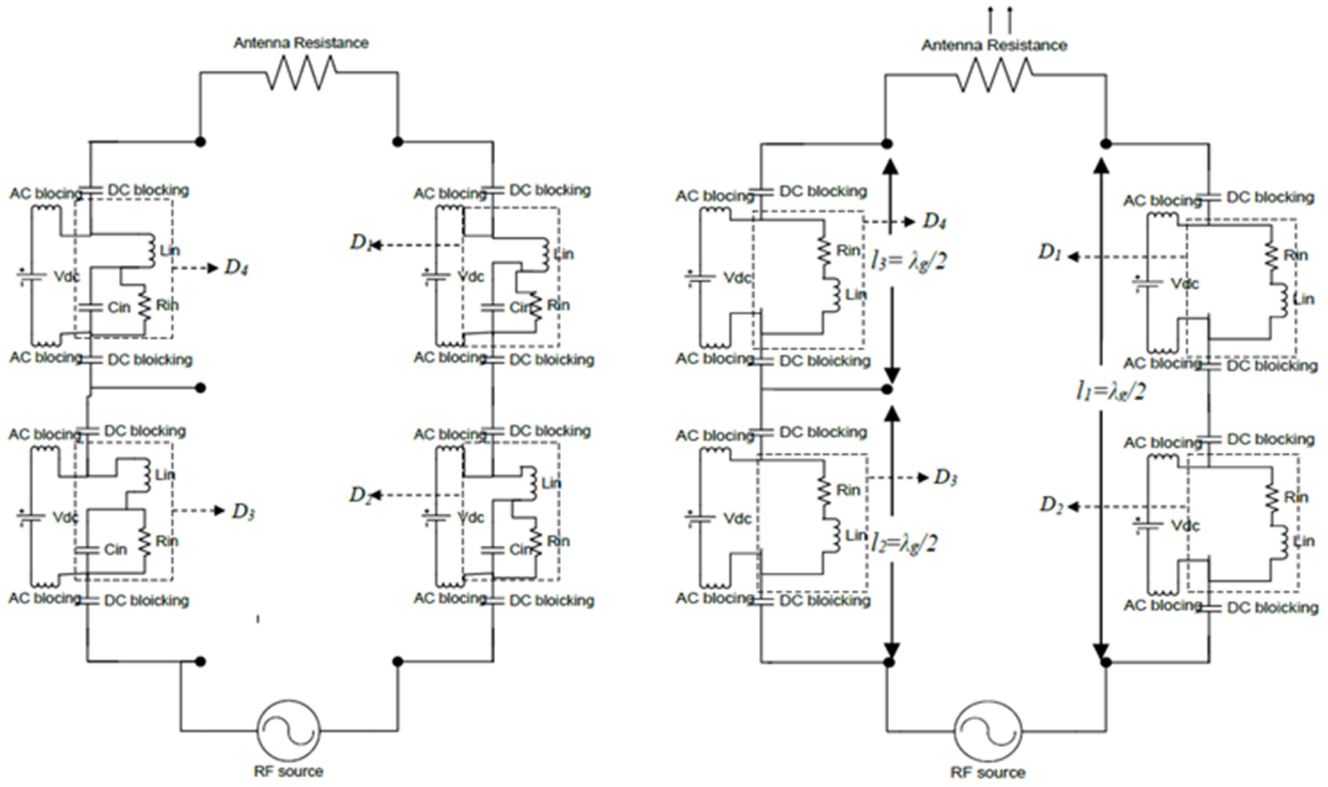

Fig. 3. Modelling of the diodes across the slots: (a) forward biasing $V_{dc} > 0$ (mode 1); (b) reversed biasing $V_{dc} <= 0$ (mode 8).

The filtering operations are controlled by monitoring the effects of the slots, across which, four PIN diodes D_1, D_2, D_3 and D_4 are carefully positioned as shown in Fig. 1 (Antenna 3). Each PIN diode has to be controlled through a biasing circuit that necessitates a DC signal (V_{DC}). The diode can be set *On* when it is forwardly biased and *Off* when inversely biased. To explain the diodes functionality along with the biasing control, the equivalent circuit model RLC are given in Fig. 3. When the diodes are forwardly biased ($V_{DC} > 0$), they shows high capacitance which allows passing AC signals, where each diode is modelled by capacitor in parallel with a small resistor, Fig. 3(a). Otherwise, they shows a high resistance to AC signals when reversely biased ($V_{DC} <= 0$) and they are modelled only by a serial resistor, as shown in Fig. 3(a) and Fig. 3(b). In simulation, S-parameters of BAR50-2V PIN diodes [20] are introduced using CST design studio. These diodes are commercially available with low-cost and with the suitable size and operating frequency for the present application. They are used in this design, in order to predict the practical behaviour of the proposed antenna rather than conventional simulation with ideal switches such as metallic stubs. S-parameters file includes the modelling of the diodes in the On and Off states. Besides, it is crucial to separate between the DC signals and the AC signals within the antenna surfaces. For this reason, a set of slots T_1 to T_6 is generated in the patch to prevent the DC signals from circulating in the entire patch surface, where T_7, T_8 and T_9 are created in the ground plane for the same reason, Fig. 1 (Antenna 3). In fact, these separations have heavily changed the antenna basic resonance; this is why a set of RF capacitors of C = 22 pF is inserted across the two ends of each biasing slot, as observed in Fig. 1 (Antenna 4). As it is known, capacitor stops DC signals while lets pass AC signals if it has small capacitive reactance X_c. for this reason, its value is chosen to be C = 22 pF to achieve less capacitive reactance value where: $X_c = 1/(2\pi fC)$. Furthermore, inductors of value 27 nH and operating frequency 2.4 GHz are used to prohibit alternative signals from flowing towards the biasing circuit. For that, the value L = 27 nH is calculated to achieve high inductive reactance where $X_L = 2\pi fL$. Finally, the optimization of Antenna 4 has been conducted in CST based on the criteria that, the reflexion coefficient is close to -5 dB over the filtered bands, while it is less than -10 dB over the rest parts of UWB spectrum. The final optimized dimensions are depicted in Table I.

TABLE I. ANTENNA DIMENSIONS.

Parameter	Value in millimeters	Parameter	Value in millimeters
W	35	d	0.5
L	35	l_1	52
W_f	3	l_2	6.5
R	6	l_3	10.39
L_g	12		

III. RESULTS AND DISCUSSION

The control of the four PIN diodes is well clarified in Table II, in which eight possible switching states are exposed. Due to the longer length of S1 compared to S2 and S3, one single diode was not enough to control its effect. Therefore, the two diodes D_1 and D_2 are incorporated to perform together like a single switch. Hence, the proposed antenna is capable of working in eight distinct operational modes, as illustrated in Fig. 4 that shows the simulation results obtained from CST for each mode.

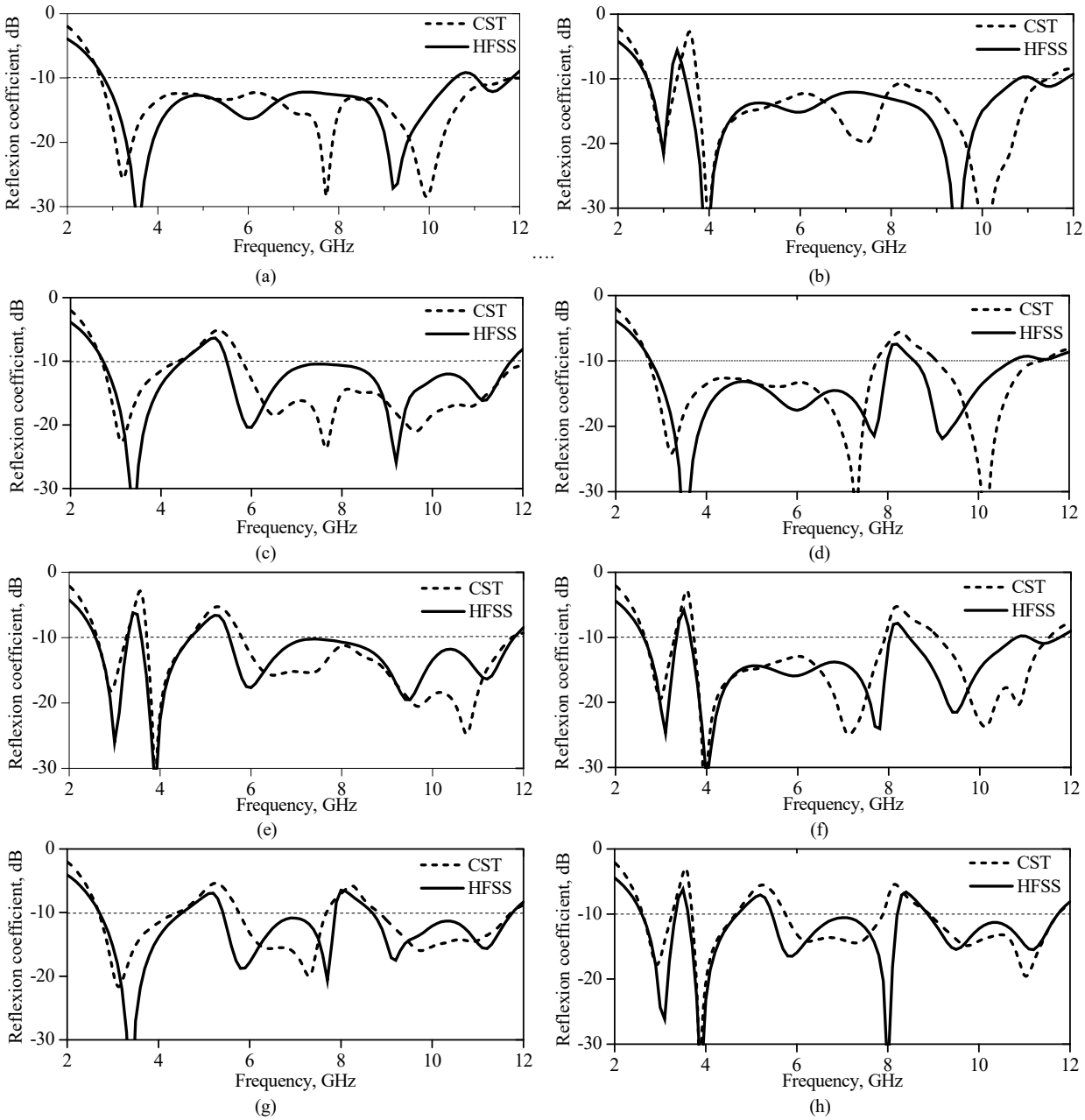

Fig. 4. Simulated reflexion coefficient of the eighth operational modes: (a) mode 1; (b) mode 2; (c) mode 3; (d) mode 4; (e) mode 5, (f) mode 6; (g) mode 7; (h) mode 8.

For the eight different modes, the antenna tunes from 3 GHz 11.5 GHz which includes the UWB spectrum 3.1 GHz–10.7 GHz. The filtering actions can be observed in the regions where the reflexion coefficient (S11) is around -5 dB. This reveals actually a high mismatching in the input impedance of the antenna which means in turn that, the antenna is prohibited from transmitting or receiving at the frequencies 3.5 GHz, 5.1 GHz and 8.2 GHz in the modes 2, 3 and 4, respectively. This touch is used to stop interferences coming from WiMAX (3.4 GHz–3.7 GHz), lower band of WLAN (5 GHz–5.4 GHz) and ITU band (8 GHz–8.4 GHz). Besides, the antenna can be reconfigured such as it filters two frequencies at once as in the modes 5, 6 and 7. Furthermore, it is capable to filter the three bands WiMAX, WLAN and ITU at the same time when it is in the mode 8. In order to support the validity of the obtained results, the proposed structure is re-simulated using different simulation software which is HFSS [21]. As a result, the behaviours of both the methods appear like similar to each other for the eight modes, as shown in Fig. 4. This confirms the validity of the results obtained with CST.

TABLE II. REAL SWITCHES CONFIGURATION.

Modes	Switching states			
	D_1	D_2	D_3	D_4
mode 1	On	On	On	On
mode 2	Off	Off	On	On
mode 3	On	On	Off	On
mode 4	On	On	On	Off
mode 5	Off	Off	Off	On
mode 6	Off	Off	On	Off
mode 7	On	On	Off	Off
mode 8	Off	Off	Off	Off

However, some discrepancies can be observed, particularly in the filtering levels obtained from HFSS. This can be explained by the fact that, in HFSS, metallic stubs

were used as switches rather than S-parameters of real PIN diodes like in CST. To demonstrate the filtering functions, surface current distributions at the modes 1, 2, 3 and 4 are pictured in Fig. 5. It can be seen that, in the mode 1, the current distribution is quasi-uniform, since that by setting all the diodes in the On state, the effects of S1, S2 and S3 are not operational, Fig. 5(a). Unlike the mode 1, strong current distribution can be observed around S1, S2 and S3, attesting their contributions in the modes 2, 3 and 4, respectively Fig. 5(a)–Fig. 5(c).

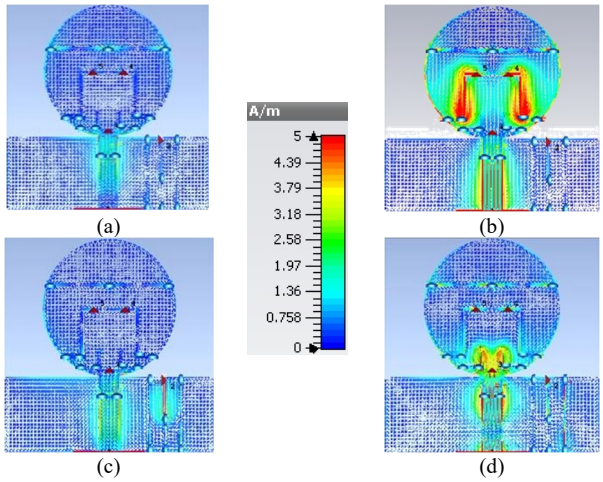

Fig. 5. Currents distribution on the antenna at: a) mode 1, b) mode 2, c) mode 3, d) mode 4.

The radiation pattern of the mode 8 obtained by the CST simulation is presented for discussion in Fig. 6, since this mode includes all the filtering functions. It can be seen that, an omnidirectional shape is achieved in both E and H planes at all simulated frequencies. The same shapes of radiation pattern obtained with HFSS simulation confirm the ones obtained with CST. Nevertheless, higher gains are obtained with HFSS. This is due to the fact that, the effect of real switches is not considered. The realized gains of the antenna in the modes 1 and 8 are presented and compared in Fig. 7. The difference between the modes 1 and 8 can be clearly observed. In the mode 1, a quasi-steady peak gain between 2 dBi and 3 dBi is obtained while in mode 8, the antenna gain exhibits a deep shrinking around the frequencies of 3.5 GHz, 5.2 GHz and 8.2 GHz. These attenuations in the peak gain can be explained by the antenna impedance mismatching due to the slot's effect. This result suggests that the filtering operations are successfully accomplished at these three frequencies of the spectrum.

IV. PERFORMANCES COMPARISON

In order to highlight the contribution of this work, it is worth to compare the performance of the proposed antenna with other structures recently reported in the literature. The comparison is addressed in Table III, in which three key parameters are under consideration: the number of the RF-switches (n), the operating modes (2^n) and the size of the whole structure. As it is demonstrated, the antenna proposed in [13] has a size of about 40 × 30 × 0.8 mm^3. It uses three PIN diodes ($n = 3$) to produce only four modes (4/8). Otherwise, the antenna reported in [14] uses five optical switches ($n = 5$) while offering only four modes (4/32). It is size is larger considering the source of optical light. Up to six operational modes (6/16) are provided by the antenna proposed in [15] where four ($n = 4$) ideal switches were used. Its size is presented in the table do not encompass the size of the biasing network. Therefore, the comparison divulges that the antenna of the present work outperforms those of previous works. It uses only four ($n = 4$) PIN to produce eight operational modes (8/16) which is the highest that has been reported. Moreover, it has the smaller size including the basing network which is about 35×35×1.6 mm^3.

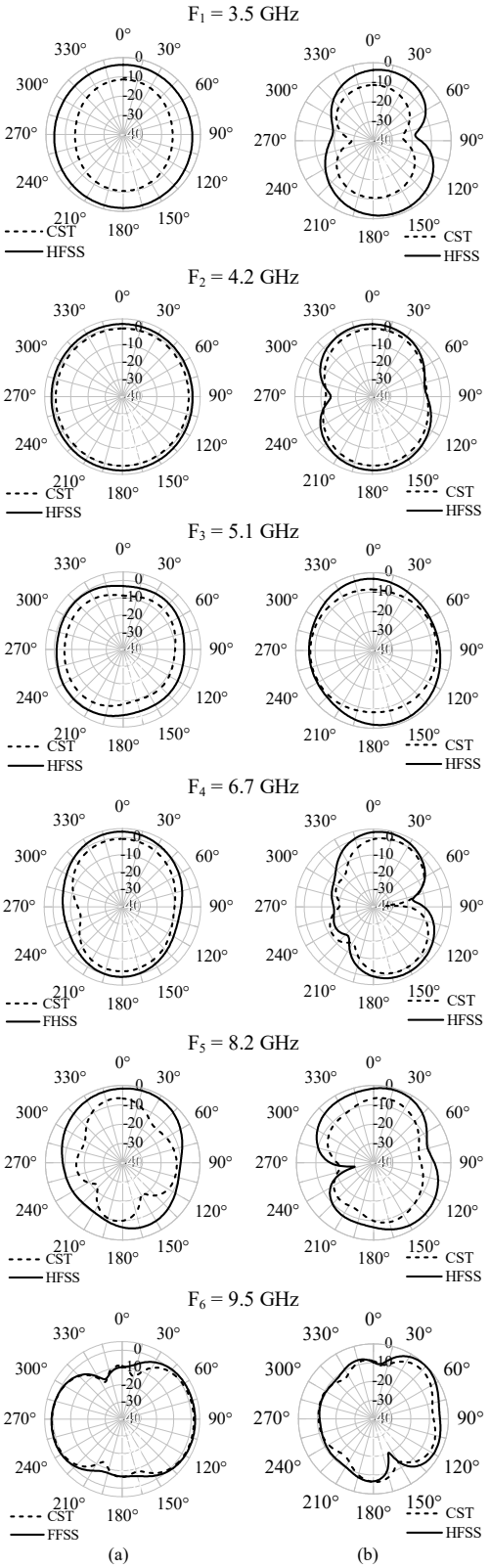

Fig. 6. Radiation pattern of mode 8 simulated in CST and HFSS: (a) E-plane/{Phi = 0°}; (b) H-plane/{Phi = 90°}.

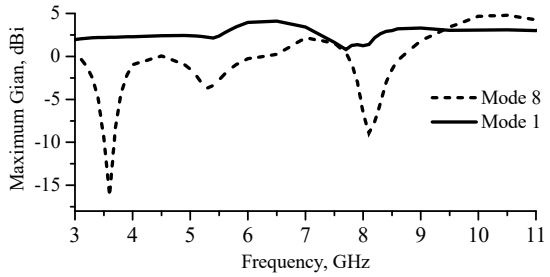

Fig. 7. Realized gain in dBi vs frequency in modes 1 and 8.

TABLE III. PERFORMANCE COMPARISON.

Antenna	Operating modes (2^n)	(n)	Size in mm^3
Ref. [13]	1-WB. 2-WB with filtering of 5.5 WLAN band GHz. 3-WB with filtering of X-band 7.5 GHz. 4-WB with filtering of WLAN 5.5 GHz and X-band 7.5 GHz.	3	40×30×0.8
Ref. [14]	1-WB with filtering of WLAN band 2.4 GHz. 2-WB with filtering of WiMAX band 3.5 GHz. 3-WB with filtering of WLAN band 5 GHz. 4-WB with filtering of ITU band 8 GHz 5.	5	25×25×0.8
Ref. [15]	UWB. UWB with filtering of WLAN 5.5 GHz, RFID 6.8 GHz, X band 11.5 GHz. UWB with filtering of WLAN 5.5 GHz, X band 11.5 GHz. UWB with filtering of X band 8.7 GHz. UWB with filtering of RFID band 6.8 GHz X band 8.7 GHz. UWB with filtering of RFID band 6.8 GHz.	4	30×31×0.8
The antenna of the proposed work	1-UWB. 2-WB with filtering of WiMAX band 3.5 GHz. 3-WB with filtering of lower-band WLAN 5.2 GHz. 4-WB with filtering of ITU band 8.2 GHz. 5-WB with filtering of WiMAX band 3.5 GHz and 5.2 GHz. 6-WB with filtering of WiMAX band 3.5 GHz and ITU band 8.2 GHz. 7-WB with filtering of Lower-band WLAN 5.2 GHz and ITU band 8.2 GHz. 8-WB with filtering of WiMAX band 3.5 GHz, lower-band WLAN 5.2 GHz and ITU band 8.2 GHz.	4	35×35×1.6

V. CONCLUSIONS

At this work, eight reconfigurable filtering states has been integrated in a simple planar monopole UWB antenna. The design has been done by two simulation software, where the results obtained by both confirm each other. The performance has been compared with those obtained in previous works, where the proposed antenna has showed the highest number of operational modes. The proposed structure is suitable for application in UWB systems where it can solve interference problem, as well, it can be used for applications where reconfigurable bandwidth is required such as in cognitive radio systems.

REFERENCES

[1] UFC Commission. FCC Revision of part 15 of the commission's rules regarding ultra-wideband transmission systems: First report and order. *Technical Report*, 2002.

[2] D. Valderas, J. I. Sancho, D. Puente, C. Ling, X. Chen, *Ultrawideband Antennas*. Imperial College Press, 2010. DOI: 10.1142/p684.

[3] M. Ur-Rehman, QH. Abbasi, M. Akram, C. Parini, "Design of band-notched ultra wideband antenna for indoor and wearable wireless communications", *IET Microwaves, Antennas & Propagation*, vol. 9, no. 3, pp. 243–51, 2014. DOI: 10.1049/iet-map.2014.0378.

[4] M. Koohestani, N. Pires, A. K. Skrivervik, A. A. Moreira, "Band-reject ultra-wideband monopole antenna using patch loading", *Electronics letters*, vol. 48, no. 16, pp. 974–975, 2012. DOI: 10.1049/el.2012.1771.

[5] T. D. Nguyen, D. H. Lee, H. C. Park, "Design and analysis of compact printed triple band-notched UWB antenna", *IEEE antennas and wireless propagation letters*, vol. 10, pp. 403–406, 2011. DOI: 10.1109/LAWP.2011.2147270.

[6] K. Luo, W. P. Ding, W. Q. Cao, "Compact monopole antenna with triple band-notched characteristics for UWB applications", *Microwave and Optical Technology Letters*, vol. 56, no. 4, pp. 822–827, 2014. DOI: 10.1002/mop.28223.

[7] D. E. Anagnostou, M. T. Chryssomallis, B. D. Braaten, J. L. Ebel, N. Sepulveda, "Reconfigurable UWB antenna with RF-MEMS for on-demand WLAN rejection", *IEEE Trans. Antennas and Propagation*, vol. 62, no. 2, pp. 602–608, 2014. DOI: 10.1109/TAP.2013.2293145.

[8] A. M. Abbosh, "Design of a CPW-fed band-notched UWB antenna using a feeder-embedded slot-line resonator", *International Journal of Antennas and Propagation*, 2008, pp. 1–5. DOI: 10.1155/2008/564317.

[9] N. Sepulveda, D. E. Anagnostou, M. T. Chryssomallis, J. L. Ebel, "Integration of RF-MEMS switches with a band-reject reconfigurable ultra-wideband antenna on SiO_2 substrate", in *IEEE Antennas and Propagation Society Int. Symposium*, 2010, pp. 1–4. DOI: 10.1109/APS.2010.5560968.

[10] S. Nikolaou, N. D. Kingsley, G. E. Ponchak, J. Papapolymerou, M. M. Tentzeris, "UWB elliptical monopoles with a reconfigurable band notch using MEMS switches actuated without bias lines", *IEEE Trans on Antennas and Propagation*, vol. 57, no. 8, pp. 2242–2251, 2009. DOI: 10.1109/TAP.2009.2024450.

[11] B. Badamchi, J. Nourinia, C. Ghobadi, A. V. Shahmirzadi, "Design of compact reconfigurable ultra-wideband slot antenna with switchable single/dual band notch functions", *IET Microwaves, Antennas & Propagation*, vol. 8, no. 8, pp. 541–548, 2014. DOI: 10.1049/iet-map.2013.0311.

[12] N. Tasouji, J. Nourinia, C. Ghobadi, F. Tofigh, "A novel printed UWB slot antenna with reconfigurable band-notch characteristics", *IEEE Antennas and wireless propagation letters*, vol. 12, pp. 922–925, 2013. DOI: 10.1109/LAWP.2013.2273452.

[13] P. Lotfi, M. Azarmanesh, E. Abbaspour- Sani, S. Soltani, "Design of very small UWB monopole antenna with reconfigurable band-notch performance", in *IEEE Sixth Int. Symposium Telecommunications (IST 2012)*, 2012, pp. 102–105. DOI: 10.1109/ISTEL.2012.6482964.

[14] H. Oraizi, N. V. Shahmirzadi, "Frequency-and time-domain analysis of a novel UWB reconfigurable microstrip slot antenna with switchable notched bands", *IET Microwaves, Antennas & Propagation*, 2017. DOI: 10.1049/iet-map.2016.0009.

[15] S. H. Zheng, X. Liu, M. M. Tentzeris, "Optically controlled reconfigurable band-notched UWB antenna for cognitive radio systems", *Electronics Letters*, vol. 50, no. 21, pp. 1502–1504, 2014. DOI: 10.1049/el.2014.2226.

[16] Y. Li, W. Li, Q. Ye, "A reconfigurable triple-notch-band antenna integrated with defected microstrip structure band-stop filter for ultra-wideband cognitive radio applications", *International Journal of Antennas and Propagation*, 2013. DOI: 10.1155/2013/472645.

[17] M. Hicham, A. Zegadi, "Design of reconfigurable filtering based UWB antenna dedicated for radar applications", in *IEEE Seminar Detection Systems Architectures and Technologies (DAT 2017)*, pp. 1–4, 2017. DOI: 10.1109/DAT.2017.7889162.

[18] Computer Simulation Technology. [Online]. Available: https://www.cst.com

[19] S. B. Cohn, "Slot line on a dielectric substrate", *IEEE Trans on microwave theory and techniques*, vol. 17, no. 10, pp. 768–778, 1969. DOI: 10.1109/TMTT.1969.1127058.

[20] Radio frequency components. [Online]. Available: https://www.infineon.com/cms/en/product/rf-wireless-control/rf-diode/rf-pin-diode/antenna-switch/bar50-02v/

[21] Higher Frequency Structure Simulator. [Online]. Available: http://www.ansys.com.

Title: Design and Implementation of Reconfigurable Antennas

Abstract

In this thesis we describe novel approaches in designing reconfigurable antennas. The proposed reconfigurable layouts are intended for integration into compact UWB communication systems and are characterized by their low profile and easy fabrication processes. Initially, the project was to design et implement some reconfigurable antennas based on conductive polymers. As a result, the first part of this thesis provides an advanced literature survey as well as an investigation on the use of tunable permittivity or conductivity in designing antennas based on conductive polymers. The second part of this thesis reports on the design of planar reconfigurable UWB antennas with interference filtering capabilities. Firstly, a planar monopole UWB reconfigurable antenna has been designed showing filtering capabilities in three narrow bands which could potentially interfere in this particular region of the spectrum. Reconfigurability allows the antenna to match to any interference cases. The presented design uses low-cost FR 4 substrates known for being light. Secondly, an extremely compact UWB single-sided reconfigurable designed antenna is described. Unlike the previous antenna, the reconfigurable filtering circuit has been exclusively implemented in the ground plane rather than in the radiating patch in order to optimize the radiation performance of the antenna. By doing so, the new design is cost effective, allowing interferences' filtering at the antenna level rather than at a later stage and avoids complex biasing control antenna circuitry.

Keywords: Antennas; Microstrip; UWB; Conductive polymers; Reconfiguration.

العنوان: تصميم وصناعة هوائيات ذات خصائص قابلة لإعادة الهيكلة

ملخص

في هذه الرسالة وصفنا طرائق جديدة في تصميم هوائيات ذات الخصائص القابلة للتحكم. فقد تم تقديم تصاميم لهوائيات مناسبة للإدماج في أنظمة الاتصالات الصغيرة الحجم وذو ترددات واسعة النطاق المنحصرة بين 3 و10 GHz. تتميز هذه الهوائيات بخاصيتين هامتين هما الهيئة الفزيائية الأقل جاذبية وسهولة التصنيع. أصلا في بداية المشروع، كنا نرغب إلى تصميم وصنع بعض الهوائيات القابلة لإعادة التكوين استنادًا إلى البوليمرات الموصلة. على هذا الأساس، يوفر الجزء الأول من هذه الرسالة مسحًا متقدمًا للأدب بالإضافة إلى دراسة حول استخدام السماحية القابلة للضبط أو الموصلية في تصميم الهوائيات باستعمال البوليمرات الموصلة. يقدم الجزء الثاني من هذه الرسالة تقريراً عن تصميم هوائيات **UWB** المستوية القابلة لإعادة التشكيل مع إمكانيات تصفية التداخل. أولاً، تم تصميم هوائي قابل لإعادة التشكيل أحادي القطب **UWB** لإظهار إمكانيات التصفية في ثلاث نطاقات ضيقة يمكن أن تتداخل في منطقة الطيف المعينة. تسمح إعادة التكوين للهوائي بالتطابق مع أي حالات تداخل. يستخدم التصميم المقدم ركائز **FR 4** منخفضة التكلفة معروفة بكونها خفيفة. ثانياً، يوصف هوائي مصمم بدقة **UWB** أحادي الجانب قابل لإعادة التحكم. بخلاف الهوائي السابق، تم تنفيذ دائرة الترشيح القابلة لإعادة التحكم على وجه الحصر في المستوى الأرضي بدلاً من التصحيح المشع من أجل تحسين أداء إشعاع الهوائي. القيام بذلك، يكون التصميم الجديد منخفض التكلفة مما يسمح بترشيح التداخلات على مستوى الهوائي بدلاً من مرحلة لاحقة ويتجنب الدوائر المعقدة لهوائي التحكم في التحيز.

الكلمات المفتاحية: الهوائيات؛ النواقل المطبوعة؛ UWB؛ لدائن ذات ناقلية كهربائية؛ عالية إعادة الهيكلة.

Titre : Conception et réalisation d'antennes reconfigurables

Résumé

Dans cette thèse, nous décrivons de nouvelles approches dans la conception d'antennes reconfigurables. Les schémas reconfigurables proposés sont destinés à être intégrés dans des systèmes de communication UWB compacts et se caractérisent par leur profil bas et leurs processus de fabrication faciles. Au départ, le travail consistait à concevoir et à mettre en œuvre des antennes reconfigurables à base de polymères conducteurs, par conséquent, la première partie de cette thèse propose une étude bibliographique avancée ainsi qu'une étude sur l'utilisation de la permittivité ou de la conductivité accordables dans la conception d'antennes à base de polymères conducteurs. La deuxième partie de cette thèse porte sur la conception d'antennes UWB planes reconfigurables dotées de capacités de filtrage aux interférences. Premièrement, une antenne reconfigurable UWB monopolaire plane a été conçue, montrant des capacités de filtrage dans trois bandes étroites susceptibles d'interférer dans cette région spectrale. La reconfiguration permet à l'antenne de s'adapter à tous les cas d'interférences. La conception présentée utilise des substrats à faible coût de FR 4 connus pour leur légèreté. Deuxièmement, Nous décrivons une seconde reconfigurable antenne UWB et qui est extrêmement compacte. Contrairement à l'antenne précédente, le circuit de filtrage reconfigurable a été mis en œuvre exclusivement dans le plan de masse plutôt que dans le patch rayonnant afin d'optimiser les performances de rayonnement de l'antenne. La nouvelle conception est peu coûteuse et permet de filtrer les interférences au niveau de l'antenne plutôt qu'à un stade ultérieur, en évitant le besoin aux circuits complexes de commande de polarisation.

Mots clés : Antennes ; Microruban ; UWB ; Polymères conducteurs ; Reconfiguration.